DEFINING THE ROLE OF LYSINE ACETYLATION IN REGULATING THE FIDELITY OF DNA SYNTHESIS

by

Onyekachi Ebelechukwu Ononye

A Dissertation

Submitted to the Faculty of Purdue University

In Partial Fulfillment of the Requirements for the degree of

Doctor of Philosophy

Department of Biology at IUPUI

Indianapolis, Indiana

December 2020

THE PURDUE UNIVERSITY GRADUATE SCHOOL
STATEMENT OF COMMITTEE APPROVAL

Dr. Lata Balakrishnan
Department of Biology

Dr. John Watson
Department of Biology

Dr. AJ Baucum
Department of Biology

Dr. John Turchi
Indiana University School of Medicine

Dr. Matthew Bochman
Department of Molecular Biology and Cellular Biochemistry Indiana University, Bloomington

Approved by:
Dr. Theodore Cummins

I dedicate this work foremost to God from whom all blessings flow. Then to my family who this couldn't have been possible without especially my parents and my brother, Azubike who has always served as a pillar of strength throughout my life. To Kola, my husband, thank you for learning to provide support through unconventional means, it hasn't gone unnoticed. To Sara, as we always say, "we're all we got." Thank you for always getting me. Vienne, words will never be enough, so here's to Fiona and Delilah! Finally, to my Diversity Church family who have been a home away from home, I dedicate this work to you as well.

ACKNOWLEDGMENTS

I'd like to thank Dr. Balakrishnan for all the ways she has impacted my life both scientifically and personally. In many ways, I have watched myself learn to persevere through the floods of life with continued hope and grit until tasks are accomplished. I attribute a portion of this to your mentorship and continued support. In the same stead, I'd like to acknowledge my committee members: Dr. Watson, Dr. Baucum, Dr. Turchi and Dr. Bochman who have not only challenged me but have equally empathized and supported me throughout my graduate journey. I owe a huge depth of gratitude to both current and past members of the Balakrishnan laboratory who have contributed to my learning by asking vital questions, teaching techniques and creating one of the best work environments. To the current and past members of the Picard laboratory (second floor lab mates) thank you for your friendship and always including me in non-lab activities. Furthermore, another round of thanks goes to the Baucum laboratory who I refer to as my second lab as I spent a lot of my time with them imaging all my gels. Thank you for your patience and engaging conversations. Finally, I'd like to acknowledge Christopher Sausen who was a graduate student in the Bochman laboratory for all his hard work towards ensuring our paper was a success.

TABLE OF CONTENTS

LIST OF FIGURES

LIST OF ABBREVIATIONS

DNA	deoxyribonucleic acid
AC	acetylated
Acetyl CoA	acetyl coenzyme A
AT	acetyltransferase
BLI	biolayer interferometry
DBD	DNA binding domain
dsDNA	double strand DNA
EMSA	electro mobility gel shift assay
FEN1	flap endonuclease
G4	G quadraplex
GluC	enodoproteinase GluC
hr.	hours
KAT	lysine acetyltransferase
kDa	kilodaltons
KDAC	lysine deacetylase
mins	minutes
MS	mass spectrometry
nt	nucleotides
OFP	Okazaki fragment processing
PCNA	proliferating cell nuclear antigen
PiNT	Pif1 N terminal domain
PTM	post translational modification
rDNA	ribosomal DNA
RFB	replication fork barrier
RPA	replication protein A
ssDNA	single stranded DNA

ABSTRACT

Accurate DNA replication is vital for maintaining genomic stability. Consequently, the machinery required to drive this process is designed to ensure the meticulous maintenance of information. However, random misincorporation of errors reduce the fidelity of the DNA and lead to pre-mature aging and age-related disorders such as cancer and neurodegenerative diseases. Some of the incorporated errors are the result of the error prone DNA polymerase alpha (Pol α), which initiates synthesis on both the leading and lagging strand. Lagging strand synthesis acquires an increased number of polymerase α tracks because of the number of Okazaki fragments synthesized per round of the cell cycle (~50 million in mammalian cells). The accumulation of these errors invariably reduces the fidelity of the genome. Previous work has shown that these pol α tracks can be removed by two redundant pathways referred to as the short and long flap pathway. The long flap pathway utilizes a complex network of proteins to remove more of the misincorporated nucleotides than the short flap pathway which mediates the removal of shorter flaps. Lysine acetylation has been reported to modulate the function of the nucleases implicated in flap processing. The cleavage activity of the long flap pathway nuclease, Dna2, is stimulated by lysine acetylation while conversely lysine acetylation of the short flap pathway nuclease, FEN1, inhibits its activity. The major protein players implicated during Okazaki fragment processing (OFP) are known, however, the choice of the processing pathway and its regulation by lysine acetylation of its main players is yet unknown. This dissertation identifies three main findings: 1) *Saccharomyces cerevisiae* helicase, petite integration frequency (Pif1) is lysine acetylated by Esa1 and deacetylated by Rpd3 regulating its viability and biochemical properties including helicase, binding and ATPase activity ii) the single stranded DNA binding protein, human replication protein A (RPA) is modified by p300 and this modification stimulates its primary binding function and iii) lysine acetylated human RPA directs OFP towards the long flap pathway even for a subset of short flaps.

CHAPTER 1. INTRODUCTION

1.1 Interplay Between Genome Stability, Cell Cycle and DNA Replication

One contributor to maintaining genome stability is faithful and error free DNA replication (1). In order to duplicate 3 billion nucleotides worth of genetic information of a human genome, the replication machinery ought to be efficient and finely regulated to ensure the following: recruitment of necessary protein players, proper and timely addition of nucleotides and correction of any associated errors. These processes are well coordinated within the context of the cell cycle where two major phases dictate the timing of cellular duplication and segregation events: interphase and mitosis or M phase outlined in figure 1.1 (2). While the M phase is the stage where nuclear division and chromosome segregation occurs, the interphase consists of two rest phases (G1 and G2) and the S phase where DNA replication is allowed to occur only once (3,4).

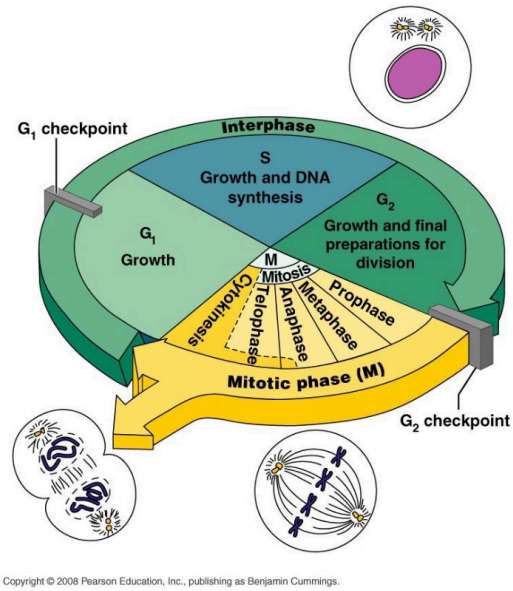

Figure 1.1 Cell cycle phases. Timing of cellular events is separated into interphase where rest phases G1 and G2 flank cell duplication that occurs in the S phase while chromosomal segregation occurs in the mitotic phase [(5)].

The concerted interplay between cell cycle regulation and DNA replication mechanisms necessitate checkpoints at these rest phases that help mitigate deleterious cellular consequences. In mammalian cells, there are two G1 checkpoints; one is referred to as the restriction point while

the other is the G1/S transition which once crossed, commits the cell to duplication in the S phase (6). Crossing this point is favored by the presence of extracellular growth factors though an alternative model suggests that only a fraction of cells enter into this uncommitted phase while others exit mitosis and continue cycling through to the next phase (7). Previous studies have demonstrated that mutations to genes encoding G1 regulatory proteins are responsible for a majority of cancers (8,9). The G2 checkpoint on the other hand ensures that the DNA is completely duplicated before proceeding to mitosis (10). It is also at this checkpoint that replication errors and damages which occur on the recently synthesized strand that are missed by the replication machinery are further repaired. This is important because incorrect genetic information contained within the genome could lead to unfavorable outcomes such as cancers, increased response to genotoxic stress and neurodegenerative disorders downstream (11).

The mechanism of DNA replication was first outlined by Meselson and Stahl who provided evidence that this process occurred semi-conservatively with both strands serving as templates during replication (12). Following this discovery, Okazaki *et al* in 1968 highlighted that replication also occurrs in a semi-discontinuous fashion with one strand synthesizing continuously and the other discontinuously (13). Since then, we refer to the continuously synthesized strand as the leading strand and the strand synthesized discontinuously as the lagging strand, a result of the anti-parallel nature of DNA (14). Over the years, more details about the mechanism of DNA replication have been discovered and the processes have been categorized into three steps: initiation, elongation and termination (15). In eukaryotes, DNA replication is initiated at multiple origins whereas bacteria typically have only one (16,17). Although eukaryotic cells contain multiple origins, not all are fired at the same time, a regulatory mechanism directed by the cell cycle (18). The initiation events start with (i) origin licensing by the inactive pre-replicative complex [origin recognition complex (ORC1-6), Cdt1 and Cdc6] which directs the loading of minichromosome maintenance complex (MCM2-7) helicase during G1-S to the origin to be fired and (ii) origin firing which induces the formation of an active helicase complex consisting of MCM, GINS and Cdc45, collectively referred to as CMG helicase which then unwinds the parent strand allowing for the replisome to be recruited for elongation (19). Following the unwinding of the parental DNA strand, the activities of the replisome bifurcate as replication proceeds to the elongation phase based on the directionality of the leading and lagging strands. Because the focus of my

dissertation is to understand the enzyme mechanism involved in lagging strand synthesis and maturation, these events are highlighted in the subsequent sections.

1.2 Correlation Between Lagging Strand Replication and Nucleosome Assembly

1.2.1 Dynamics of Lagging Strand Replication

Given that replicative polymerases only synthesize in the 5' – 3' direction, the lagging strand inherently poses a challenge to the replicative process as the template DNA mirrors the directionality of the polymerase consequently hindering the daughter strand from being able to be synthesized in the correct orientation (20). Polymerases also have another "rule of action" as defined by Mitra and Kornberg wherein, only one nucleotide is added to the new chain at a time (21). However, due to the fact that polymerases are unable to synthesize *de novo*, the addition of nucleotides must be preceded by an initiating primer (22). Therefore, to circumvent these highlighted predicaments, the cell replicates the lagging strand discontinuously and elongation is initiated by DNA polymerase alpha (Pol α) (13,23,24).

Pol α , the first eukaryotic polymerase to be discovered, is a heterotetrameric protein that catalytically functions both as a primase and a polymerase (25). Its primase function is associated with the p48 subunit in conjunction with its p58 accessory subunit synthesizing approximately 8-10 RNA molecules (26). Following RNA primer extension, there is a switch to its polymerase function which is induced by steric clashes that exist between the length of the RNA primer and the primase causing the p58 subunit to rotate its C terminus and giving way to the p180 subunit (27,28). The p180 subunit primarily catalyzes the polymerase reaction, but it does so in tandem with p70 synthesizing about 20-30 nucleotides of DNA (27). Similar to other B family polymerases, Pol α has an exonuclease catalytic domain (29). However, it is often referred to as an error prone polymerase because this domain while present, is inactive permitting errors associated with misincorporated nucleotides and ribonucleotides (20). Previous work has shown that Pol α creates mutational hotspots during lagging strand replication as 1.5% of the mature genome is comprised of DNA synthesized by this error prone polymerase (30,31).

Once the RNA-DNA initiating primer has been synthesized, Pol α is displaced by the action of replication factor C (RFC), the clamp loader which binds to the nascent strand at the 3'OH position and loads proliferating cell nuclear antigen (PCNA) onto it, a process to which the

single stranded DNA binding protein (SSDBP), replication protein A (RPA) is recruited (32-34). The concerted activities of these proteins promote polymerase switching from Pol α to the lagging strand polymerase, polymerase delta (Pol δ) (35,36). This polymerase requires the binding of PCNA to processively extend about 100-200 nucleotides of DNA at each primer tract (37-39). These short segments of replicated DNA are termed Okazaki fragments (OFs) and in a bid to form a fully functional DNA strand, must be processed (40). Processing ensures that the initiating RNA-DNA primer is removed so as to prevent possible mutagenicity. Additionally, it ensures that these short segments are ligated in a DNA-DNA fashion as the presence of RNA within this duplex will give rise to instability, as a result of the fact that RNA contains a highly reactive 2' OH group that can react with the aqueous environment causing shortened templates (41).

In an attempt to rid the cell of an accumulation of RNA, the lagging strand polymerase, Pol δ not only possesses synthesis activities, but also exhibits strand displacement functions when in close proximity to downstream OFs as shown in figure 1.2 (42). Work by Maga *et al* shows that as the polymerase synthesizes the upstream OF, in conjunction with PCNA and RPA, its processivity is amplified, displacing the downstream OF into a flap whose size is limited by the presence of the SSDBP (37). Due to the complementarity of the displaced flap and the newly synthesized upstream OF to the template, there is an equilibration into a structure known as a double flap (43). There are two proposed pathways for processing this flapped intermediate and they have been delineated as the short flap and long flap pathway (40,44). In the short flap pathway, which is believed to be the predominant method by which OFs are processed, a structure specific protein, flap endonuclease 1 (FEN1) physically interacts with the clamp PCNA.

This interaction stimulates the activity of FEN1 by 10-fold allowing it bind to the newly equilibrated, short double flap substrate (45,46). Upon binding, FEN1 threads through to the base of the flap, bending it at a 100° angle, a possibility that can only exist when the dsDNA contains a break or a flap and cleaves creating a nick (47). This process is referred to as nick translation and it is through the constant repetition of this process that the RNA-DNA initiator primer is removed (48). Finally, once DNA-DNA ends are revealed, the resulting nick can then be sensed and sealed by DNA Ligase I or its *S. cerevisiae* homolog Cdc9 which also tethers onto PCNA (49-51).

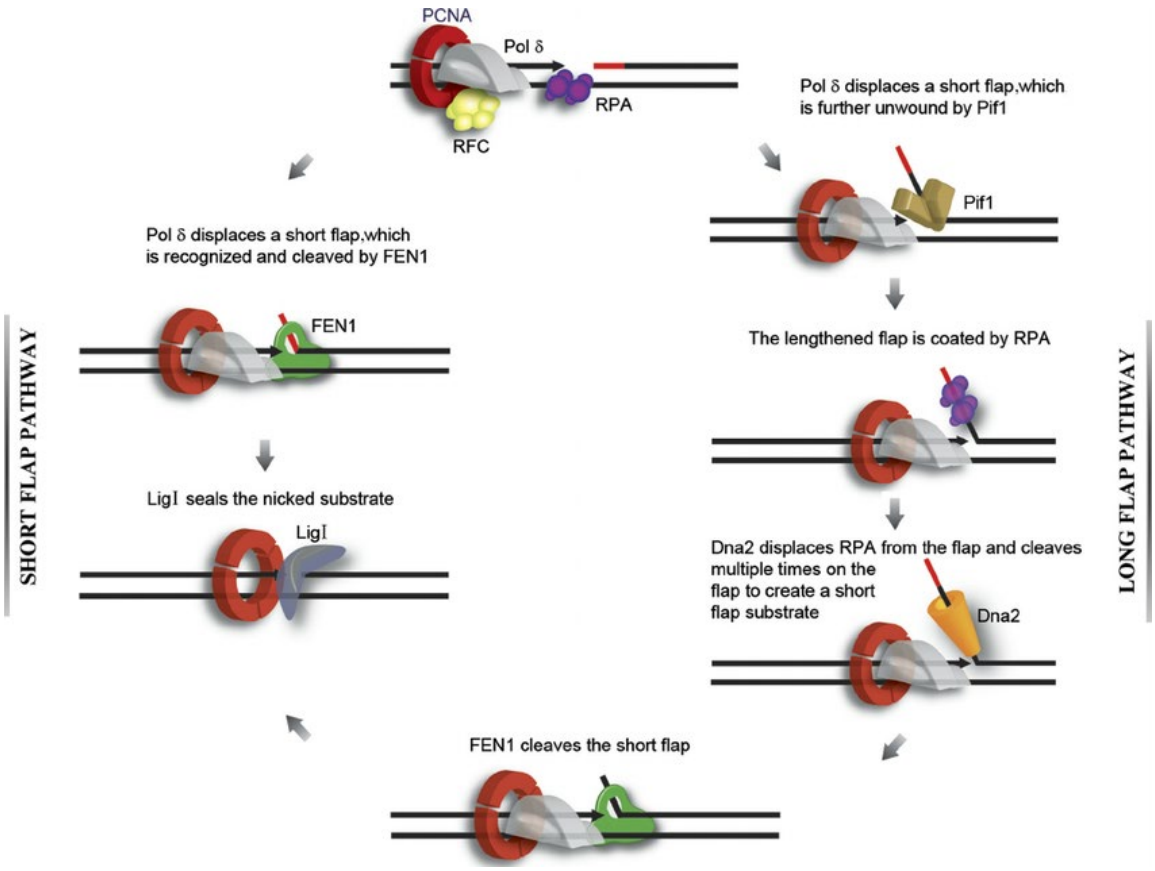

Figure 1.2 Elongation phase of lagging strand DNA synthesis. Okazaki fragment processing pathways outlining the short and long flap pathway proteins [1].

While most OFs are processed via the short flap pathway, studies have shown that an alternative route exists for flap processing (52). This pathway has been termed the long flap pathway and is utilized when short flaps become lengthened due to a variety of reasons (49,52). One such scenario where this could occur is when FEN1 is disengaged from the replisome as a result of possible post translational modifications (PTMs) or stimulated strand displacement activity of Pol δ (53,54). Another instance where the long flap pathway is activated is in the presence of a helicase, petite integration frequency (Pif1) (55). This 5' – 3' helicase has been demonstrated to precede the lagging strand polymerase unwinding the downstream OF and creating a lengthened flap as a result (56). As flap length increases, RPA binds with high affinity preventing the formation of fold back structures and preventing the DNA from inappropriate degradation by cellular nucleases which has a catastrophic impact on genomic stability (57). The

binding of RPA to these flaps is refractory to FEN1 cleavage and necessitates the presence of another nuclease, Dna2 (58). Dna2 serves as both a nuclease and helicase which displaces RPA and sequentially cleaves the flap substrate multiple times leaving a 5-6nt terminal product, a fundamental difference in its catalytic activity when compared to FEN1 (59). At this point, FEN1 is able to cleave the shortened flap and Lig I can seal the nick created.

The presence of both of these pathways highlight that the cell has regulatory mechanisms in place wherein it engages one pathway over the other. Ultimately, the choice of OFP should promote the highest level of replication fidelity, especially as there are about 50 million OFs that are synthesized and ligated on the lagging strand during one round of the mammalian cell cycle (60). It is therefore imperative that the cell invests into redundant proteins and pathways that aid in the removal of RNA-DNA primers synthesized by Pol α which initiates thousands of OFs as incorporation of any errors during this process present the cell with dire consequences.

1.2.2 Nucleosome Assembly

In 2012, work by Smith and Whitehouse showed that Okazaki fragment processing (OFP) is closely associated with nascent nucleosome deposition (61). This work provided insight into the correlation between DNA replication processes and the components of nucleosomal assembly. It revealed that OFs are ligated at nucleosomal dyads and this relationship serves as a form of regulation for both the length of OFs and determining the position of nucleosome deposition as one could alter both properties by changing components of either process (61). Other work has also demonstrated the importance of these interactions as depletion of the histone chaperones, chromatin assembly factor 1 (CAF-1) and anti-silencing function 1 (Asf1) slow down the rate of DNA replication (62). The results of these studies, came as no surprise given that DNA is compacted around histones to form chromatin as identified by Walther Flemming (63). The nucleosome is a functional unit of chromatin containing a histone octamer and 146 bp of DNA (64). The histone octamer consists of two copies of histone H2A, H2B, H3 and H4 and during nascent nucleosome assembly, CAF-1 mediates the formation and transfer of a histone H3 and H4 tetramer to the nucleus (65). CAF-1 is further recruited to the replication fork by PCNA the homotoroidal clamp, allowing the deposition of this H3-H4 nucleosome precursor (66). Following this, H2A-H2B quickly associate forming a mature nucleosome (67). These core histone proteins each contain a lysine rich tail and a globular domain impacting its overall charge (68). The final

histone to be added is histone H1 which is believed to be necessary for exit out of S phase. As with DNA replication, histones are exclusively expressed during the S phase of the cell cycle demonstrating the consistent interplay and regulation of both processes (69-71).

When considering nucleosome assembly and its components, it is imperative to visualize them within the context of how they exist in the cell and understand the underlying principles guiding their mechanism of actions. The compaction of DNA around histones is defined by (i) the attraction that occurs due to the interaction between negatively charged DNA and positively charged lysine rich histones and (ii) the need to fit the entire genome into a 2-10μm cellular compartment called the nucleus (72). This tight packaging which serves as medium of protection for the naked DNA, also precludes it from being accessible to other cellular components that might need to interact with it for different cellular events. Therefore, to navigate this functional hindrance, certain levels of regulation have been implemented to provide access to the DNA for key biological processes. One major form of regulation that has been widely studied is the post translational modification (PTM) of histones (72).

PTMs are classified as modulations arising from the reversible and irreversible addition or deletion of chemical moieties to amino acids, the addition of covalent crosslinks to multiple protein domains and the proteolytic processing of certain regions of a protein (73). Functionally, PTMs extend a protein's diversity by impacting its cellular localization, as well as promoting changes to its structure, catalytic activity and interactions with other proteins and cellular co-factors (74). It is on this basis that PTMs act as a form of regulation of not only histone – histone interactions, but also histone – DNA interactions as some of these PTMs inherently affect the net charge of the histones. The first identification of a histone modification was made in 1964 and since then, over 30 different modifications have been observed (75,76). These histone modifications including methylation, ubiquitination, acetylation, ADP ribosylation and more recently SUMOylation have shown that nucleosome structure and stability can be greatly impacted such that the nucleosomes exist in either a fully wrapped or less wrapped state controlling access to the DNA (75,77).

1.3 Lysine Acetylation as a Reversible Post Translational Modification of Histone Proteins

Histone tails are one of the points of modification for several PTMs. One such PTM that has been widely studied and modifies these lysine rich tails is lysine acetylation, which was first described over 50 years ago by Vincent Allfrey (78). Lysine acetylation is a reversible chemical

modification wherein an acetyl moiety is transferred from acetyl-CoA to the ε - amino group of a lysine residue as shown in figure 1.3 (79,80). Conserved across prokaryotes to eukaryotes, this modification serves two functions on histones: (i) it neutralizes the positive charge of the lysine residues limiting its affinity for the negatively charged DNA and (ii) it recruits necessary transcription factors containing acetyl lysine motifs/bromodomains (64,81). By disrupting the overall net charge of histones, lysine acetylation promotes the decondensation / unwrapping of nucleosomes providing access to the DNA for replication and other downstream cellular events (80). The reverse reaction termed deacetylation promotes condensation or the tight packing of nucleosomes into heterochromatin (82). Although this modification could be non-enzymatic as is the case in the mitochondria where there are high levels of acetyl-CoA, more often than not, the reversible reaction is mediated by two groups of enzymes lysine acetyl transferases (KATs) that are termed "writers" and lysine deacetylases (KDACs) often referred to as "erasers" (64). The tight regulation of both enzymes mediates gene activation and repression respectively (83,84). Previously, the terms used to describe these group of enzymes were histone acetyl transferases (HATs) and histone deacetylases (HDACs) until it was identified that they could modify non-histone proteins as well (85).

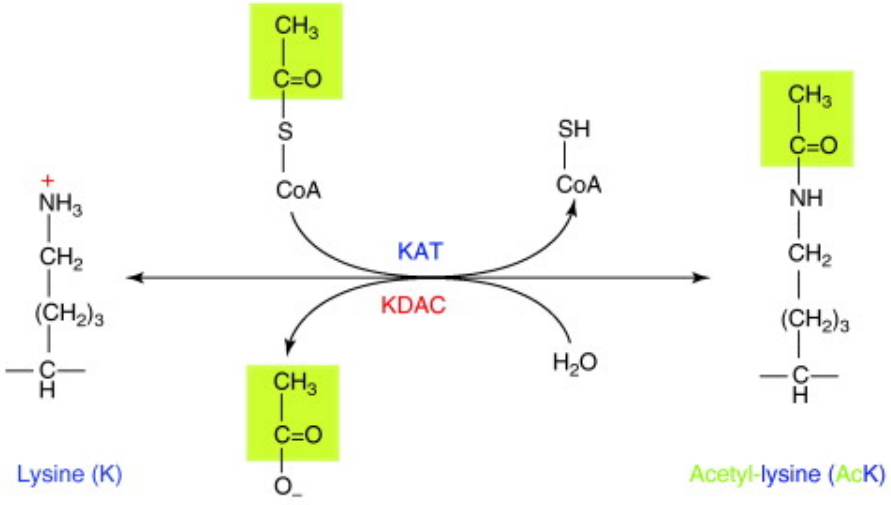

Figure 1.3 Lysine acetylation as a post translational modification. Reversible acetylation and deacetylation reaction of a lysine residue mediated by KATs and KDACs respectively [86].

1.3.1 Regulators of Lysine Acetylation: KATs and KDACs

KATs

There are two types of KATs that promote the addition of an acetyl moiety to lysine residues and they are classified on the basis of their substrate specificity and localization: nuclear or type-A and cytoplasmic or type-B KATs (83). Type-A KATs are responsible for mediating the acetylation of free histones in chromatin while the type-B KATs acetylate nascent histones aiding in their localization and deposition to the replication fork for nucleosomal assembly (84). Over 21 KATs have been identified in humans and about 10 in *S .cerevisiae* (80,87). In addition to categorizing KATs on the basis of subcellular localization, type-A HATs can also be grouped into 3 different families on the basis of their mode of action and sequence homology across species: (i) GCN5 related N-acetyl transferases (GNATs), (ii) the MOZ, Ybf2, Sas2 and Tip60 family of acetyl transferases (MYST) and (iii) p300/CREB binding protein acetyl transferases (p300/CBP) (88). All three families of KATs possess a similar acetyl-CoA binding motif Q/RxxGxG/A although the mechanism of acetylation differs as detailed below (80,89).

GCN5 related N-Acetyltransferases (GNAT)

Contained within this family of acetyltransferases is Gcn5, it the prototypical member. In *S. cerevisiae*, Gcn5 exists within a multiprotein complex referred to as the SAGA complex consisting of Spt, Ada2, Gcn5 and Ada3 (90). It catalyzes the acetylation of both histone H3 and H4 with preference given to H3 when in the complex (91). Previous work demonstrates that in the absence of Gcn5, cells accumulate in the G2/M phase and are more sensitive to DNA damage highlighting that this KAT is necessary for cell cycle progression (92). Furthermore, work by Burgess *et al* revealed that Gcn5 is required for CAF-1 mediated replication coupled nucleosome assembly (93). Other proteins in this family are the human Gcn5 homolog, KAT2A and PCAF (KAT2B) (94). In this family, the process of lysine acetylation proceeds sequentially in three steps: deprotonation of the ε amine group of the lysine to be acetylated by a glutamine residue in the KAT's active site (Glu80) followed by a transient intermediate structure formed between the protein's lysine residue and the bound acetyl-CoA which promptly releases Co-ASH leaving a final lysine acetylated product as shown in Figure 1.4 (68).

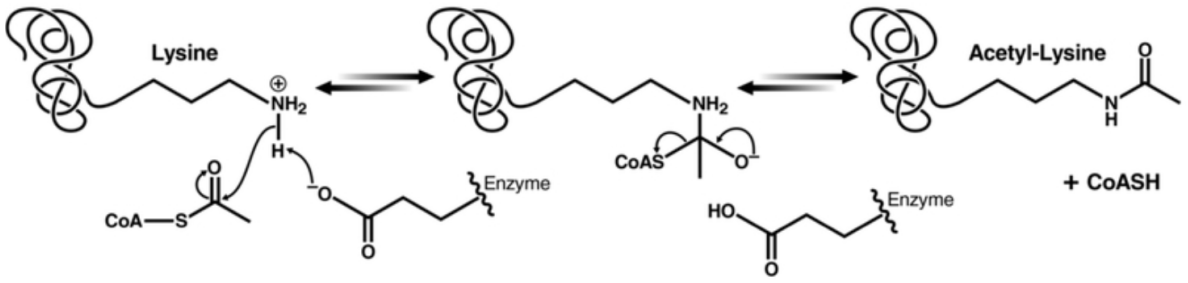

Figure 1.4 GNAT and MYST family mechanism of action. Formation of deprotonated intermediate before the release of Co-ASH to form an acetylated lysine product [80]. "Reprinted (adapted) with permission from (Ibrahim et al, 2018). Copyright (2020) American Chemical Society."

P300/CREB Binding Protein Acetyltransferases (p300/CBP)

In this family of KATs, p300, CBP and Rtt109 are all members. The first member of this family to be identified was p300 and it was discovered a little under 40 years ago where it was observed to function as a transcriptional activator associated with the E1 A protein (95). A few years later, CBP was discovered to have high homology with p300 and was grouped in the same category. They were later observed to function as KATs that could mediate the transfer of acetyl groups to histone and non-histone proteins alike (96,97). The yeast homolog of these human proteins is Rtt109 and although structurally similar, functions slightly differently from the other two (98).

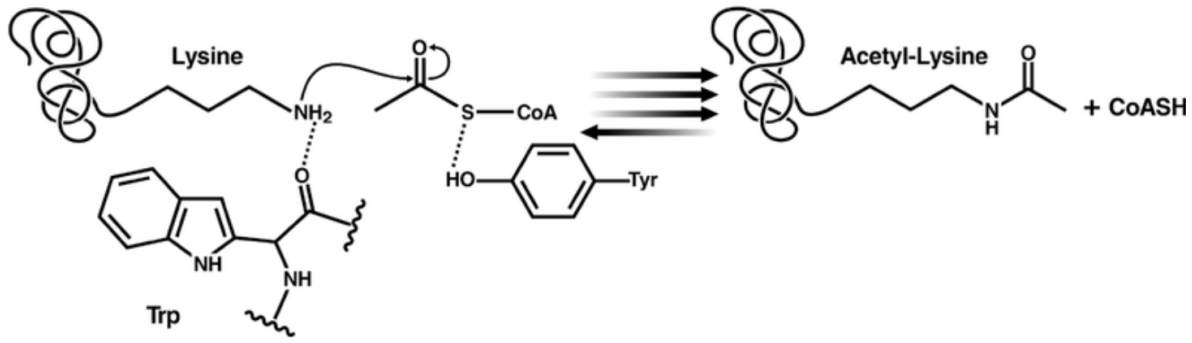

Figure 1.5 p300/CBP "Hit and Run" mechanism of action. Rapid release of Co-ASH and acetyl lysine product [80]. "Reprinted (adapted) with permission from (Ibrahim et al, 2018). Copyright (2020) American Chemical Society."

Unlike the other KAT families, their mechanism of action is referred to as a "hit and run" or Theorell-Chance transfer mechanism. Here, the transfer is rapid and mediated by aromatic residues lying within the shallow catalytic pocket of the protein that direct the lysine residue for nucleophilic attack by the acetyl CoA (99). The tyrosine residue then protonates the sulfhydryl group of CoA releasing it as depicted in Figure 1.5 (80).

MYST Acetyltransferases

This family of acetyltransferases was named according to its founding members: MOZ, Ybf2, Sas2 and Tip60 (100). They contain a conserved MYST domain among species that is made up of a zinc finger domain and an acetyl-CoA binding motif (101). Similar to GNATs, they also exist in multiple protein complexes. For example, the yeast Esa1 protein, a Tip60 homolog functions with nucleosome acetyltransferase of histone H4 (NuA4) complex (102). This protein is necessary for cell cycle progression as a deletion of its gene is embryonically lethally (103). It also has been detected to acetylate H4 histone tails (104). Mechanistically, MYST family of KATs require deprotonation by a glutamine residue as highlighted in Figure 1.4 though it was previously thought that this reaction was mediated by cysteines (105).

KDACs

The deacetylation reaction is mediated by KDACs, which have been categorized into two groups based on their dependency on Zn^{2+} or NAD^{+} cofactors (106). The classical family of deacetylases is Zn^{2+} dependent and consists of three classes of KDACs: Class I, II and IV while the NAD-dependent KDACs describe class III/sirtuins (107). The first reference to deacetylation was made in 1977 by Riggs et al who discovered that n-butyrate causes histone modifications in HeLa cells (108). Subsequently, various enzymes that were able to remove acetyl and other acyl groups from lysine resides were discovered. Similar to KATs, although these enzymes mediate the removal of acetyl groups, they do so in unique ways. Class I, II and IV KDACs act similarly in that three amino acids stabilize the acetyl-lysine in the protein's catalytic site and the Zn2+ cofactor polarizes the C-O group making the carbonyl carbon more electrophilic as indicated in Figure 1.6A. This carbon is then nucleophilically attacked by water molecules as activated by a histidine residue. Finally, a tyrosine reside on the KDAC stabilizes the transition state as the acetyl group is removed

from the lysine residue (109). Sirtuins on the other hand deacetylate by binding the acetyl-lysine within its active site, a necessary step for nicotinamide hydrolysis. This hydrolytic reaction gives rise to an *O*- alkylamidate intermediate wherein the acetyl group on the 1' carbon is attacked as outlined in Figure 1.6B (110). The cyclic intermediate formed is further attacked by a water molecule resulting in a deacetylated lysine and a 2'- acetyl-ADP-ribose (111).

Class I KDACs

This group contains human KDAC 1, 2, 3 and 8 and their yeast homolog, Rpd3 (112). Similar to KATs, these KDACs also exist within a complex like Rpd3 which belongs to the nucleosome remodeling and deacetylase complex (NuRD) (113). In mammalian cells, the NuRD complex consists of both KDAC1 and 2 which share ~85% sequence identity (114). KDAC1 and 2 also form complexes with Sin3 and Co-REST (115). Though expressed in all tissues, they are localized to the nucleus where they function (116). In mice, inhibition of KDAC1 leads to cell cycle arrest as a result of the increased expression of p21, a cyclin dependent kinase (CDK) inhibitor (117). Deletion of KDAC2 although not embryonically lethal leads to heart defects (118). KDAC3 has only ~34% sequence identity with KDAC8 making it the most related class I KDAC (119). Knockout of this deacetylase in mice are embryonically lethal while a deletion of KDAC8 leads to cranial defects (120).

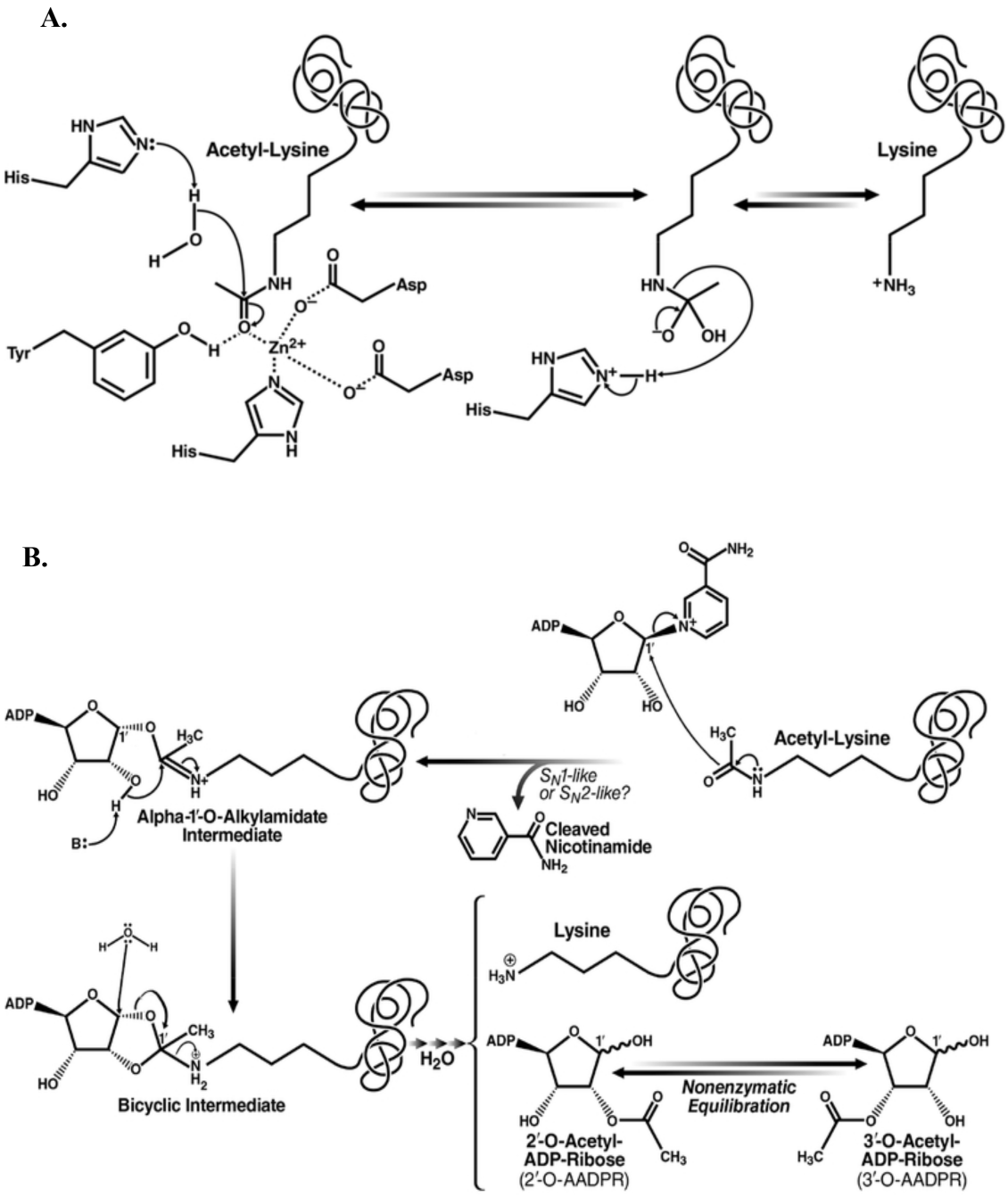

Figure 1.6 Mechanism of action of KDACs. A) Class I, II and IV KDACs require Zn^{2+} cofactor and water molecules for deacetylation reaction B) Sirtuins formation of an *O*-alkylamidate intermediate [80]. "Reprinted (adapted) with permission from (Ibrahim et al, 2018). Copyright (2020) American Chemical Society."

Class II KDACs

This class is further subdivided into 2 groups: Class IIa and IIb and contained within each class are KDAC 4, 5, 7, 9 and KDAC 6 and 10 respectively. This class shuttles between both the nucleus and the cytoplasm depending on certain cellular modifications and localization signals such as phosphorylation (121,122). In yeast, class II KDACS are fore mostly represented by Hda1 which was discovered in 1996 by Carmen *et al* and over the years has been outlined to function in complex with Hda2 and Hda3 (123,124). Class IIa enzymes share a highly conserved C-terminal catalytic domain (125). They are expressed in specific tissues such as the heart and brain making them markedly different from class I KDACs which are ubiquitously expressed (126,127). In mice, a knockout of some of these KDACs results in cardiac defects and excessive bone formation highlighting their importance in specific tissues (128,129). In mammalian cells, class IIb enzymes are mostly cytoplasmic and are represented by double deacetylase domains (130). Interestingly, KDAC 10 has been discovered to be a poor lysine deacetylase, but a strong polyamine deacetylase showing that these KDACs are not limited to one modification (131). Knockout of this class in mice yields no observable phenotype (132).

Class III KDACs/Sirtuins

In the 1990's the first member of this family, silent information regulator (Sir2) was identified in yeast (133). Upregulation of Sir2 seemed to extend the cell's lifespan in an NAD^+ dependent manner highlighting its impact in regulating transcriptional silencing (134,135). NAD^+ has always been viewed in terms of catalyzing reduction-oxidation reactions in the cell, but in the last decade, its role in acting as a substrate for deacetylation activities has garnered much interest (136). In mammalian cells, there are seven sirtuins (SIRT1-7) belonging to four different classes based on the homology of their sequences: SIRT1-3 are class I sirtuins while SIRT 4, SIRT5 and SIRT 6-7 belong to class II, III and IV respectively (137). SIRT1 and 7 are localized to the nucleus though SIRT 1 can be shuttled to the cytoplasm where SIRT 2 also localizes (138-140). SIRT 3-5 all contain a mitochondrial localization sequence while SIRT 7 is localized to the nucleolus (141-144).

Class IV KDACs

There is only one KDAC in this class and that is KDAC 11 which is the most recently discovered deacetylase (145). It appears to be most closely related to Class I HDACs but serves unique functions. It primarily localizes to the nucleus and as of yet has not been shown to deacetylate any histone, though its activity on non-histone proteins has been detected (146). In addition, KDAC11 has been shown to remove long-chain acyl groups from lysine resides other than acetyl moieties (147)

1.4 Lysine Acetylation as a Modifier of Non-Histone Proteins

While this modification has been attributed to the regulation of histone proteins for over a century, it has now been shown that it is not limited to just one subset of proteins. It is important to note that while most proteins (80-90%) are N-terminally acetylated, internal lysine acetylation serves a different function (148). Choudhary and colleagues have been at the forefront of using proteomic techniques to detect novel proteins that are modulated by lysine acetylation (149). An outline of some of the functional roles lysine acetylation plays in numerous pathways mediated by its non-histone targets is provided below.

1.4.1 Transcription Activation

The first non-histone protein to be identified as being able to undergo acetylation was p53, a transcription co-activator (150). Lysine acetylation of p53 by TIP60/MOF (K120) and p300 (K164 and C-terminus) activates the protein by abolishing its binding with p21 and Mdm2, a repressor that prevents p53 responsive genes from being activated and ultimately cell arrest (151). Because p53 needs to be tightly regulated within the cell, Md2 recruits KDAC1 or SIRT1 to deacetylate p53 (152). Additionally, acetylation of Mdm2 by p300 promotes its interaction with the deubiquitinase USP7 and ultimately, p53 ubiquitination (153). Another transcription factor that is impacted by lysine acetylation is NF-κB whose two subunits (p65 and p50) are acetylated altering transcription activation (154).

1.4.2 Cytoskeletal Stability

All isoforms of actin have been reported to be acetylated and this modification enhances their stability which is important as they inform cell shape and motility (155). Additionally, other regulatory proteins that are involved with the cytoskeleton are also acetylated such as cofilin and contarctin which are modulated by p300 and deacetylated by KDAC6 resulting in regulated cell motility (156). Other microtubules modified by this PTM include both α and β-tubulin which when acetylated downregulates tubulin polymerization (157).

1.4.3 Protein Aggregation

Aggregation is a hallmark of a myriad of neurological disorders including Alzheimer's disease where in tau protein aggregation is defined as an early marker of the disease (158,159). Ordinarily, tau proteins mediate microtubule assembly and contribute to neuronal morphology (160). However, previous work has revealed that tau proteins can be modified by p300 and CBP and this modification leads to an inhibition of its cellular degradation thereby accumulating these proteins (161). Conversely, in mice, inhibition of p300 ameliorates the effect of tau induced memory deficit and hippocampal atrophy highlighting that the tight regulation of tau proteins by lysine acetylation has dire neurological consequences (162).

1.4.4 Cellular localization

In addition to cellular localization signals attached to proteins, lysine acetylation has been shown to aid in shuttling proteins from one cellular location to another or affecting the ability of proteins to localize to certain areas. Lysine acetylation of the RECQL4 helicase interrupts its engagement with nuclear import factors thereby preventing its transport and causing it to accumulate in the cytoplasm (163). Additionally, nuclear import proteins are also regulated by lysine acetylation themselves such as importin-α1 which when acetylated by p300/CBP aids in its association with importin-β (164).

1.4.5 DNA Replication

The replicative process requires intricate regulation to ensure that genome stability is maintained. Coupled with PTMs like phosphorylation that regulate the cell cycle and time when this process occurs, lysine acetylation has been revealed to be another method of fine-tuning replication to ensure high fidelity processing (165). Glozak *et al* discovered that the licensing factor Cdt1 is modified by KAT2A and KAT2B, offering it protection from being degraded by ubiquitination (166). Interestingly, at least three of the proteins implicated during lagging strand replication have been identified to be regulated by this PTM. FEN1, the short flap endonuclease is lysine acetylated by p300 and this inhibits its binding and cleavage properties (53). Conversely, its functional interacting partner in the long flap pathway, Dna2 shows improved DNA binding and cleavage when acetylated by p300 (167).

Given the proximity and interaction between histone deposition and lagging strand replication, it is no surprise that these OFP proteins are acetylated. It is on the basis of these observations that this study was founded. We sought to elucidate if other lagging strand proteins specifically Pif1 and RPA could be acetylated. Furthermore, we probed the cellular contexts wherein this modification was activated on the proteins and finally, detailed the impact of lysine acetylation on their biochemical properties. This study reveals that though the process of DNA replication is already optimized to perform high fidelity synthesis, its mechanisms can be further fine-tuned by lysine acetylation to promote higher fidelity processing via the long flap pathway. This decision to process Okazaki fragments in this manner ensures that the majority of misincorporated errors are removed resulting in improved genome stability.

CHAPTER 2. NUCLEAR PIF1 IS POST TRANSLATIONALLY MODIFIED AND REGULATED BY LYSINE ACETYLATION

Chapter 2 along with Appendix A were originally published in Journal of Biological Chemistry. Ononye, O. E., Sausen, C. W., Balakrishnan, L., and Bochman, M. L. (2020) Lysine Acetylation Regulates the Activity of Nuclear Pif1. *J Biol Chem*

2.1 Abstract

In *S. cerevisiae*, the Pif1 helicase functions to impact both nuclear and mitochondrial DNA replication and repair processes. Pif1 is a 5'-3' helicase, which preferentially unwinds RNA-DNA hybrids and resolves G-quadruplex structures. Here, we report lysine acetylation of nuclear Pif1, which influences both its cellular and core biochemical activities. Using Pif1 overexpression toxicity assays, we determined that the acetyltransferase NuA4 and deacetylase Rpd3 are primarily responsible for dynamically acetylating nuclear Pif1. Mass spectrometry analysis revealed that Pif1 was modified throughout the protein's sequence on the N-terminus (K118, K129), helicase domain (K525, K639, K725), and C-terminus (K800). Acetylation of Pif1 exacerbated its overexpression toxicity phenotype, which was alleviated upon deletion of its N-terminus. Biochemical assays demonstrated that acetylation of Pif1 stimulated its helicase activity, while maintaining its substrate preferences. Additionally, both the ATPase and DNA binding activities of Pif1 were stimulated upon acetylation. Limited proteolysis assays indicate that acetylation of Pif1 induces a conformational change that may account for its altered enzymatic properties. We propose an acetylation-based model for the regulation of Pif1 activities, addressing how this post translational modification can influence its role as a key player in a multitude of DNA transactions vital to the maintenance of genome integrity.

2.2 Introduction

At the core of all cellular transactions, such as replication, repair, and transcription, is the need for biological machines to gain access to the genetic information stored within the DNA duplex (168). Along with chromatin remodeling, access to the DNA is provided through either the active or passive action of helicases, which function to unwind double-stranded DNA (dsDNA) into its complementary single strands. Approximately 1% of the genes in eukaryotic genomes code for helicases, and to date, over 100 RNA and DNA helicases have been discovered (169,170). These motor proteins function by coupling ATP hydrolysis to mechanical movement to break the hydrogen bonds between complementary base pairs in dsDNA (169). One such DNA helicase, Pif1, was first identified in a screen for genes that influence the frequency of mitochondrial DNA recombination in *Saccharomyces cerevisiae* (171). Since its initial discovery, Pif1 has been characterized as a member of the Superfamily 1B group of helicases, which translocate along single-stranded DNA (ssDNA) in the 5' to 3' direction (172). Unlike some members in this superfamily, Pif1 only binds to DNA, but preferentially unwinds RNA-DNA forked duplexes and structured regions such as G-quadruplexes (G4s) and R-loops (170,173-177).

Following its initial discovery in yeast mitochondria over 20 year ago, Pif1 has been shown to also localize to the nucleus, where it participates in a myriad of DNA transactions. It functions in Okazaki fragment maturation, wherein it lengthens the flap ahead of DNA polymerase δ, allowing RPA to bind to the displaced flap (56). Recently, it was determined that the rate of replication on lagging strands containing G4s is delayed in the absence of Pif1, underscoring the need for Pif1 to unwind regions that are difficult to replicate due to the presence of DNA secondary structures (178). Pif1 also stimulates the activity of polymerase δ during break-induced replication through bubble migration (179). Furthermore, prior to mitosis, Pif1 helps to resolve R-loops and aid in protein displacement from tDNA (tRNA genes) (175), while within the ribosomal DNA (rDNA), it is required for maintaining arrest at the replication fork barrier (RFB) (180). Additionally, Pif1 acts as a negative regulator of telomerase, both at telomeric ends and sites of double-strand breaks (DSBs) where it prevents telomere addition, allowing for the recruitment of DSB repair factors (181-184). Given Pif1's involvement in a plethora of cellular activities, it still remains a mystery how its numerous activities are regulated.

Structurally, Pif1 is divided into three domains: N-terminus, helicase core, and C-terminus. A wealth of research has improved our understanding of the structural motifs and related functions

of the helicase domain, but in comparison, little is known about the N- and C-terminal domains of Pif1. Currently, these regions are postulated to be modular accessory domains that may serve as regulatory regions (176,185,186). We hypothesize that the functional significance of these domains may help to maintain specific folds that are necessary for protein function and establish points for post translational modifications (PTMs) (187). Protein PTMs serve to expand a protein's functional toolbox by altering cellular localization and impacting protein structure, function, and availability while mediating novel interactions with other proteins or nucleic acids (188). Acetylation of the ε-amino group on a lysine residue is one such PTM that has been studied in the context of modulating chromatin architecture for many decades (189-191). However, many non-histone proteins are also modified by acetylation, including replication/repair-associated helicases such as Dna2 (167), BLM (192), and WRN (193).

In addition to reports of acetylation of multiple helicases, many functional interacting partners of Pif1 in the Okazaki fragment maturation pathway, namely, Dna2 (167), FEN1 (194), PCNA (195), and RPA (196,197) are also modified by lysine acetylation. Since the sequence coding for Pif1 is fairly rich in lysine residues (~10% of the whole sequence), an amino acid that serves as a good target for many PTMs, we were interested in investigating the acetylation dynamics of Pif1. In the current study, we aimed to specifically explore the lysine acetylation status of Pif1, identify the enzymes that dynamically mediate this modification, and elucidate the impact of acetylation on the protein's cellular functions and alterations to its biochemical activities. Using Pif1-FLAG overexpression constructs, we compared cellular toxicity in wild-type and acetyltransferase or deacetylase mutant strains. Based on the growth phenotypes, we determined that the acetyltransferase (KAT), NuA4 (Esa1), and its counteracting deacetylase (KDAC), Rpd3, are responsible for regulating Pif1 overexpression toxicity *in vivo*. The Pif1 N-terminal domain (PiNt) was critical for this toxicity regulation, as N-terminally truncated Pif1 (Pif1ΔN) did not behave in the same manner as the full-length Pif1. Additionally, using *in vitro* Piccolo NuA4 (Esa1)-acetylated recombinant protein, we evaluated the impact of this modification on Pif1's biochemical functions - DNA unwinding, G4 resolvase activity, DNA binding, and ATPase activity - and observed a stimulation in all four activities in the acetylated form when compared to the unmodified form of the protein. The results of our cellular assays and *in vitro* studies indicate that lysine acetylation serves as an important regulator of Pif1 activity within the cell.

2.3 Results

2.3.1 Cellular Acetylation Status Modulates Pif1 Overexpression Toxicity *In Vivo*

Acetylation dynamics within the cell are tightly regulated by KATs and counteracting KDACs (198). These lysine modifiers regulate both histone and non-histone proteins, thereby impacting biochemical activities and cellular processes (199). Because the lysine-rich sequence of Pif1 makes it a target for modification by acetylation, we were interested in defining the effect of this modification on the functional activities of Pif1 within the cell. To understand the impact of global cellular acetylation on the function of Pif1, we initially sought to alter the acetylation dynamics in the cell by creating either KAT or KDAC mutant strains. It has previously been reported that the overexpression of Pif1 in *S. cerevisiae* is toxic to cell growth (200-202). Therefore, we used this overexpression toxicity phenomenon to develop a phenotypic assay to determine the impact of cellular acetylation. Our hypothesis was that altering the cellular levels of acetylation may influence Pif1 interactions with other proteins and/or its own function, thereby altering the overexpression toxicity phenotype. A galactose-inducible overexpression plasmid was used to overexpress Pif1 in wild-type, acetyltransferase mutant, and deacetylase deletion mutant cells. However, the growth kinetics (*i.e.*, length of lag phase, doubling rate, and terminal cell density) of *S. cerevisiae* cells are affected by multiple variables in a somewhat stochastic manner (203). Thus, it can be difficult to compare growth curves between independent experiments using the same strain, let alone comparing strains with multiple genetic backgrounds.

To overcome these limitations of cell growth analyses, we developed a data analysis method to specifically focus on the effect of Pif1 overexpression regardless of strain background. First, cell growth was monitored by measuring the optical density of liquid cultures at 660 nm (OD_{660}) over 48 FEN1, and the mean OD_{660} for each strain was calculated. Then, to determine the effect of Pif1 overexpression on growth, the mean OD_{660} of cells grown in galactose-containing medium was divided by the mean OD_{660} of the same strain grown in glucose-containing medium, which strongly represses the *GAL1/10* promoter. Finally, this galactose/glucose ratio for each Pif1-overexpressing strain was normalized to the same ratio from an empty vector control. The normalized growth value for each genotype is interpreted as the toxic effect of Pif1 overexpression in that specific genetic background. The results of these experiments are shown in Figure 2.1. Here, we recapitulated the toxicity of Pif1 overexpression reported by others (200-202), finding an

approximately 50-60% reduction in wild-type growth upon overexpression of the helicase (Figure 2.1A).

To determine if acetylation of Pif1 had an effect on overexpression toxicity, we performed similar experiments in KAT mutant cells. Acetyltransferases representative from the Gcn5-related N-acetyltransferase (GNAT) family, the MYST family, and p300/CBP family were chosen for our studies (204). The genes encoding the Gcn5 (GNAT) and Rtt109 (p300/CBP) KATs are non-essential and can be cleanly deleted, but the catalytic subunit Esa1 of the NuA4 complex (MYST) is essential (205,206), so the temperature-sensitive *esa1-414* allele (207) was used. This allele has reduced KAT activity at 30°C but full activity at 25°C. Pif1 overexpression in the *esa1-414* background caused significantly ($p < 0.001$) reduced toxicity compared to wild-type when grown at the restrictive temperature (30°C) but not at the permissive temperature (25°C) (Figure 2.1B). No such effect was observed upon Pif1 overexpression in the *gcn5Δ* and *rtt109Δ* backgrounds, suggesting that NuA4 (Esa1) acetylates Pif1 *in vivo* and that acetylation is connected to Pif1 overexpression toxicity.

To address this hypothesis further, the effects of Pif1 overexpression were assessed in a set of *S. cerevisiae* strains each lacking a single KDAC (Figure 2.1C). If hypo-acetylation resulted in better growth upon Pif1 overexpression in the *esa1-414* cells, then hyper-acetylation in one or more KDAC-null backgrounds should exacerbate the toxicity. Indeed, we observed significant ($p < 0.001$) increases in Pif1 overexpression toxicity in cells lacking either the KDAC, Rpd3 or Hda2 (Figure 2.1C). Unfortunately, we could not test for synergistic Pif1 toxicity in a double *rpd3Δ hda2Δ* mutant strain because that combination of KDAC deletions is synthetically lethal (*data not shown*). These results indicate that hyperacetylation of Pif1 in cells lacking Rpd3 or Hda2 leads to increased toxicity upon helicase overexpression. Furthermore, the experiments in Figure 2.1B suggest that NuA4 (Esa1) mediates Pif1 acetylation *in vivo*, and Rpd3 and/or Hda2 are responsible for deacetylating Pif1 (Figure 2.1C). It should be noted that NuA4 and Rpd3 are known to have balancing activities *in vivo* (207), lending credence to these results, and thus, we focused on Rpd3 instead of Hda2 herein.

2.3.2 Pif1 Acetylation is Dynamically Regulated by NuA4 and Rpd3

Because Pif1 overexpression toxicity was significantly altered in specific KAT and KDAC mutant strains, we were interested in directly confirming if the lysine residues on Pif1 were

acetylated in these backgrounds. Based on the results obtained in Figure 2.1B and C, we investigated the acetylation status of overexpressed Pif1-FLAG in the acetylation proficient (*rpd3Δ)* and acetylation deficient (*esa1-414*) strains that displayed significant difference in overall cell viability compared to the wild-type strain. To assess Pif1 acetylation, we immunoprecipitated the lysates with anti-acetyl lysine antibody, followed by immunoblotting with anti-FLAG antibody. Input and phosphoglycerate kinase (Pgk1) served as a loading control in all experiments. The western blot results showed increased Pif1 acetylation in the *rpd3Δ* lysate (1.7-fold) and decreased Pif1 acetylation in the *esa1-414* lysate compared to the wild-type (compare lane 2 and 3 to lane 1 respectively, Figure 2.2A), consistent with the results in Figure 2.1. These results further confirm that Pif1 acetylation is regulated by the action of NuA4 (Esa1) and its counteracting partner, Rpd3.

To test the efficiency of recombinant Piccolo NuA4 (Esa1/Epl1/Yng2 subunits) for acetylating Pif1, we used a previously established *in vitro* acetylation protocol to modify recombinant Pif1 (194). Using an anti-acetyl lysine antibody, we were able to detect lysine acetylation of Pif1 on the Piccolo NuA4-modified Pif1 but not on the unmodified form (Figure 2.2B), confirming that Piccolo NuA4 was capable of acetylating Pif1. Similarly, autoradiography of *in vitro* acetylated Pif1 also showed the helicase to be modified, in addition to the autoacetylation of the Esa1, Epl1, and Yng2 subunits of Piccolo NuA4 (*A- 1*). Further, using tandem mass spectrometry analysis, we were able to identify six acetyl lysine sites on the *in vitro*-modified Pif1: K118, K129, K525, K639, K725, and K800 (Figure 2C). An example of an acetylation spectrum detecting the +42 Da mass shift is shown in *A*- 2. These results establish a Pif1 acetylation signature that defines two sites of modification in the N-terminal domain (K118, K129), three in the helicase domain (K525, K639, K725), and one on the C-terminus (K800). The two modified residues clustered in the PiNt were intriguing because while the function of the PiNt is still being elucidated, it has already been shown to regulate some of Pif1's activities and alter its overexpression toxicity *in vivo* (201). To investigate this further, we used an N-terminal domain truncation of Pif1 (Pif1ΔN) lacking amino acids 1-233 to determine the role of the PiNt in Pif1 acetylation. We found that similar to modifying the full-length Pif1, Piccolo NuA4 (Esa1) was also able to *in vitro* acetylate recombinant Pif1ΔN (Figure 2.2B) and detected sites K525, K639, K725 and K800 to be acetylated using mass spectrometry. Additionally, acetylation of previously determined lysine sites on the helicase and C-terminal domains in the absence of PiNt were confirmed by mass spectrometry.

2.3.3 The Absence of the PiNt in Acetylation Mutant Strains Impacts Overexpression Toxicity

To assess the contribution of the PiNt to acetylation-dependent toxicity, we used the Pif1ΔN construct in our overexpression toxicity assay, investigating the same genetic backgrounds as in Figure 2.1. As previously reported (201), Pif1ΔN was less toxic in this assay in wild-type cells than full-length Pif1 (Figure 2.3A and 2.3B), exhibiting a toxicity value of ~0.8 compared to 0.4, respectively. No decrease in toxicity was observed in the *esa1-414* cells nor in any other KAT deletion strain (Figure 2.3A). Because wild-type cells over-expressing Pif1ΔN already showed robust growth, this result is unsurprising.

Among the KDAC mutant strains, deletion of the PiNt rescued the increased toxicity of Pif1 overexpression in *hda2Δ* cells (Figure 2.3B). Deletion of *RPD3* still resulted in increased toxicity relative to wild-type cells ($p < 0.01$), upon Pif1ΔN overexpression (Figure 2.3B), but this still represented a significant growth improvement compared to full-length Pif1 overexpression in *rpd3Δ* cells ($p < 0.0001$). Indeed, growth in *rpd3Δ* cells led to a 51% toxicity increase when Pif1 was overexpressed, compared to only a 20% toxicity increase with Pif1ΔN (Figure 2.3C). There were no significant effects of Pif1ΔN overexpression in the other KDAC deletion backgrounds. The reduction of acetylation effects on Pif1ΔN toxicity compared to full-length Pif1 indicates that the PiNt is critical for acetylation-altered activity *in vivo*.

2.3.4 Acetylation Stimulates Pif1's Helicase Function

Pif1 is a structure-specific helicase, and the order of its preferential unwinding of substrates is RNA:DNA forks > DNA:DNA forks > 5' tailed DNA:RNA duplex > 5' tailed DNA:DNA duplex (208). We designed forked and tailed duplex substrates to aid in determining the impact of lysine acetylation on the helicase activity of Pif1. Because Pif1 is a non-processive helicase, assays were performed using unmodified (UM) and Piccolo NuA4 (Esa1) *in vitro*-acetylated (AC) forms of the protein under multi-turnover conditions, such that more unwound products could be visualized given the experimental parameters used. Under these conditions, Pif1 was able to rebind to its DNA substrate after initial dissociation, allowing for multiple rounds of binding followed by unwinding. The amplitude (*a measure of the percentage of DNA molecules that are completely unwound by the helicase during the course of the reaction)* of unwinding was compared between UM-Pif1 and AC-Pif1 on different cognate helicase substrates. We observed that Pif1 acetylation

led to ~3-fold increase on a DNA-DNA fork (Figure 2.4A), DNA-DNA tail (Figure 2.4C), and RNA-DNA tail substrates (Figure 2.4D) and ~2-fold increase on an RNA-DNA fork (Figure 2.4B). Both RNA-DNA substrates had higher amplitudes than their DNA-DNA counterparts, confirming that indeed, the nature of the nucleic acid within the duplex region of the displaced strand dictates Pif1's preference for certain substrates over others (208). Furthermore, the Pif1 helicase is additionally known to unwind stable G4 structures, which can hinder DNA replication (178). Therefore, using a G4 substrate, we determined the impact of acetylation on G4 resolution under similar conditions (209). Identical to its other preferred substrates, we observed ~2-fold stimulation of unwinding when Pif1 was acetylated (Figure 2.4E). Formation of a stable G4 structure was confirmed by performing a synthesis assay using Pol δ in the presence of unmodified and acetylated forms of the helicase (Figure 2.4F). DNA pol δ alone was unable to synthesize on the G4 substrate past the gap region, indicating the presence of a stable G4 structure. However, in the presence of both UM-Pif1 and AC-Pif1, we observed synthesis past the gap and into the G4 region. The AC-Pif1 displayed the highest stimulation of pol δ synthesis, including the formation of a full-length product, presumably because AC-Pif1 was more efficient at G4 structure resolution than UM-Pif1.

To study the impact of acetylation on helicase activity in the absence of the PiNt, experiments were also performed using the UM- and AC-Pif1ΔN recombinant protein. Under multi-turnover conditions, acetylation increased the amplitudes of forked duplex unwinding (~2-3-fold) analogous to the full-length protein (Figures 2.4A and 2.4B). However, we observed decreased unwinding of tailed substrates by AC-Pif1ΔN compared to full-length AC-Pif1 (Figures 2.4C and 2.4D). These data demonstrate that although Pif1ΔN retains the preference for RNA-DNA substrates, it is not equally affected by acetylation in the same manner as the full-length protein, indicating that the PiNt may be involved in the altered biochemistry of AC-Pif1. Additionally, for the G4 substrate, although acetylation of PifΔN yielded a ~2-fold increase in the amplitude of unwinding relative to UM-PifΔN, our results suggest that deletion of the PiNt had an impact on Pif1's interaction with this substrate (Figure 2.4E). A comparison of the amplitude of unwinding at the highest time-point for every substrate is summarized in Figure 2.4G. Control experiments showed that neither the presence of Piccolo NuA4 (Esa1) nor acetyl CoA alone impacted helicase activity, but acetylation of Pif1 was necessary to observe stimulation of helicase activity (*A- 3*).

Results from our multi-turnover helicase assays demonstrated that acetylation of Pif1 led to an increase in the amount of unwound products formed compared to UM-Pif1. We then inquired if this increase was due to a change in the rate of Pif1 unwinding when the helicase was modified by lysine acetylation. To address this, helicase assays were performed under single-turnover conditions, where the protein was trapped by the addition of an excess of unlabeled oligonucleotide, permitting only one round of binding and unwinding of its substrate. We ensured that the presence of the protein trap did not affect the unwinding kinetics of the protein (*data not shown*). The rate of unwinding of the DNA-DNA fork by UM-Pif1 was $0.409 \pm 0.210\ s^{-1}$, while that of its acetylated form was $0.368 \pm 0.132\ s^{-1}$ (Figure 2.5A). Comparatively, the rate of unwinding of the RNA-DNA fork by UM-Pif1 was $0.344 \pm 0.208\ s^{-1}$, and that of AC-Pif1 was $0.344 \pm 0.151\ s^{-1}$ (Figure 2.5B). Thus, the data obtained from the single-turnover assays showed that irrespective of the forked substrate (DNA:DNA or RNA:DNA fork) incubated with the helicase, acetylation did not influence the rate of unwinding. However, we observed that there was still an increase in helicase activity (as measured by the amplitude) on an RNA:DNA fork substrate compared to a DNA:DNA fork substrate, following the previously established phenomenon that Pif1 preferentially unwinds RNA-DNA forks (210). Additionally, AC-Pif1 displayed ~3-fold stimulation in the formation of unwound product compared to UM-Pif1 on a DNA:DNA fork substrate, and ~ 2-fold stimulation on a RNA:DNA fork substrate (Figure 2.5A and 2.5B) as measured by their amplitudes. Negligible unwinding of the tailed substrates was found under the experimental conditions used for single-turnover studies (*data not shown*). Interestingly, our results suggest that lysine acetylation does not stimulate Pif1 unwinding by affecting its unwinding rate. Instead, acetylation may make the protein more processive as the amplitude of unwound product formed was increased when substrates were incubated with AC-Pif1. Taken together, these results show that lysine acetylation improves the helicase-catalyzed unwinding of both forked and tailed substrates. They also show that this PTM preserves the protein's preference and processivity for RNA-DNA hybrids.

2.3.5 ATPase Activity of Pif1 is Increased upon Lysine Acetylation

As a helicase, Pif1 utilizes the energy produced from ATP hydrolysis to translocate along ssDNA and unwind the DNA duplex. Due to the coupling of its helicase activity to ATP hydrolysis, we sought to determine if acetylation also impacts Pif1's ATPase activity, using an NADH-coupled spectrophotometric assay (211). This assay operates on the principle that steady-state

hydrolysis of ATP is proportional to NADH oxidation. Because Pif1 is a DNA-stimulated ATPase, we measured the change in absorbance associated with NADH oxidation and ultimately ATP hydrolysis in the presence of a 45-nt ssDNA at 340 nM over a 30-min period. We found a ~3-fold stimulation in the rate of ATP hydrolysis (Figure 2.6A) when full-length Pif1 was acetylated compared to its unmodified form, suggesting that this modification co-stimulates the helicase-coupled ATPase activity of Pif1. Comparatively, the rate of ATP hydrolysis of Pif1ΔN displayed no significant difference between the unmodified and acetylated forms of the helicase. Interestingly, we observed that the rate of ATP hydrolysis of PifΔN was higher than that of the full-length protein (Figure 2.6B), implying that the PiNt may further play a role in regulating Pif1 ATPase activity.

2.3.6 Acetylation Enhances Pif1's Substrate Binding Ability

This binding to a single-stranded region on the DNA precedes its ATPase activity and ultimately its unwinding function. Therefore, we speculated that the stimulation in helicase-catalyzed unwinding observed upon acetylation might correlate with differential binding of Pif1 to its substrate. To determine this, biolayer interferometry (BLI) technology was used to measure the affinity of UM- and AC-Pif1 to a biotinylated 45-nt ssDNA oligonucleotide immobilized on a streptavidin biosensor. We found that the binding affinity of AC-Pif1 was two-fold stronger than UM-Pif1, with K_D values of 7.2 ± 0.3 nM and 19.1 ± 5.1 nM, respectively (Figure 2.7A). A representative sensorgram showing the binding curves when 125 nM of UM- and AC-Pif1 were incubated with 500 nM of 45 nt ssDNA is presented in Figure 2.7B. These results show that acetylation of Pif1 leads to higher affinity ssDNA binding. Furthermore, we observed that the UM- and AC-Pif1 ssDNA association rates differed, but their dissociation rates were similar, supporting the hypothesis that the increased amounts of substrate unwound by AC-Pif1 *vs.* UM-Pif1 might be due to faster association and stronger affinity for ssDNA when Pif1 is acetylated. Evaluating DNA:DNA fork binding via EMSAs also revealed a difference in the binding affinities of UM-Pif1 and AC-Pif1, confirming the results obtained from the BLI analyses (Figure 2.7C).

Based on these results, we hypothesized that AC-Pif1ΔN would show a similar binding trend when compared to UM-Pif1ΔN. However, we observed that acetylation had no impact on the binding affinity of the truncated protein, as the calculated K_D values were 14.1 ± 1.5 nM and 15.2 ± 3.3 nM for UM-Pif1ΔN and AC-Pif1ΔN, respectively (Figure 2.7A). Moreover, these

values are similar to unmodified full-length Pif1 (19.1 ± 5.1 nM). This suggests that while Pif1ΔN can bind to ssDNA similar to Pif1, it is not affected by acetylation in the same manner. We hypothesized that acetylation may drive a conformational change in the Pif1 structure that does not occur for Pif1ΔN, and to test this, we next examined changes in Pif1 structure induced by acetylation using limited proteolysis.

2.3.7 Acetylation Alters the Conformation of Pif1, likely mediated through the N-terminal Domain

To date, there are no published atomic-level structures of full-length *S. cerevisiae* Pif1 including its N-terminal domain (212,213), presumably due to the challenges presented by the predicted native disorder of the PiNt (201). Being unable to crystallize full-length UM-Pif1 and AC-Pif1, we instead used limited proteolysis assays to determine if a gross conformational change plays a role in AC-Pif1's altered biochemical activities. If a conformational change occurs in solution upon Pif1 acetylation, then the protease digestion patterns of UM-Pif1 and AC-Pif1 should differ. We incubated recombinant Pif1 with GluC protease for various lengths of time; GluC was chosen instead of an enzyme such as trypsin or LysC to prevent lysine acetylation from inhibiting the protease. We found that full-length UM-Pif1 was nearly completely degraded within the first 15 min, with lower molecular weight digestion products continuing to form over 60 min (lanes 2 – 4, Figure 2.8A). In contrast, a proportion of full-length undigested AC-Pif1 remained even after 60 min, with minor small peptide (20-35 kDa) product formation (lanes 6 – 8, Figure 2.8A).

Next, we repeated this assay with recombinant UM- and AC-Pif1ΔN proteins to determine the role of the PiNt in acetylation-driven conformational changes. We observed that UM-Pif1ΔN was more resistant to GluC proteolysis than UM-Pif1, with at least a portion of undigested UM-Pif1ΔN evident at all time points (lanes 2-4, Figure 2.8B). This suggests that the PiNt is a major target of GluC activity in the context of UM-Pif1. Indeed, although we do not know the sequences of the digested species created by limited proteolysis, it should be noted that the highest molecular weight digestion product of UM-Pif1 is approximately the same size as undigested Pif1ΔN (Figures 2.8A and B), perhaps indicating that the PiNt is easily removed from Pif1 upon GluC digestion. Further, unlike with full-length Pif1, AC-Pif1ΔN was only slightly protected from GluC digestion compared to UM-Pif1ΔN, with both proteins exhibiting similar proteolytic cleavage

patterns and rates of digestion (compare lanes 2 – 4 to lanes 6 – 8, Figure 2.8B). Taken together, these data indicate that acetylation induces a conformational change in Pif1, which occurs either directly in the PiNt or which requires the PiNt for allosteric changes.

2.4 Discussion

While the enzymatic functions of the Pif1 helicase have been extensively characterized, the precise mechanisms by which the activities of this helicase are coordinated to impact a variety of nuclear DNA transactions remain unknown (213-217). Pif1's cellular abundance is predicted to be low (218), and aberrant Pif1 levels in the cell lead to deleterious effects. Deletion or depletion of Pif1 from the nucleus results in telomere hyperextension and telomere addition to double-stranded breaks (219). Conversely, as described previously (200,201) and in Figure 2.1A, overexpression of Pif1 is toxic to cells, inhibiting cell growth. These studies demonstrate that the activity of the protein is regulated in the cell by one or more means. Indeed, phosphorylation is known to regulate Pif1's role in telomere maintenance (220). However, the role of other PTMs in regulating Pif1 activities has not yet been elucidated. In our current study, we determined the acetylation dynamics of Pif1 *in vivo* and, using *in vitro* biochemical assays, defined alterations to its various enzymatic activities upon modification. We speculate that lysine acetylation is a mechanism used by the cell to regulate the function of Pif1 for different nuclear DNA transactions.

Acetylation of histone tails helps to neutralize the positive charge on lysine residues, causing the destabilization of the chromatin architecture and thereby allowing biological machineries to gain access to the DNA (221). Enzymes responsible for dynamically modifying histone residues can also interact and acetylate non-histone proteins, including proteins associated with DNA replication and repair (79,199). Our toxicity assay for Pif1 overexpression in different KAT and KDAC mutant strains pointed to the KAT, NuA4, and its counteracting partner KDAC, Rpd3, as responsible for cellular Pif1 acetylation (Figures 2.1B, 2.1C and 2.2A). The KAT activity of Esa1 is linked to cell cycle progression, potentially by regulating transcription (103). In *S. cerevisiae*, Rpd3 is also associated with cell cycle control by regulating replication origin firing (222). Both Esa1 and Rpd3 also play an important role in the DNA repair process, albeit these studies are in connection with histone acetylation (104). Because both the acetylation modifiers are in close contact with chromatin during cell cycle progression and repair, it is not surprising that they would also play a role in modifying Pif1, a helicase associated with replication and repair.

Our Pif1 toxicity assay, while quantitative, will not catch subtle modifications (singular or multiple lysine acetylation on Pif1) that other redundant KATs and KDACs may be able to accomplish. In addition to NuA4 (Esa1), other KATs can potentially also interact with and acetylate Pif1 during different cellular events. For example, the gene encoding the KAT Rtt109 is essential when Pif1 is over-expressed (200). While we observed *in vitr*o acetylation of Pif1 using the KAT Gcn5, we did not observe in Pif1 acetylation with recombinant Rtt109. Similarly, deletion of both these KATs did not alleviate toxicity in the Pif1 overexpressed strains. However, we also found Hda2 to play a subtle role in the deacetylation process, though, its impact may not have been as high as Rpd3, based on the toxicity studies (Figure 2.1B). Thus, although NuA4 (Esa1) and Rpd3 may serve as the primary modifiers of Pif1, we cannot rule out the activity of other KATs and KDACs in regulating Pif1 acetylation, because these modifiers display redundancy in their cellular functions (223). Although we did not evaluate if acetylation of Pif1 is coordinated along with cell cycle phases in our current study, previous work demonstrates that acetylation of other replication proteins, including FEN1 and PCNA, does not display cell cycle specificity (53,224). Nonetheless, considering that Pif1 partakes in multiple DNA transactions, lysine acetylation may be specifically regulated in response to a genome maintenance event requiring alterations to specific activities of Pif1.

Acetylation of recombinant proteins has its own caveats, including that the *in vitro* acetylation reaction never goes to completion and, in the absence of other protein regulators, tends to be promiscuous (225). However, the six lysine residues we report to be modified on Pif1 were acetylated in multiple independent *in vitro* reactions, thus making them robust potential targets for modification by Piccolo NuA4 (Esa1) (Figure 2.2C). Of these lysine residues, two resided in the PiNt, three in the helicase domain, and two in the C-terminus. The fact that this modification is not limited to a certain segment/domain of the protein suggests that many of the various biochemical properties of the protein could be impacted. Pif1's helicase core alone houses the seven conserved amino acid motifs common to this family where the direction of ssDNA translocation is determined, ATP hydrolysis, and ssDNA binding occur (226-228). Lysine acetylation of the BLM helicase is similarly spread across its different domains, allowing for regulation of its functions during DNA replication and the DNA damage response (192).

Helicase assays performed using *in vitro*-modified Pif1 revealed a significant stimulation in its unwinding activity upon acetylation compared to the unmodified form. This stimulation was

apparent on all substrates tested, even though the levels of stimulation differed based on the specific substrate being unwound (Figure 2.4F). The single-turnover and multi-turnover helicase reactions confirmed that the increased helicase unwinding was due to increased processivity and not due to a faster rate of unwinding (Figures 2.4 and 2.5). In addition to Pif1's helicase activity, its ATPase function was also stimulated when the protein was acetylated (Figure 2.6). However, because Pif1 is a DNA-stimulated ATPase, it is difficult to determine if this stimulation is due to faster ATP hydrolysis or if faster DNA binding allows ATP hydrolysis to occur more rapidly. Future work using order-of-addition ATPase assays could help to delineate between these two possibilities.

Characterization of DNA binding activity demonstrated increased binding by AC-Pif1 compared to UM-Pif1 (Figure 2.7). At a first glance, this observation is counterintuitive because one would expect lower nucleic acid binding affinity when the positive charge on lysine is neutralized by acetylation. However, Pif1 was acetylated at a single site, K725, located within the DNA binding domain (DBD) (229), while the other modified sites were found throughout the protein. Alterations in binding activities could depend on sites modified within and outside the DBD, and how each of those individual lysine charge neutralization events impact the overall binding of a protein. Of the six Pif1 lysine residues we found to be acetylated *in vitro*, one residue, K525, is conserved in hPIF1 (K485). K485 makes contact with ssDNA, and mutation of this residue to alanine results in decreased ssDNA binding affinity (214). In yeast, K525 may be important for the regulation of Pif1 DNA binding and acetylation-altered activity, which mutational analysis would elucidate further. Acetylation of other proteins, such as p53 (230), Gata-1 (231), and Stat3 (232), all serve as examples of proteins displaying increased binding affinities for specific DNA substrates when acetylated. Interestingly, acetylation of replication protein A (RPA) promotes its displacement from ssDNA during DSB repair (233), and acetylated FEN1 displays lower substrate binding affinity (53). All of these proteins are hypothesized to undergo conformational changes upon acetylation, which may alter their ability to interact with and bind to their cognate substrates.

Pif1 has a large N-terminal domain (PiNt) making up almost one-third of the protein, and this domain is predicted to be natively disordered (201). Due to the ability to mutate the N-terminus and still retain helicase activity, we focused on characterizing the two acetylation sites on the N-terminal domain. Overexpression toxicity assays revealed that deletion of the PiNt resulted in

lesser toxicity compared to wild-type Pif1 when cellular acetylation dynamics were altered (Figure 2.3). Because the PiNt is predicted to be natively disordered, we hypothesized that it might undergo a conformational change when Pif1 is acetylated, thus impacting the biochemical properties of the helicase domain. Acetylation has been documented to cause conformational changes in a number of other proteins. For instance, PCNA is acetylated in response to DNA damage, and this induces long-range conformational changes in the protein, distal from the acetylation site (224). Similarly, the DNA binding protein TCF4 is suggested to change conformations when acetylated in a complex with DNA (234), and Beta 2-glycoprotein changes from a closed to open conformation upon acetylation (235).

Limited proteolysis is a method of detecting protein conformational changes that does not require crystallization or large amounts of protein, which are currently both obstacles when working with AC-Pif1. The altered digestion and degradation patterns in the acetylated form of Pif1 compared to the unmodified form indicate changes in the tertiary structure of the protein (Figure 2.8). Similarly, because AC-Pif1ΔN displayed the same digestion pattern as UM-Pif1ΔN, we speculate that the PiNt is necessary for the acetylation-based conformational change. It may be that the acetylated residues in the helicase and/or C-terminal domain are responsible for changes in the PiNt, similar to the allosteric changes that acetylation drives in PCNA. Alternatively, a combination of residues in every domain might require acetylation for these changes to take place. The structure of the PiNt is unknown, but the transition from a closed to an open conformation like Beta 2-glycoprotein upon acetylation could explain how Pif1 ssDNA binding affinity increases. Additional study, including high-resolution structures of full-length UM-Pif1 and AC-Pif1, is needed to address these questions and further understand how acetylation affects Pif1 structure.

The impetus for studying Pif1 lysine acetylation was triggered by the observation that multiple proteins involved in the Okazaki fragment maturation pathway are also acetylated. Studies *in vitro* have shown that Pif1 promotes increased strand displacement synthesis by the lagging strand DNA pol δ (236). Increased strand displacement allows for the creation and cleavage of longer 5' displaced flaps. While genetic and biochemical studies support a redundant alternate long flap pathway for Okazaki fragment maturation, this model is largely based on *in vitro* reconstitution assays. One hypothesis for creating longer flaps in the cell is to completely remove the initiator RNA/DNA primer on the lagging strand that is synthesized by the error-prone DNA polymerase α (40). Another possibility to consider is if $Rad27^{FEN1}$ disengages from the

replisome, it may unintentionally allow for the creation of longer flaps within the cell, thereby necessitating an alternate pathway for flap processing. Along with acetylation of other Okazaki fragment proteins, including Rad27^{FEN1} and Dna2, Pif1 modification may push the creation of longer flaps during the maturation process, allowing for higher fidelity synthesis (Figure 2.9). Recent evidence from the Rass group provides an alternate explanation for the observation that the lethality of *dna2Δ* is suppressed by *pif1Δ* (237). In this study, they show that in *dna2Δ* cells, Pif1 mediates checkpoint activation following replication stress, which leads to replication fork stalling. These stalled replication forks are resolved through break-induced replication or recombination-dependent replication (RDR), both of which utilize the Pif1 helicase for efficient D-loop structure resolution. Acetylation of Pif1 may also play a role in coordinating the checkpoint response and recruitment of proteins during stalled replication.

AC-Pif1 was also shown to be more efficient at G4 structure resolution (Figure 2.4E). Though the unmodified form of Pif1 is capable of efficient G4 resolution, due to increased binding affinity of the acetylated form, AC-Pif1 could potentially resolve tandem G4 structures more effectively than UM-Pif1 (Figure 2.9). Thus, while finely regulated concentrations of AC-Pif1 may be critical to the maintenance of overall genome stability, increases in AC-Pif1 levels may overwhelm the replication machinery by generating longer ssDNA segments, leading to cellular toxicity. Other studies have shown similar results supporting this hypothesis. For instance, SV40 T-antigen inhibits Okazaki fragment processing when in a higher-concentration hexameric state, but it supports Okazaki fragment processing when in a lower-concentration monomeric state (238). Dysregulation of Rad5, an enzyme involved in post-replication repair in yeast and humans, leads to cisplatin sensitivity when both deleted or overexpressed (239). The study of human PIF1 (hPIF1) has also demonstrated the deleterious consequences of Pif1 helicase misregulation. The transfection of cultured primary neurons with hPIF1 is toxic, increasing the risk of cell death (240). Further, human tumor cells rely on hPIF1 for protection from apoptosis (241), whereas hPIF1 depletion in normal cells increases replication fork arrest (242). The L319P hPIF1 mutant is linked to breast cancer and cannot suppress the lethality of Pfh1 deletion in *S. pombe* (243), indicating that mutant hPIF1 activity could also lead to cancer cell growth. These studies demonstrate that regulation of PIF1 family helicases is critical not just in *S. cerevisiae* but also in humans, and as such, acetylation of hPIFif1 may be a conserved modification used by the cell to regulate hPIF1 activity.

In conclusion, we propose that lysine acetylation of Pif1 is a regulatory mechanism that dynamically alters the cellular enzymatic activity of the helicase. While this study serves as the first report of acetylation-based regulation of Pif1, many questions remain unanswered. The precise timing and cellular triggers of Pif1 acetylation are still unknown. Likewise, how acetylation affects Pif1's interactions with other proteins and cellular localization remain to be determined. Here, we report the importance of the N-terminus in regulating acetylation-dependent Pif1 activity. While the C-terminus, also predicted to be disordered, serves as an important point of contact for PCNA during BIR (236), we are currently unaware of how specific lysine residue acetylation impacts this domain. Crosstalk between PTMs is commonplace, and as such, acetylation may be connected to Pif1 phosphorylation or other lysine residue dependent PTMs. Studies designed to answer these and other remaining questions regarding Pif1 activity and regulation will be important to further our understanding of how Pif1 achieves its multi-faceted role of maintaining genomic integrity.

2.5 Materials and Methods.

2.5.1 Strains, media, and reagents

The *S. cerevisiae* strains used are listed in Tables A- 1 and A-2. The cells were maintained on rich medium (YPD) or synthetic drop-out medium and transformed with overexpression plasmids using standard methods. Escherichia coli strain NiCo21(DE3) (New England Biolabs) was transformed with the pLysS plasmid (Novagen) to create the NiCo21(DE3) pLysS strain. The *E. coli* cells were maintained on LB medium supplemented with antibiotics (50 µg/ml kanamycin, 34 µg/ml chloramphenicol, and/or 100 µg/ml ampicillin as needed). Liquid cultures were grown in 2X YT medium for protein overproduction and supplemented with the same antibiotics. dNTPs were purchased from New England Biolabs (Ipswich, MA). Oligonucleotides were purchased from IDT (Coralville, IA) and are listed in Table A- 4. Chemical reagents were purchased from Thermo-Fisher, Sigma, or DOT Scientific.

2.5.2 Overexpression toxicity assays

Plasmid pESC-URA was used for the galactose-induced overexpression of proteins in S. cerevisiae. Empty pESC-URA vector or pESC-URA-Pif1 (WT or mutant) was transformed into the indicated yeast strains, and transformants containing the plasmid were selected on SC-Ura drop-out media. Fresh transformants were then grown in liquid SC-Ura medium containing 2% raffinose for 16 FEN1, the cells were harvested and washed with sterile water, and then diluted to an OD660 of 0.01 in SC-Ura supplemented with either 2% glucose or galactose. A 200-µL volume of each culture was added in duplicate to wells in 96-well round bottom plates, and each well was overlaid with 50 µL of mineral oil to prevent evaporation. The plate was monitored using a Synergy H1 microplate reader (BioTek), taking OD660 measurements at 15-min intervals for 48 FEN1, with linear shaking occurring between readings. The plate reader also incubated the cells at 25 or 30°C as indicated. The mean of the OD660 readings for each Pif1-expressing strain grown in galactose was divided by the mean OD660 of the same strain grown in glucose. This mean value was normalized to that of cells from the same genetic background containing empty vector to produce a toxicity value for each Pif1 variant in each yeast genotype. Plasmids used in this study are detailed in Table A- 3.

2.5.3 Protein purification

S. cerevisiae Pif1 was over-expressed in NiCo21(DE3) pLysS cells and purified as previously reported (184), with slight modification. To increase the yield of SUMO-Pif1, up to 10 mL TALON resin was used in the form of tandem 5-mL TALON HiTrap columns in the initial capture of recombinant protein from lysate. The Pif1ΔN mutant (176) lacked the first 233 amino acids of the helicase. Recombinant Pif1ΔN protein was expressed and purified in an identical manner to full-length wild-type (WT) Pif1. The *S. cerevisiae* Piccolo NuA4 complex (consisting of Esa1, Epl1, and Yng2) was over-expressed using the polycistronic expression system developed in the Tan laboratory and purified from BL21(DE3) pLysS cells as previously described (244). *S. cerevisiae* pol δ was purified by co-expressing the pol 3, pol 31, and GST-pol 32 plasmids in BL21(DE3) cells and purifying as previously described (245).

2.5.4 *In vitro* acetylation

In vitro acetylation of Pif1 was performed using two complementary methods. In the first method, purified recombinant Pif1 (Pif1 or Pif1ΔN) was incubated with the Piccolo NuA4 complex (Esa1/Epl1/Yng2) in the presence of acetyl-CoA in 1X HAT buffer (50 mM Tris-HCl (pH 8.0), 10% (v/v) glycerol, 150 mM NaCl, 1 mM dithiothreitol (DTT), 1 mM phenylmethylsulfonyl fluoride, and 10 mM sodium butyrate) for 30 min at 30°C. For proteins analyzed via mass spectrometry, DTT was omitted from the reaction buffer.

In the second method, Pif1 was *in vitro* acetylated using the same protocol as above, but the reactions were incubated for 60 min. Subsequently, the reaction mixture was loaded onto a TALON affinity column. Because Esa1 was 6X-His tagged, the Piccolo complex remained bound to the column, whereas the acetylated Pif1 was eluted by the column wash buffer (50 mM sodium phosphate (pH 7.5), 300 mM NaCl, 1 mM PMSF, 5 mM β-mercaptoethanol, 10% (v/v) glycerol, and 7 µg/uL pepstatin A). The eluate was analyzed by SDS-PAGE and Coomassie staining and found to contain no contaminating proteins or subunits from the acetyltransferase.

A ratio of 1:1:10 [Pif1/ Pif1ΔN):acetyltransferase:acetyl-CoA] was maintained for all acetylation reactions. Results described in this report used AC-Pif1 that was obtained using the second method. However, results for all biochemical assays were confirmed using AC-Pif1 obtained using both methods.

2.5.5 Mass spectrometry

Tandem mass spectra from *in vitro* Piccolo NuA4 (Esa1)-acetylated full-length Pif1 were collected in a data-dependent manner with an LTQ-Orbitrap Velos mass spectrometer running XCalibur 2.2 SP1 using a top-fifteen MS/MS method, a dynamic repeat count of one, and a repeat duration of 30 s. Enzyme specificity was set to trypsin (or Lys-C when cleaved with this protease), with up to two missed cleavages permitted. High-scoring peptide identifications were those with cross-correlation (Xcorr) values ≥1.5, delta CN values ≥0.10, and precursor accuracy measurements within ±3 ppm in at least one injection. A mass accuracy of ±10 ppm was used for precursor ions, and a mass accuracy of 0.8 Da was used for product ions. Carboxamidomethyl cysteine was specified as a fixed modification, with oxidized methionine and acetylation of lysine residues allowed for dynamic modifications. Acetylated peptides were classified according to gene

ontology (GO) annotations by Uniprot. Lysine residues identified as being modified in three or more independent *in vitro* reactions, cleaved with either trypsin or Lys-C, are reported.

2.5.6 Western blotting

Pif1 protein and the acetylation levels of over-expressed Pif1-FLAG were probed in WT, *rpd3Δ*, and *esa1-414* cells. Cells were grown in YPD or selective media and harvested at OD_{660} = 1.0. Harvested cells were lysed by incubation for 10 min at 95˚C in yeast lysis buffer (0.1 M NaOH, 0.05 M EDTA, 2% SDS, and 2% β-mercaptoethanol). Then, 5 µL of 4 M acetic acid was added for every 200 µL lysate, and the mixture was vortexed for 30 s. Lysates were incubated again at 95˚C for 10 min, and the soluble fraction was collected by centrifugation (246). Overexpression levels of Pif1 and Pif1ΔN were detected by immunoblotting with anti-FLAG antibody (Millipore Sigma A8592). For loading controls, the levels of Pgk1 were detected by immunoblotting with an anti-Pgk1 antibody (Fisher 22C5D8). Acetylation of cellular Pif1 was detected by immunoprecipitating cell lysate with anti-acetyl lysine antibody (CST 9441) resin and immunoblotting with an anti-FLAG M2 antibody (Millipore Sigma A8592). Specifically, Protein G Dynabeads (Invitrogen 10007D) were incubated with anti-acetyl lysine antibody (CST 9441) with end-over-end rotation for 4 FEN1 at 4°C, followed by the addition of 1 mg of cell lysate, which was then rotated overnight at 4°C. The beads were washed three times in the washing buffer provided with the Dynabead kit, and the beads were resuspended in 2X Laemmli buffer, boiled, and analyzed by SDS-PAGE followed by western blotting using the anti-FLAG M2 antibody. The fold-change in Pif1 acetylation was determined by first normalizing to the PGK-1 loading control, followed by comparing the levels of total Pif1 to the modified form of Pif1.

To detect *in vitro*-acetylated Pif1, 2.5 µM of purified protein, unmodified (UM-Pif1) or acetylated (AC-Pif1; acetylated protein obtained by the second method above), was separated by 4-15% gradient SDS-PAGE and immunoblotted with the anti-acetyl lysine antibody.

2.5.7 Oligonucleotides

Synthetic oligonucleotides were purchased from Integrated DNA Technologies. The lengths and sequences (5'-3') of each oligonucleotide are listed in Table A- 4. For helicase assays, the template was 5'-labeled using the IR 700 dye synthesized by IDT. The IR-labelled template

primer (T1) was annealed in IDT duplex buffer to oligonucleotide D1, D2, D3, or D4 to generate the DNA fork, RNA fork, DNA tail, or RNA-DNA tail substrate (respectively) in a 1:4 ratio. Oligonucleotides employed in BLItz assays contained a 3' biotin tag to allow for binding to the streptavidin biosensors. The G4 template (T2) was radiolabeled with [γ-^{32}P] ATP from Perkin Elmer and incorporated at the 5′ end using polynucleotide kinase as previously described (194). The template was further purified on a 12% sequencing gel containing 7 M urea. The radiolabeled T2 oligonucleotide was annealed to oligonucleotide D5 in a buffer containing 20 mM Tris (pH 8.0), 8 mM $MgCl_2$, and 150 mm KCl in a 1:4 ratio. All annealing reactions were incubated at 95°C for 5 min and then slowly cooled to room temperature as previously described (209).

2.5.8 Electrophoretic mobility gel shift assay (EMSA)

The binding affinities of UM-Pif1 and AC-Pif1 were measured by incubating increasing concentrations of the protein (100 and 200 nM) with 5 nM DNA fork substrate in 1X EMSA buffer (50 mM Tris-HCl (pH 8.0), 2 mM DTT, 30 mM NaCl, 0.1 mg/mL bovine serum albumin, and 5% (v/v) glycerol). The reactions were incubated at 30°C for 10 min, and samples were loaded onto a pre-run 8% polyacrylamide native gel. The gel was electrophoresed at a constant 250 V for 1 FEN1 and imaged using an Odyssey imaging system (700-nM filter). Using Image Studio, the densitometry of each band was used to calculate binding affinity with the equation: *[(bound product) / (bound product + substrate remaining) * 100]*.

2.5.9 BLItz analysis

To measure the binding kinetics of the different forms of Pif1 to single-stranded (ss)DNA, 500 nM of a biotinylated 45-nt substrate (T1) was diluted in 1X HAT buffer and coated onto a streptavidin dip read biosensor for 120 s (Pal Forte Bio, CA, USA.) A baseline was established for all biosensor reads by immersing them in 1X HAT buffer for 30 s. Following the baseline reading, 4 μL of the corresponding form of Pif1 at varying concentrations (62.5, 125, 250, and 500 nM) was applied to the biosensor for 150 s to measure association. Upon completion, the biosensor was then immersed in 550 μL of 1X HAT buffer to establish dissociation kinetics for another 150 s. The shift in wavelength was recorded, and the binding affinity (K_D) was analyzed using ForteBio software.

2.5.10 Helicase assay

The unwinding efficiency of the different forms of Pif1 was assessed on a wide variety of substrates using either multi- or single-turnover assays. For multi-turnover reactions, 5 nM substrate was incubated with 1 nM Pif1 at 30°C for 0, 0.5, 1, 2, 3, or 4 min. Reactions were performed in helicase buffer (50 mM Tris-HCl (pH 8.0), 2 mM DTT, 30 mM NaCl, 0.1 mg/mL bovine serum albumin, 5% (v/v) glycerol, 4 mM $MgCl_2$, and 8 mM ATP) and terminated with 80 mM EDTA, 0.08% SDS, and 50% formamide (final concentration) as previously described (209). For single-turnover reactions, 1 μM protein trap (T50) and 75 nM cold trap complementary to the labelled strand were added to prevent reannealing. Reactions under these conditions were started by adding 8 mM ATP and 4 mM $MgCl_2$. Samples were loaded onto pre-run 8% native polyacrylamide gels and electrophoresed for 30-45 min at 250 V. Gels were imaged using an Odyssey imaging system (700-nM filter) and quantified using Image Studio. The percentage of substrate unwound was calculated using the following equation: *% unwound = [(unwound product) / (unwound product + substrate remaining) * 100]*. Unwinding data were fit to the equation $A(t) = A(1-e^{kut})$ using Graphpad Prism, where A is the amplitude of product formation, k_u is the rate of unwinding, and t is time (247).

2.5.11 ATPase assay

ATP hydrolysis was measured using an NADH coupled assay in the presence of 3 μM ssDNA (unlabeled T1) and 10 nM helicase. The reaction buffer (10 mM ATP, 10 mM $MgCl_2$, 1 mM phosphoenolpyruvate, 10 U/mL pyruvate kinase, 16 U/mL lactate dehydrogenase, and 0.8 mM NADH) was pre-loaded into 96-well plates. To start the reaction, protein and DNA were added, and absorbance readings at 340 nm were recorded every 60 s for 30 min using a BioTek Cytation 5™ multi-mode plate reader. The rate of hydrolysis was determined as previously reported (248).

2.5.12 Proteolysis assay

Proteolysis assays were performed at 30˚C for up to 60 min. Pif1 proteins were diluted in 25 mM Na-HEPES, 5% glycerol, 50 mM NaOAc, 150 μM NaCl, 7.5 mM MgOAc, and 0.01%

Tween-20, and GluC protease was diluted in 100 mM ammonium bicarbonate. Proteolysis reactions were performed at a 1:250 GluC:Pif1 ratio. To assess proteolysis, 6 µg of protein was mixed with SDS-PAGE loading dye and chilled on ice at the indicated time points. The stopped reactions were ultimately electrophoresed on 10% SDS-PAGE gels for 45 min at 150 V and stained with Coomassie Brilliant Blue staining dye.

2.6 Acknowledgements

This work was funded by grants from the National Science Foundation (1929346) and Indiana CTSI Core Pilot Grant to L.B. and National Health Institutes (1R35GM133437) and American Cancer Society (RSG-16-180-01-DMC) to M.L.B. We would like to thank Dr. Song Tan for sharing the Piccolo NuA4 (Esa1) expression construct. Additionally, we would like to acknowledge Dr. Amber Mosley, IUSM Proteomics Core and the IU Bloomington Proteomics Core for help with the mass spectrometry analysis.

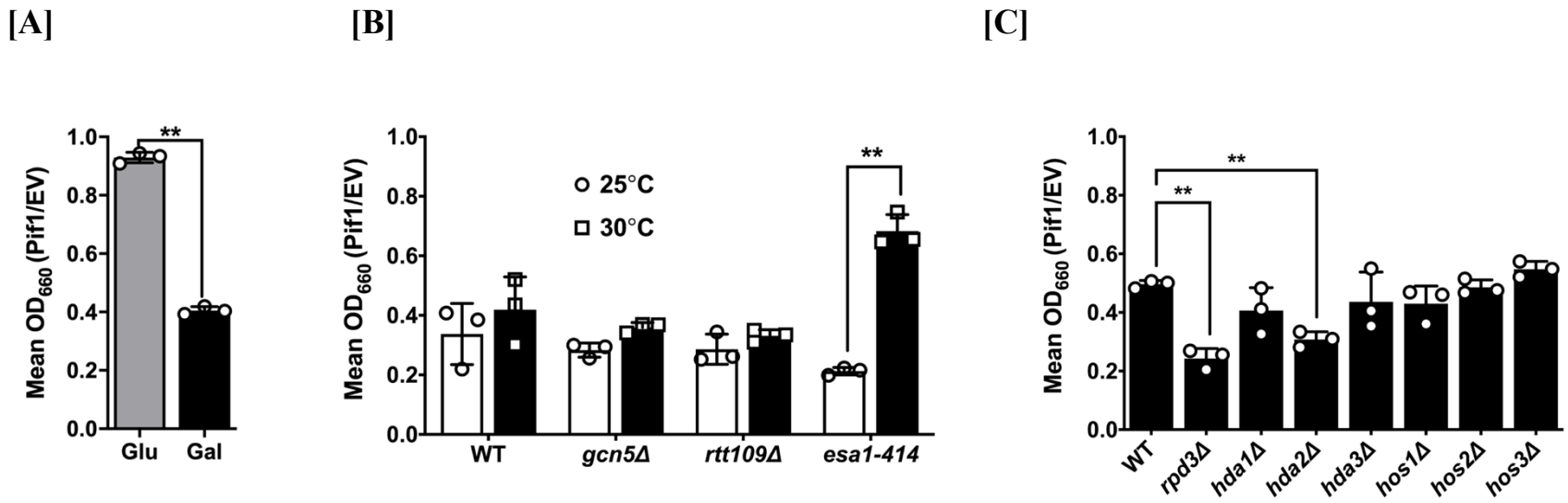

Figure 2.1 Pif1 over-expression toxicity is altered based on cellular acetylation levels.

[A] A galactose-inducible Pif1 expression vector, along with the empty vector, were transformed into wild-type cells. Growth was monitored over 48 FEN1, and the mean OD660 of Pif1-expressing strains was normalized to that of the empty vector in both glucose- and galactose-containing media. [B] Pif1 was overexpressed in acetyltransferase deletion (gcn5*Δ* and rtt109*Δ*) or temperature-sensitive (esa1-414) mutants at permissive (25°C) and restrictive (30°C) temperatures. [C] Pif1 was overexpressed in the indicated deacetylase mutant strains. The graphed values represent the average of ≥3 independent experiments of technical duplicates, with error bars corresponding to the standard deviation. **p<0.001. Data obtained by Christopher Sausen Ph.D

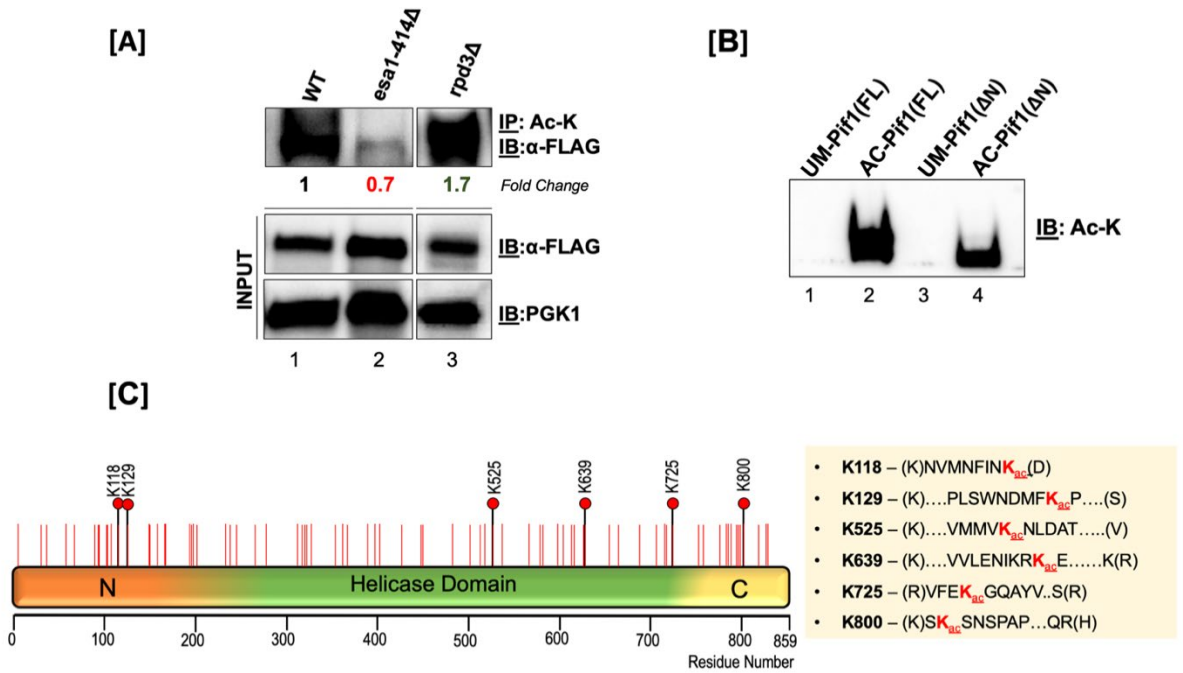

Figure 2.2 Pif1 is acetylated both in vivo and in vitro.

[A] Top Panel: S. cerevisiae lysates from WT (lane 1), esa1-414 (lane 2), and rpd3*Δ* (lane 3) backgrounds were immunoprecipitated with anti-acetyl lysine (ac-K) antibody-coated Protein G-dynabeads and immunoblotted with anti-FLAG antibody (1:1000); middle Panel: 10% of input immunoblotted with the anti-FLAG antibody and; bottom panel: PGK-1 antibody (1:10,000). Fold change in Pif1 acetylation is indicated. [B] Immunoblot of unmodified Pif1 (lane 1), NuA4 (Esa1) in vitro-acetylated full-length Pif1 (lane 2), unmodified Pif1ΔN, and NuA4 (Esa1) in vitro-acetylated Pif1ΔN probed with anti-Ac-K antibody. [C] Schematic of the full-length Pif1 sequence. The positions of all of the lysine residues in the sequence are denoted with red lines, and all acetylated lysine residues identified by mass spectrometry are denoted with black lines and red filled circles

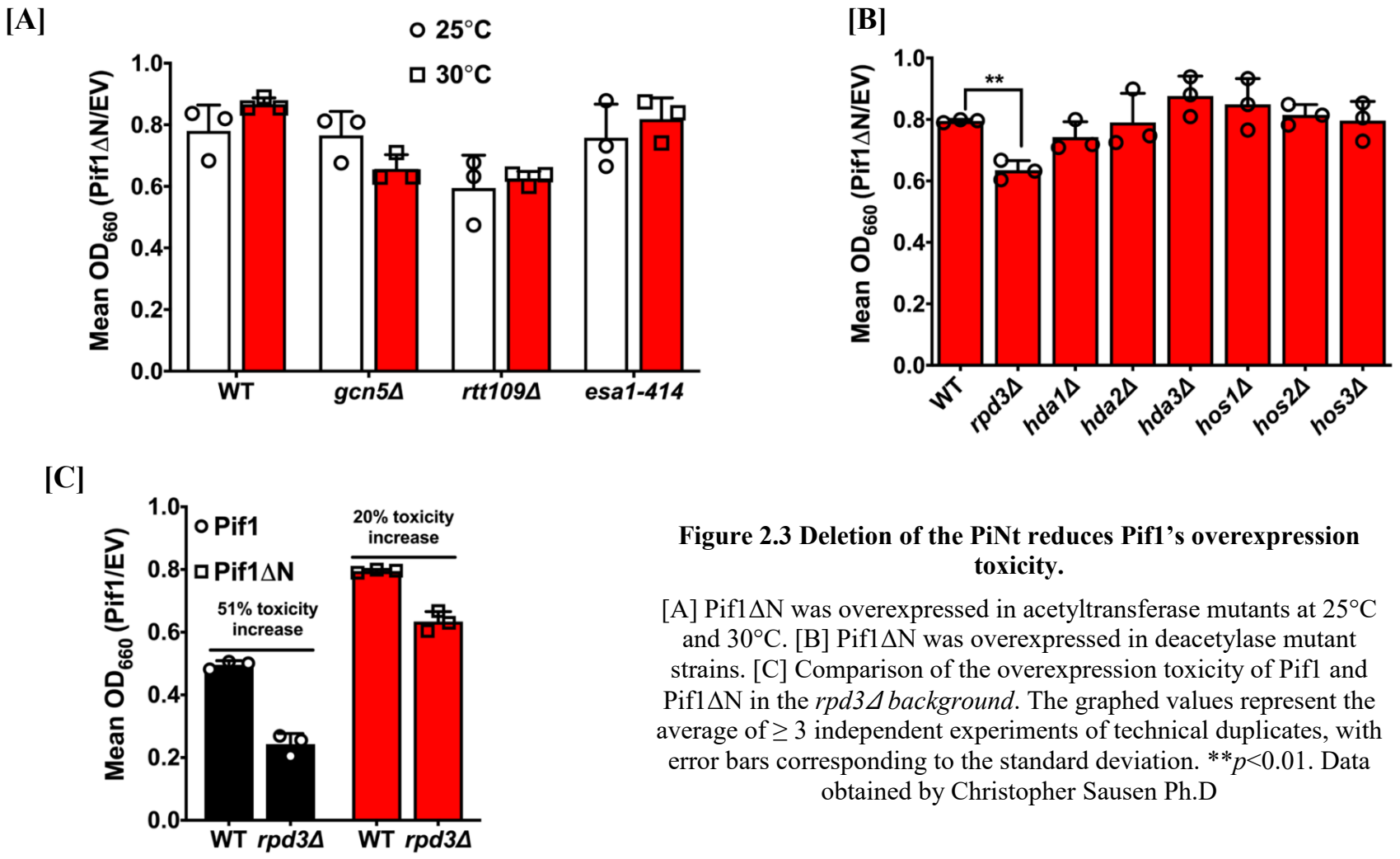

Figure 2.3 Deletion of the PiNt reduces Pif1's overexpression toxicity.

[A] Pif1ΔN was overexpressed in acetyltransferase mutants at 25°C and 30°C. [B] Pif1ΔN was overexpressed in deacetylase mutant strains. [C] Comparison of the overexpression toxicity of Pif1 and Pif1ΔN in the *rpd3Δ background*. The graphed values represent the average of ≥ 3 independent experiments of technical duplicates, with error bars corresponding to the standard deviation. ** $p<0.01$. Data obtained by Christopher Sausen Ph.D

Figure 2.4 Measurement of Helicase Activity Under Multi Turnover Conditions.

The kinetics of 1nM of full length and N-terminus deleted Pif1 helicase activity under multi turnover condition were assessed over 6 time points (0'', 30'',1',2', 3' and 4') in the presence of 5nM IR labelled [A] DNA fork, [B] RNA fork, [C] DNA tail and [D] RNA Tail. [E] cMyc-G4 template stabilized by K^+ was annealed to a complimentary 5' radiolabeled 21 nt ssDNA and the kinetics of Pif1 structure resolving activity was measured by the accumulation of the radiolabeled substrate over 6 time points (0", 1', 2.5', 5', 7.5', and 10'). Black line with open squares represents Pif1-FL and dotted black lines with filled squares represents acetylated form of Pif1-FL. Red line with open triangles represents Pif1ΔN and dotted red lines with filled triangle represents acetylated form of Pif1ΔN. F) The synthesis activity of 23 nM S. cerevisiae DNA polymerase delta (pol δ) was assayed on 5 nM cMyc-G4 substrate in the absence (lane 1) and presence of increasing concentrations (5 and 10 nM) of UM-Pif1 (lanes 3, 4) and AC-Pif1 (lanes 5, 6). The reactions were performed in a reaction buffer containing 20 mM Tris HCl (pH 7.8), 8 mM $Mg(CH_3COO)_2$, 100 mM KCl, 1 mM DTT, 0.1 mg/mL BSA, 100 μM dNTPs, and 1 mM ATP for 10 min at 30ºC. Reactions were terminated using 2X termination dye and were immediately heated to 95°C and loaded onto a pre-warmed denaturing polyacrylamide gel (12% polyacrylamide, 7 M urea), and reaction products were separated by electrophoresis for 80 min at 80 FEN1, subsequently dried, and analyzed, G) Comparison of amplitude of unwinding by Pif 1 (UM/AC-FL and UM/AC-ΔN) on different substrates. Data from the analysis was fit to a first order reaction [A{1-exp[-(ku*X)], in which A is the amplitude of the reaction, ku is the apparent rate constant of unwinding and X is time. Values are represented as mean $\pm$ SEM of at least three independent experiments

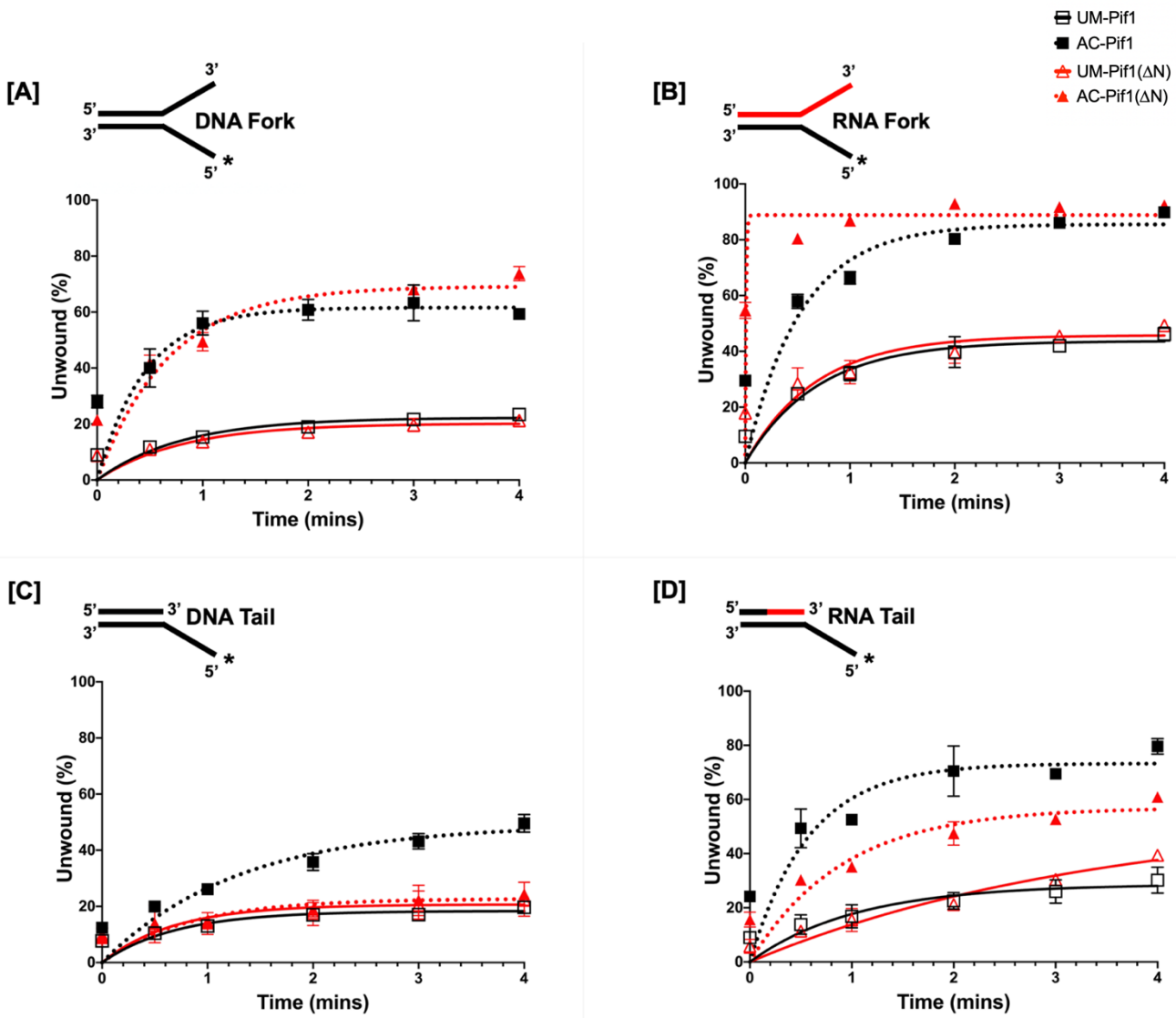
[A]
DNA Fork
3'
5'
3'
5'
*
Unwound (%)
Time (mins)
[B]
RNA Fork
UM-Pif1
AC-Pif1
UM-Pif1(ΔN)
AC-Pif1(ΔN)
[C]
DNA Tail
[D]
RNA Tail

Figure 2.4 continued

[E]

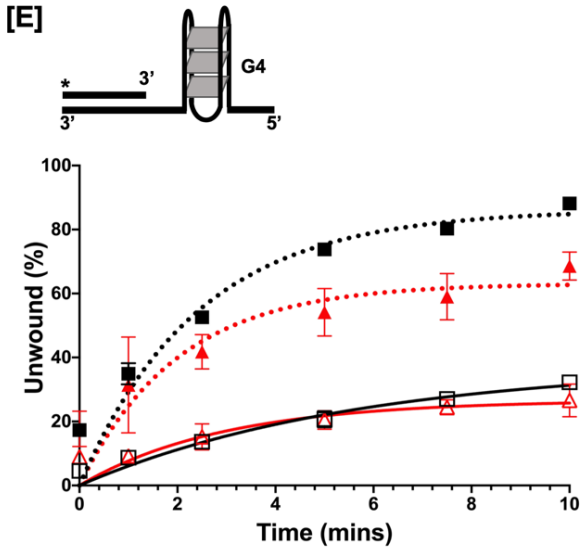

[F]

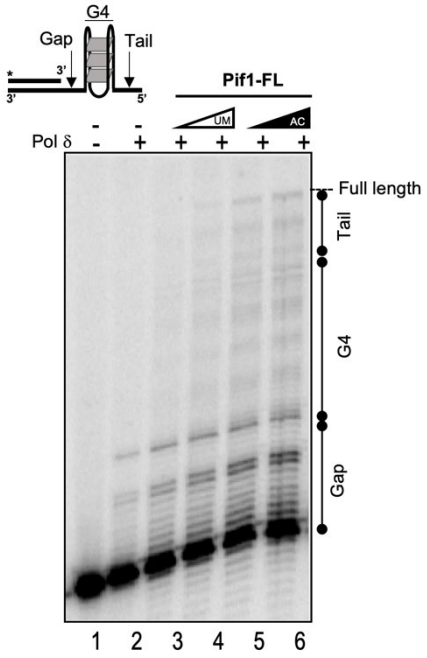

[G]

Pif1	DNA Fork	RNA Fork	DNA Tail	RNA Tail	G4
UM - FL	22.2 ± 2.2	43.6 ± 2.7	18.3 ± 1.5	28.6 ± 4.0	39.4 ± 13.1
AC - FL	61.6 ± 5.7	85.5 ± 6.1	49.2 ± 4.7	73.3 ± 6.0	80.8 ± 8.2
UM - ΔN	20.1 ± 2.2	45.7 ± 4.4	20.6 ± 2.2	54.7 ± 6.3	27.1 ± 2.8
AC - ΔN	69.1 ± 5.1	88.8 ± 7.8	22.7 ± 2.6	57.0 ± 4.8	58.7 ± 5.5

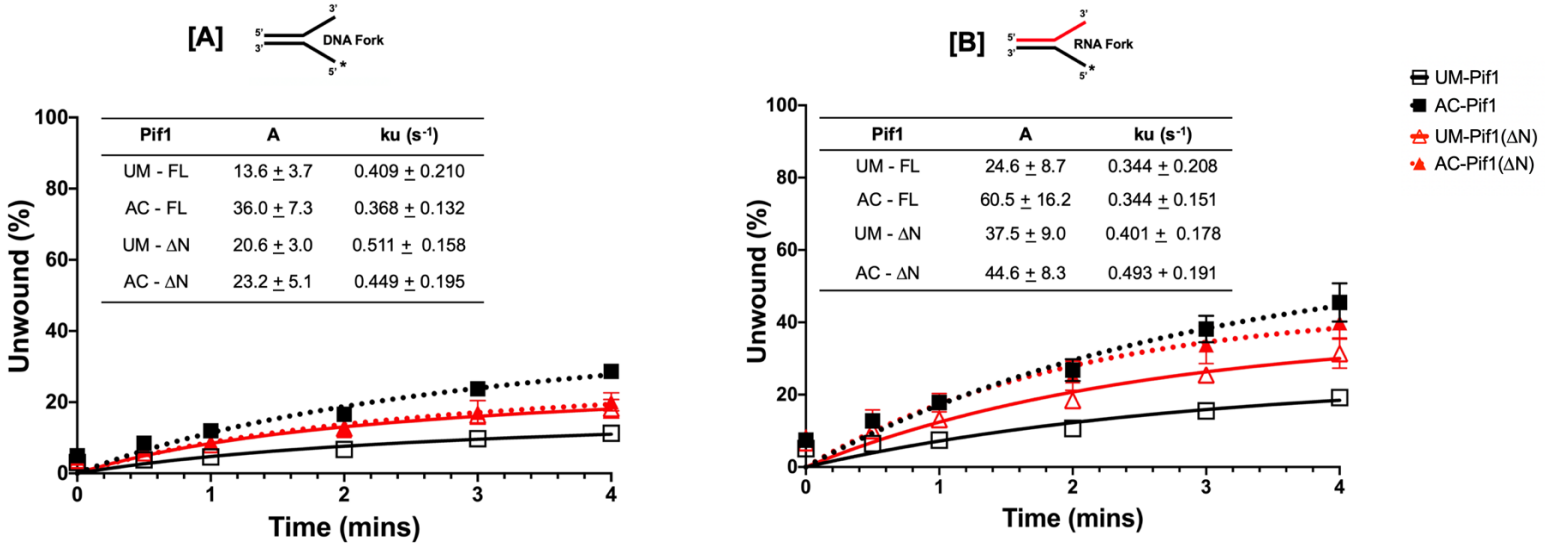

Pif1	A	ku (s^{-1})
UM - FL	13.6 ± 3.7	0.409 ± 0.210
AC - FL	36.0 ± 7.3	0.368 ± 0.132
UM - ΔN	20.6 ± 3.0	0.511 ± 0.158
AC - ΔN	23.2 ± 5.1	0.449 ± 0.195

Pif1	A	ku (s^{-1})
UM - FL	24.6 ± 8.7	0.344 ± 0.208
AC - FL	60.5 ± 16.2	0.344 ± 0.151
UM - ΔN	37.5 ± 9.0	0.401 ± 0.178
AC - ΔN	44.6 ± 8.3	0.493 + 0.191

Figure 2.5 Measurement of Helicase Activity Under Single Turnover Conditions.

The single turn over kinetics for measuring unwinding activity of 1nM of full length and N-terminus deleted Pif1 helicase activity was assessed in the presence of a protein trap (T50) and DNA trap (unlabeled 45mer complementary to displaced strand) over 6 time points (0'', 30'',1',2', 3' and 4') in the presence of 5nM IR labelled [A] DNA fork and [B] RNA fork. Data from the analysis was fit to a first order reaction [A{1-exp[-(ku*X)], in which A is the amplitude of the reaction, ku is the apparent rate constant of unwinding and X is time. Black line with open squares represents Pif1-FL and dotted black lines with filled squares represents acetylated form of Pif1-FL. Red line with open triangles represents Pif1ΔN and dotted red lines with filled triangle represents acetylated form of Pif1ΔN. Data from the analysis was fit to a first order reaction [A{1-exp[-(ku*X)], in which A is the amplitude of the reaction, ku is the apparent rate constant of unwinding and X is time. Values are represented as mean ± SEM of at least three independent experiments.

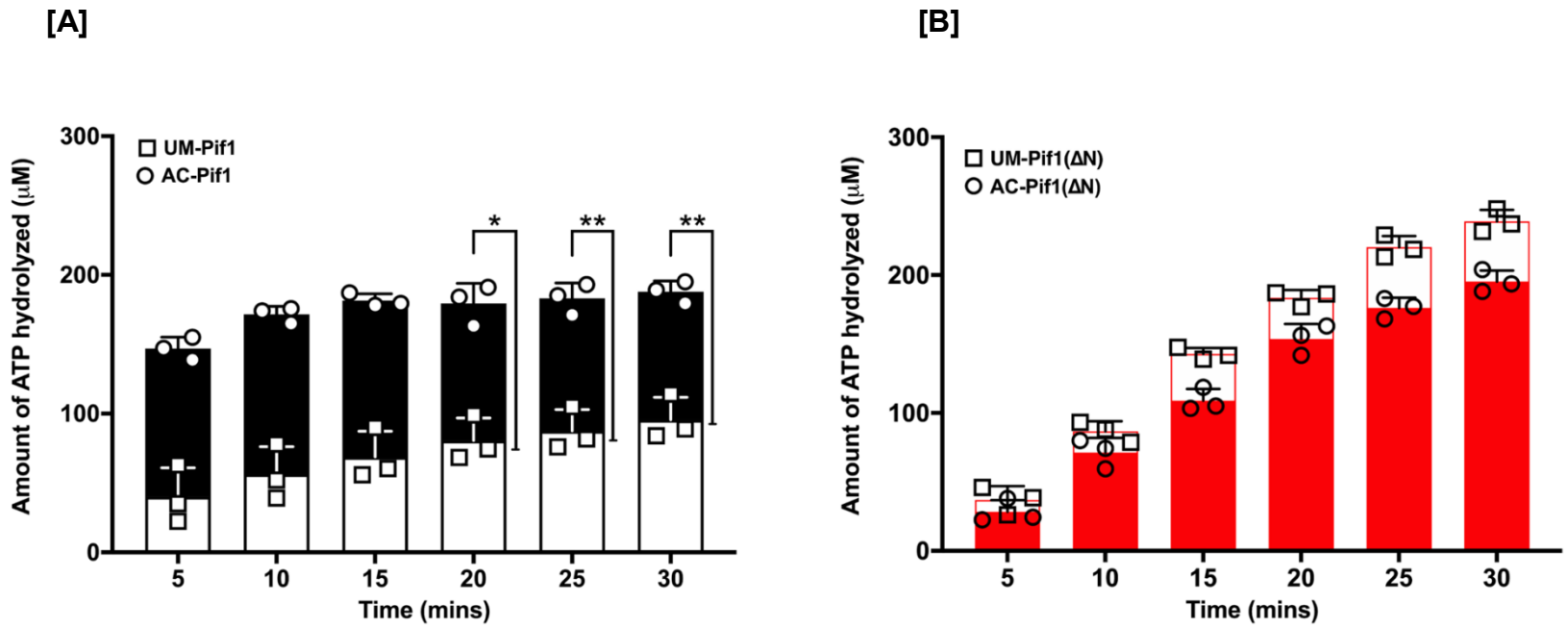

Figure 2.6 Pif1 ATPase is stimulated upon acetylation.

Using an NADH-coupled assay, the rate of ATP hydrolysis by [A] UM-Pif1 (open black bars) and AC-Pif1 (filled black bars) and [B] UM-Pif1ΔN (open red bars) and AC-Pif1ΔN (filled red bars) was measured in the presence of 45-nt ssDNA. Values are represented as the mean $\pm$ SEM of at least three independent experiments. *$p<0.05$, **$p<0.01$

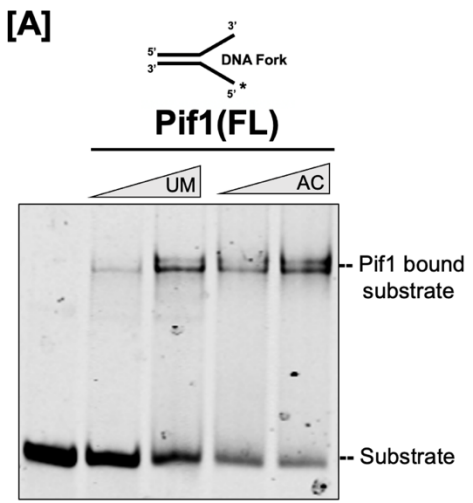

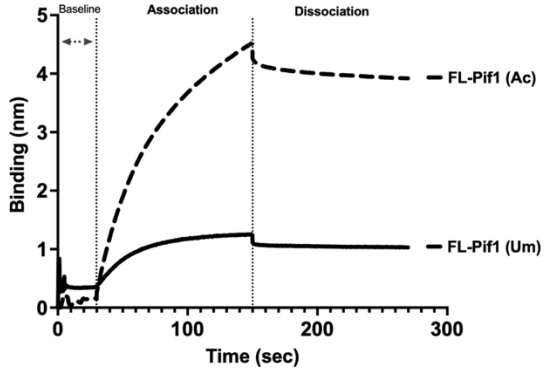

[C]

Pif1	K_D (in nM)
UM - FL	19.1 ± 5.1
AC - FL	7.2 ± 0.30
UM - ΔN	14.1 ± 1.5
AC - ΔN	15.2 ± 3.3

Figure 2.7 Characterizing Pif1 Binding Properties. Increased binding affinity induced by lysine acetylation.

[A] EMSA of increasing concentrations of Pif1 (100 and 200 nM) in both its unmodified and acetylated form bound to 5 nM of a DNA fork substrate. [B] Sensogram displaying measured binding kinetics of 125 nM Pif1 to an immobilized biotinylated 45nt biotinylated ssDNA using BLItz technology. [C] Binding affinity (K_D) of the unmodified and acetylated forms of Pif1-FL and Pif1ΔN.

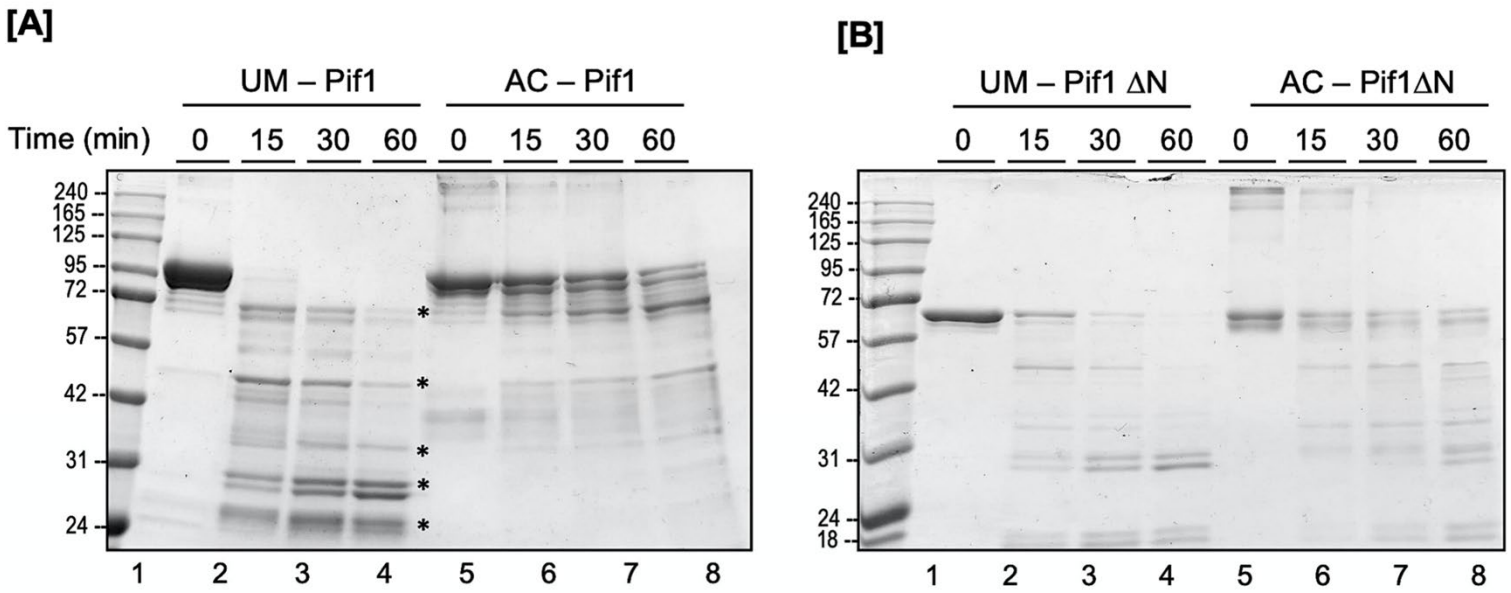

Figure 2.8 **Acetylation of Pif1 Induces a Conformational Change.**

A time course GluC degradation reaction of unmodified and acetylated [A] Pif1 and [B] Pif1ΔN is shown. [C] Quantitation of degraded products by full-length Pif1 [open squares (unmodified) *vs* black filled squares (acetylated)] and Pif1ΔN [open triangles (unmodified) *vs* red filled triangles (acetylated)]. Data obtained by Christopher Sausen Ph.D

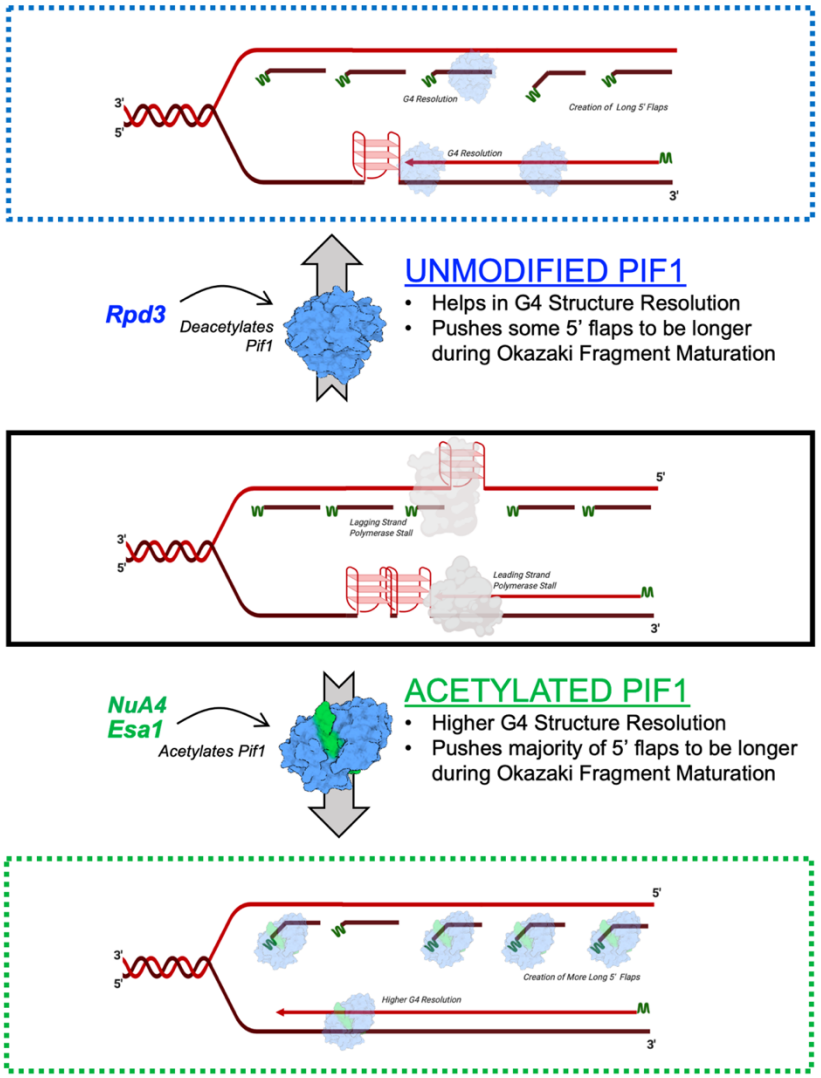

Figure 2.9 Model for Altered Acetylated Pif1 Activities

Middle Panel: Replication fork with two tandem G4 structures on the leading strand and one G4 structure on the lagging strand (replication stalled) and Okazaki fragments (RNA primers indicated in green). Top Panel: Unmodified Pif1 (or deacetylated by KDAC, Rpd3) is able to resolve one G4 structure on the leading strand and the G4 structure on the lagging strand allowing for synthesis of Okazaki fragments. Presence of UM-Pif1 (or deacetylated) allows for displacement of a few long 5' flaps during Okazaki fragment maturation. Bottom Panel: Acetylated Pif1 [by KAT, NuA4 (Esa1)] resolves the tandem G4 structures on the leading strand, resolves and allows synthesis over the G4 structure and pushes the majority of the flaps to be longer during Okazaki fragment maturation.

CHAPTER 3. LYSINE ACETYLATION OF REPLICATION PROTEIN A (RPA) ALTERS ITS BINDING PROPERTIES TO SINGLE STRANDED DNA

3.1 Abstract

Replication Protein A (RPA), a single-stranded DNA binding protein (ssDBP), is vital for various aspects of genome maintenance such as replication, recombination, repair and checkpoint activation. Binding of RPA to ssDNA protects it from degradation by cellular nucleases, prevents secondary structure formation and illegitimate recombination. In our current study, we identified the acetyltransferase, p300 to be capable of acetylating endogenous RPA on the 70kDa subunit. Interestingly, cell cycle status and exposure to specific DNA damaging agents impacted the acetylation status of RPA. Based on this observation, we evaluated the effects of lysine acetylation on the biochemical properties of RPA. Investigation of binding properties of RPA revealed that acetylation of RPA increased its binding affinity to ssDNA compared to unmodified RPA. The improvement in binding efficiency was most evident on the smaller length ssDNA oligomers. Acetylated RPA also bound more stably to ssDNA compared to the unmodified form of the protein. Our results suggest that during replication, the acetylation-based enhancement in the DNA binding properties of RPA may alter the choice of the lagging strand DNA processing pathway to prefer the longer flap pathway for processing, thereby improving genome fidelity.

3.2 Introduction

Replication protein A (RPA) is a highly conserved heterotrimeric protein in eukaryotes, and is involved in various aspects of DNA metabolism such as DNA replication, repair and recombination (249). Present at relatively high concentrations within human cells of ~1 μM (Klein et al, 2015), it functions as the major single strand DNA (ssDNA) binding protein (250). During various DNA transactions, high affinity binding of RPA to ssDNA stabilizes the DNA and protects it from degradation from cellular nucleases (251). Stabilization of ssDNA structure by RPA also prevents the formation of stable secondary structures that could impede DNA transactions (252) . Additionally, RPA serves to function as a platform for the assembly of a multitude of replication and repair associated proteins during various biological events. RPA was first isolated from HeLa cells where it was shown to play an important role in Simian Virus 40 (SV40) replication (253). RPA in eukaryotes is composed of 3 subunits: RPA1, RPA2 and RPA3 with molecular weights of 70kDa, 32kDa and 14kDa respectively (254). All three subunits are important for the formation of a stable and functional RPA complex.

RPA1 has four oligosaccharide/oligo nucleotide binding (OB) domains called DNA binding domains (DBDs) A, B, C and F, while RPA2 and RPA3 have one OB domain each - DBD D and DBD E, respectively (251,255). Different RPA DBDs are activated depending on the length of the ssDNA bound to it (256). It was previously suggested that RPA shows a sequential mode of interaction with ssDNA; (i) low affinity binding to ~8 nt ssDNA where DBD A and DBD B of RPA1 would interact (257), (ii) medium affinity binding to ~18-20 nt ssDNA with DBD A, B and C or RPA1 interacting, and (iii) high affinity binding to ~28-30nt ssDNA which implicated all three DBDs of RPA1 (A,B,C) and additionally DBD-D of RPA2 (257). However, multiple recent studies have updated the modular binding model to propose a dynamic binding model for RPA to ssDNA, wherein the binding of RPA to substrate is stable, however, it must be dynamically bound such that it easily hands-off the ssDNA substrate to its interacting protein partners (258). This model has been further improved in a study using hydrogen-deuterium exchange mass spectrometry (HDX-MS) to show dynamic binding by DBD-A and DBD-B and more stable binding by the TriC core made up of DBD-C, D and E (259).

During DNA replication, unwinding of the duplex DNA necessitates binding and protection by RPA on both the leading and lagging strand ssDNA templates (260-262). On the

leading strand, RPA inhibits priming by DNA polymerase alpha/primase (pol α), however, on the lagging strand, the priming function of pol α is stimulated in the presence of RPA (35). Additionally, RPA also influences lagging strand synthesis by stimulating the strand displacement activity of DNA polymerase δ (pol δ), which functions to create a 5' flap structure (263). In most circumstances, this structure is recognized, bound and cleaved by flap endonuclease 1 (FEN1) (46). However, creation of long 5' flaps permits stable binding of RPA to displaced flaps preventing FEN1 cleavage (57,264). Processing of RPA bound 5' flaps, requires the nuclease/helicase, Dna2, to displace RPA and cleave the flap to a length that is not optimal for RPA rebinding (265). FEN1 then cleaves the remainder of the flap allowing for ligation and maturation of the Okazaki fragments. Thus RPA functions as a governing switch that dictates the choice of flap processing during Okazaki fragment maturation (57).

RPA not only binds to ssDNA in order to direct synthesis, but it also works in conjunction with helicases to promote strand unwinding (257), especially with BLM helicase and WRN helicase (266). These protein-protein interactions allow for the removal of secondary structures that could be formed during the replication process. RPA has also been shown to possess strand annealing properties in the presence or absence of secondary structures (257). Bartos *et al* showed that in the presence of ssDNAs containing secondary structures, an increased amount of RPA led to a transient melting of the structures allowing the ssDNAs to anneal to their complimentary strands forming double stranded DNA (dsDNA) (257).

Furthermore, RPA plays an equally important role in DNA repair as it does in DNA replication. RPA has been implicated in the base excision repair (BER) pathway as it physically interacts with Uracil DNA glycosylase (UNG), an enzyme required for the removal of uracil formed from the deamination or misincorporation of cytosine (267-269) and thereby stimulating long flap BER pathway (267). During double-strand break DSB repair, the complementary strands are cut at similar positions in two places close to one another. These breaks lead to dissociation and inappropriate recombination with other ssBPs or other ssDNA (270). There are two pathways through which DSBs are repaired: non-homologous end joining (NHEJ) and homologous recombination (HR) (271). While NHEJ does not require sequence homology for repair, HR does, and thus this pathway is limited to G2 and S phases of the cell cycle (272). RPA is one of the proteins which when phosphorylated, works with phosphorylated Rad51 to find a homologous region for repair of the damaged strands (270). It is believed that other post-translational

modifications of RPA could be involved in DNA repair *via* HR but the exact details are unknown (272).

The ssDNA binding function of RPA and its interaction with protein partners are regulated within the cell using a variety of post translational modifications (PTMs). The most extensively characterized modification is that of RPA phosphorylation, specifically on the N terminus of the RPA2 subunit. Differential phosphorylation of RPA2 occurs during various phases on the cell cycle, with phosphorylation of RPA2 linked to the G1 to S transition (273) and dephosphorylation linked to the mitotic phase. RPA2 is also phosphorylated on exposure to various DNA damaging agents such as hydroxyurea (HU) and UV irradiation suggesting a role for phosphorylation in mitigating the damage response (254,274). Interestingly, the lysine residues on RPA1 are also subject to multiple forms of modifications, some of which may function as competing modifications. For example, RPA1 is known to undergo acetylation, SUMOylation, ubiquitinylation, and crotonylation. SUMOylation of RPA1 is known to recruit Rad51 to the location of damage where it is repaired by homologous recombination (275). Another PTM observed on all three subunits of RPA is ubiquitination (276). Following DNA damage, RPA-ssDNA recruits Ataxia telangiectasia and Rad3-related protein (ATR), ATR interacting protein (ATRIP) kinase and Pre-MRNA Processing Factor 19 (PRP19) complex to trigger phosphorylation and ubiquitination of RPA, which in turn activates ATR-ATRIP and the DNA damage response (DDR) (276,277). As a part of UV damage response, RPA was shown to undergo lysine acetylation (165). Lysine acetylation of RPA1 altered the efficiency of the nucleotide excision repair process (165). A recent report characterized RPA1 crotonylation in response to camptothecin (CPT) induced DNA damage, wherein they showed that the modification greatly enhanced the protein's interaction with ssDNA (278). While lysine mono-methylation of RPA1 has been identified in proteomic analysis, thus far, there are no reports characterizing this modification.

Our interest in understanding the regulatory mechanism of lysine acetylation on enzyme activity stemmed from the observation that multiple proteins involved in lagging strand maturation are modified by lysine acetylation. Acetylation of FEN1 and Dna2 imparted opposing effects on these proteins with FEN1 showing decreased nuclease activity whereas, Dna2 showed stimulated cleavage function. Since RPA is known to govern the choice of the lagging strand maturation pathway, in our current work we characterized the impact of lysine acetylation on the binding

property of RPA. Contrary to previous reports, we found that in addition to PCAF and GCN5, RPA1 is also acetylated by the acetyltransferase p300, both *in situ* and *in vitro* (165,279). The main role of p300 is to act as a transcription coactivator that aids in chromatin remodeling making it accessible for transcription (280,281). Additionally, p300 has also been shown to acetylate many DNA replication and repair proteins (FEN1 (167), Dna2 (167), WRN (193), Pol beta (282)). Our work reveals additional lysine acetylation sites on RPA1 than previously reported. We also found increase in levels of RPA1 acetylation to correspond with the G1/S phase of the cell cycle and also observed acetylated RPA directly at the replication fork. Similar to previous reports we observed an increase in RPA acetylation on exposure to UV damage and direct association of RPA1 with damaged forks. We further analyzed alterations in the dynamic binding of RPA on lysine acetylation and found that acetylation stimulates the binding activity of RPA to bind stably to shorter length ssDNA. The acetylated form of RPA was also slower in dissociating from the ssDNA compared to the unmodified form of RPA, in presence of a high excess of competing substrate. Additionally, the melting and annealing properties of RPA are also influenced by lysine acetylation. Our data suggests that changes to the binding function of acetylated RPA will undoubtedly impact protein-protein interactions, wherein RPA hands-off the substrate to other proteins in either replication or repair pathways.

3.3 Results

3.3.1 *In Vivo and In Vitro* Acetylation of RPA by acetyltransferase, p300

A study analyzing the acetylation status of proteins in a whole cell extract using high-resolution mass spectrometry (MS) identified residues K163, K167 and K259 on hRPA1 to be modified by lysine (K) acetylation (165). A subsequent study using serial enrichments of different post-translational modifications found that in addition to RPA1 (K163 and K577), RPA3, the 14 kDa subunit, (K33, K39) was also acetylated (283). In studies using HEK293T cells, the RPA1 subunit was co-transfected with different acetyltransferases, and only GCN5 and PCAF was reported as capable of acetylating RPA1 (196,197). Since numerous proteins in the DNA replication and repair pathway were modified by another KAT, p300, and because proteomic analysis identified acetylation signatures on RPA1 that could potentially be linked to p300 related signatures we wanted to test the ability of p300 in modifying RPA. To test endogenous RPA

acetylation, in the absence and presence of p300, we used the colon cancer wild-type cell line HCT116, and a p300 deficient cell line (HCT116^{p300-}), derived from HCT116 by targeting the exon 2 of the EP300 gene. Additionally, we also tested acetylation of RPA in HCT116^{p300-} cell line, transfected with increasing concentrations (1 µg or 2.5 µg) of plasmid expressing EP300 cDNA (HCT116^{p300-} + EP300). We observed RPA1 to be acetylated in all three cell lines using immunoprecipitation followed by western blot analysis. Acetylation levels of RPA1 was measured by immunoprecipitating proteins using a pan-acetyl lysine antibody, followed by immunoblotting with RPA1 antibody. Comparing the acetylation levels of RPA1, we observed ~ 2- fold reduction in the acetylation levels of RPA1 in HCT116^{p300-} compared to HCT116 cells (Figure 3.1A). On transfection with increasing concentrations of EP300 cDNA into the HCT116^{p300-} cells, we observed a corresponding increase in levels of acetylated RPA1 (Figure 3.1A). This observation indicates that p300 can acetylate endogenous RPA. Though RPA1, showed decreased level of acetylation in the p300 deficient cell line, compared to wild-type, we still observed basal levels of RPA1 acetylation. This suggests that in addition to p300, other redundant acetyltransferases, as previously reported, are capable of endogenously expressed RPA. Expression levels of the other KATs in both the wild-type and p300 deleted cells are shown in *Figure B-1A*. We repeated this experiment in HEK293T cells and observed a p300 associated dose-dependent increase in levels of endogenous RPA1 (*Figure B-1B*). We also tested acetylation status of RPA2 and RPA3 from both HCT116 and HEK293 cells but did not detect any lysine acetylation on these subunits (*data not shown*).

In-vitro acetylation of RPA1 by p300 was further confirmed using autoradiography (Figure 3.1B) and western blot analysis (Figure 3.1C). Unmodified RPA and acetylated RPA (modified using the catalytic domain of p300 and ^{14}C-acetyl CoA) were subjected to separation by SDS-PAGE gel electrophoresis and stained using Coomassie Brilliant Blue (CBB). We detected all three subunits of RPA on the stained gel (lanes 1, 2, Figure 3.1B). Autoradiography of the same gel revealed that in addition to the autoacetylation of the catalytic domain of p300, RPA1 and RPA3 (to a small extent) were also acetylated (lane 4, Figure 3.1B). We also analyzed RPA acetylation by western blot analysis using a pan acetyl lysine antibody and found RPA1 to be robustly acetylated by p300 (lane 3, Figure 3.1C) and the full-length p300 (lanes 3, 4, Figure 3.1C) to be autoacetylated. We did not detect acetylation of either RPA2 or RPA3 by western blotting (data not shown).

In order to study the role of RPA acetylation on its enzymatic properties, we used the full-length acetyltransferase, p300, to *in vitro* modify full length RPA containing all three subunits. Sites of acetylation on the p300 modified RPA, was determined using tandem mass spectrometry (MS/MS) on tryptic peptides. All peptide masses matched theoretical masses for tryptic peptides for human RPA. Spectra for acetylated peptides showed a mass change of +42 daltons indicating addition of an acetyl group (Figure B-2). Lysine sites that were previously identified to be acetylated on RPA1 in the proteomic analysis of whole cell extracts were also identified in our mass spectrometry analysis (K163, K167, K259, K489, K502 and K577). We were unable to identify any lysine residues on RPA2 or RPA3 that were *in vitro* acetylated by p300. However, this does not imply that these sites are not modified *in vitro*, as the absence of peptides containing these acetylated sites could be due to the poor ionization of the acetylated peptide, or the mass of the peptide being out of range for the set experimental values. Stoichiometric values for the extent of acetylation were not determined in these experiments. Of note, proteomic studies have also identified lysine residues K163, K167, K489, K502 and K507 on RPA1 to be potential targets for other forms of post-translational modifications such as ubiquitination (U), sumoylation (S) and mono-methylation (M) (Figure 3.1D), suggesting that there could be competing or combinatorial PTM on the protein.

3.3.2 RPA acetylation peaks during the G1/S phase of the cell cycle

Cellular events dictate the PTM status of proteins, in order to modify its properties, and thereby enhance the repertoire of the cellular proteome. Since RPA is vital to DNA replication stability and fidelity, we first determined if the cell cycle impacts the acetylation status of RPA. HEK293T cells were synchronized during different cell cycle phases as described in Materials and Methods and the levels of RPA1 acetylation during the different cell phases was determined. We used a pan-acetyl lysine antibody to immunoprecipitate acetylated proteins from different cell cycle phases, followed by immunoblotting for RPA1 to determine the acetylation status. We also performed this experiment in reverse, wherein we used RPA1 antibody to immunoprecipitate and a pan-acetyl lysine antibody to immunoblot and although we obtained similar results, the blots displayed significant background pixilation (*data not shown*). As shown in Figure 3.2A, total levels of RPA1 and acetylated RPA1 were altered during different cell cycle phases. Quantitation of AcRPA1 normalized to RPA1 levels, showed that acetylation of RPA1 peaked during the G1/S,

followed by S phase of the cell cycle (Figure 32B). Cell synchronization were confirmed by probing for the differential expression of cyclins during the various phases (*Figure B-3A*).

While there was a global increase in the acetylation of RPA1 during the G1/S phase, we were particularly interested in determining the acetylation status of RPA1 associated to the replication fork. In order to directly assess acetylation of RPA, we developed an antibody recognizing acetylated K163 of RPA1 ($RPA1_{K163ac}$). This antibody eliminated the need to immunoprecipitate acetylated proteins followed by immunoblotting using a pan-acetyl antibody. Specificity of the antibody to detect the K163 acetylated residue of RPA1 was confirmed using ELISA (*Figure B-4*). However, while anti-$RPA1_{K163ac}$ only detects a 70 kDa band on *in vitro* modified samples, it also detects ~ a 55 kDa band in cellular extracts, which corresponds to a proteolytic product (*Figure B-5*). This proteolytic product was shown to be stabilized on binding to ssDNA (284). Isolation of proteins on naked DNA (iPOND) technique using the $RPA1_{K163ac}$ revealed a similar trend to our previous study, wherein, we observed the high levels of RPA1 acetylation in the G1/S and S phase compared to other phases of the cell cycle (Figure 3.2C). These results indicate acetylation levels of RPA1 are regulated in response to the cell cycle. We were unable to enrich the iPOND eluates in order to immunoprecipitate RPA1 and probe its acetylation using a pan-acetyl lysine antibody.

3.3.3 RPA is acetylated in response to DNA damage repair

Next, we asked if DNA damage regulates acetylation of RPA, since both Dna2 and FEN1 show increased acetylation on UV damage (167). HEK293T cells were exposed to various DNA damaging agents such as hydroxyurea (HU), methane methoxy sulfonate (MMS), ultraviolet radiation (UV), and etoposide (ETP) and the change in acetylation pattern of RPA1 was analyzed. DNA damage was confirmed by the presence of markers such as phospho Chk1 (p-Chk1), phospho Chk2 (p-Chk2), phospho p53 (p-p53) and phospho H2AX (p-H2AX) (*Figure B-6*). Similar to both Dna2 and FEN1, RPA1 also showed increase in acetylation on exposure to UV radiation and did not display detectable increase in acetylation in response to other forms of damaging agents (Figure 3.3A). RPA1 levels were normalized and fold increase in levels of acetylated RPA1 levels were calculated and plotted in Figure 3.3B. Alterations in the phosphorylation of RPA32 serves as a control for known changes in response to DNA damaging agents (Figure 3.3C). Cells are known to undergo global hyperacetylation in response to either MMS (285) or UV (286) damage. Similar

to the cell synchronization studies (Figure 3.2D), we were interested in determining if the increase in cellular pools of acetylated RPA1 could be correlated to the RPA that is directly associated with the damaged fork. Using the iPOND assay we probed for the acetylation status of RPA1 directly associated with the damage fork using anti-RPA1$_{K163ac}$ and found that acetylated RPA1 correlated directly with repair of UV damaged forks. Overall, our results suggest that similar to checkpoint kinases that are activated in DNA damage response, RPA1 acetylation could specifically be involved in mediating the UV-induced damage response.

3.3.4 Acetylation of RPA increases its ssDNA binding affinity

Binding of RPA to ssDNA is initiated by weak dynamic interactions at lengths of ~ 8-10 nt involving the A and B domains, while high affinity binding of RPA requires ssDNA to be ≥ 28 nucleotides. We tested the binding efficiencies of unmodified and acetylated RPA on different length oligomers (20, 24, 29 and 32 nt) using electromobility gel shift assays (EMSAs). Based on the length of the ssDNA and known binding properties of RPA, we expected weaker binding to the 22 and 24 nt oligomers compared to high affinity binding to the 29 and 32 nt oligomers. To measure binding, we titrated varying concentrations of RPA (5, 10, 25 nM) in the presence of ssDNA (5 nM) and incubated at 37°C for 10 minutes. Following incubation, the reactions were loaded onto a 6% native gel, electrophoresed, and subsequently analyzed. Binding results indicated that RPA (unmodified and acetylated forms) showed binding to all 4 different length oligomers. Interestingly, irrespective of the length of the oligomer, the acetylated form of RPA showed higher binding efficiency compared to the unmodified form. However, it is important to note that the fold stimulation in binding of the acetylated form compared to the unmodified form correlated with the lengths of the oligomers. The 22nt oligomer showed the highest fold stimulation in binding by acetylated RPA (compare lanes 6 – 8 to lanes 14-16, 22-24, 30-32, Figure 3.4A). Smeared pattern of binding to the 22 and 24nt oligomer is consistent with dynamic binding property of RPA to shorter oligomers. Incubation of RPA and p300 in the absence of acetyl coenzyme A showed that it bound similar to the unmodified RPA. Additionally, RPA incubated with acetyl coenzyme A in the absence of p300 bound similarly to the unmodified RPA. The acetyltransferase, p300 was unable to bind to the substrate, suggesting that the observed shift was only due to RPA's interaction with the substrate (*Figure B-7*). The control experiments show that the increased binding

efficiency of acetylated RPA was due to lysine modification on the protein and not due to stabilizing interactions with the acetyltransferase.

In order to further characterize RPA-ssDNA interactions in real time, we used the label-free biolayer interferometry (BLI) technology to measure protein association and dissociation. Streptavidin biosensors were coated with 10 μM of different length biotinylated oligomers (20, 24, 28, 32 and 45 nt) for a period of 100 seconds and allowed to associate with specific concentrations of either unmodified RPA (RPA), RPA incubated with p300 (RPA+AT) or acetylated RPA (Ac-RPA) for a period of 300 seconds and then moved to a buffer wherein dissociation was measured for a period of 300 seconds. The resulting sensorgram allowed measurement of association and dissociation rate constants (k_a and k_d) and the equilibrium binding constant (K_D). An example of the sensorgram showing the association and dissociation of 100nM protein (RPA, RPA+AT, Ac-RPA) with a 28 nt oligomer is shown in Figure 3.4B. Measurements for binding of different concentrations of RPA with different length oligonucleotides were calculated and K_D values determined (Figure 3.4C). Measured binding constants of the unmodified form of RPA agreed with previously reported steady state measurements (287-289). For every tested length of oligonucleotide, we found that the acetylated form of RPA had significantly lower K_D compared to the unmodified RPA or the RPA bound to p300 (in the absence of acetyl coenzyme A). Calculation of the fold change in K_D revealed that similar to the EMSA results, fold change in binding constant was the highest for the shortest length oligonucleotide (20 nt) and the lowest for the longest length oligonucleotide (45 nt) measured (Figure 3.4D). The lower stimulation of binding for the longer length oligonucleotide was expected since RPA is capable of binding to oligonucleotides of this length with high affinity without the need for additional stimulation by acetylation.

3.3.5 Correlating sites of lysine acetylation on RPA1 to the increase in binding properties

To determine if there was a correlation between increased binding and the number of acetylation sites in the protein's DBD, we tested mutants of RPA1 subunit containing varying number of DBDs and acetylation sites. The DBD-F mutant contained only DBD-F domain and the linker region with 2 acetylation sites (K163 and K167); the FAB mutant contained DBD-F, DBD-A and DBD-B with 5 acetylation sites (K163, K167, K259, K331 and K379); the A1/A2 mutant contained two DBD-A domains fused together and two acetylation sites (K259) and ΔF-RPA

mutant contained all DBDs except DBD-F as well as 7 acetylation sites (K259, K331, K379, K443, K489, K502 and K577) (Figure 3.5). *In vitro* acetylation of the RPA1 mutants were confirmed both by autoradiography and by tandem mass spectrometry (*data not shown*). Unmodified and acetylated RPA1 mutants were incubated with a 30 nt TAMARA-labeled ssDNA and their binding affinities were analyzed by EMSA. Both the unmodified and acetylated forms of DBD-F mutant did not bind to the substrate. This was an expected result, since the DBD-F mutant does not contain any DBDs. However, this also confirms that acetylation on sites K163 and K167 alone cannot change the binding property of this mutant. Additionally, this result further shows that p300 does not complex with DNA to create a gel shift. Acetylation of all of the other mutants (FAB, A1/A2, and ΔF-RPA) showed increased DNA binding compared to their corresponding unmodified forms (Figure 3.5). From the observed fold change in binding efficiencies, we were unable to directly correlate number of acetylated lysine sites to a specific increase in binding property. Our results suggest that acetylation of one or more lysine residues in RPA1 results in increased ssDNA-binding efficiency, irrespective of the location of the acetylation sites with respect to the DBDs.

3.3.6 Acetylated RPA binds more tightly to its substrate compared to the unmodified form

It has been previously shown that ssDNA bound RPA rapidly dissociates in the presence of free RPA (258), however, it can remain stably bound to the ssDNA for many hours (290). Given that many biological pathways are dependent on the assembly of RPA on ssDNA and the subsequent hand-off to its interacting protein partners, we were interested in comparing the dissociation of unmodified and acetylated RPA in the presence of a competitor ssDNA substrate. For the competition assays, we chose two ssDNA substrates, a 24 nt and 28 nt substrate. Since only substrates longer than 28-30 nt are bound efficiently by RPA, we expected weaker binding on a 24 nt ssDNA and tighter binding to 28 nt ssDNA (291). We used higher concentration of RPA (unmodified and acetylated) to prebind the 24 nt ssDNA substrate compared to the 28 nt ssDNA substrate, in order to ensure 100% binding of RPA on the shorter length substrate. We pre-bound either unmodified RPA or acetylated RPA to a TAMARA-labeled 24 nt or a 28 nt ssDNA and allowed it to incubate for 2 minutes. We then introduced different fold excess (100, 250, 500 and 1000-fold) of a competitor substrate (unlabeled 28 nt substrate) and allowed it to incubate with the reaction for 8 minutes. The reactions were then analyzed using EMSA and the results are

graphically represented in Figure 3.6. The 28 nt competitor unlabeled ssDNA was able to compete off unmodified RPA from both the 24 nt and 28 nt substrate at much lower concentrations compared to the acetylated form of RPA. In the presence of 500-fold excess competitor, nearly 80% of the bound unmodified RPA had dissociated from both the 24 nt (black line, Figure 3.6) and 28 nt substrate (pink line, Figure 3.6). However, at the same concentration of the competitor, only ~33% of Ac-RPA was displaced from the 28 nt (pink dotted line, Figure 3.6) substrate and ~61% from the 24 nt substrate (black dotted line, Figure 3.6). Similarly, when all of the bound unmodified RPA was displaced in the presence of 1000-fold competitor, 77% of acetylated RPA was displaced from the 24 nt substrate (black dotted line, Figure 3.6) and 60% from the 28 nt substrate (pink dotted line, Figure 3.6). This data suggests that the acetylated form of RPA bound more tightly to the substrate and requires a significantly higher amount of competing substrate to be dissociated from its already bound state.

3.4 Discussion

In the present study, we demonstrate that RPA is acetylated *in vitro* by acetyltransferase p300. This was confirmed by mass spectrometry where nine lysine residues (K163, K167, K259, K489, K502 and K577) acetylated on the RPA1 subunit were identified. There was no acetylation observed on RPA2 and RPA3 subunits of the RPA complex. For most proteins, lysine residues near the DNA binding domains generally activate binding activity while those within the DNA binding domains usually repress binding efficiency to the substrate (199,292). Four of the six lysine sites identified in our study lie within the DBDs of RPA1. K259 resides within DBD-A, while K489, K502 and K577 are in DBD-C. The remaining two sites (K163 and K167) lie in the linker region between DBD-F and DBD-A. Interestingly, only K577 of the six lysine sites identified are conserved across species.

Acetylation of lysine residues on various proteins has been shown to activate or repress DNA binding depending on the proximity of the lysine residues to the DNA binding domains (199,292). Typically, addition of an acetyl group to a positively charged lysine residue results in neutralizing the charge on the amino acid, and in turn reducing affinity of the protein to the negatively charged DNA substrates. However, *in vitro* characterization of acetylated RPA1 revealed that acetylation increases its ssDNA binding affinity and its dsDNA melting property while reducing its ssDNA annealing function. This is likely due to alterations in the conformation

of the RPA1 subunit upon acetylation, which could potentially also impact interaction with both ssDNA as well as other protein interacting partners. Acetylation of p53 has been reported to open its normally closed conformation and increase DNA binding, thereby affecting its transcriptional activity (150). Similar to p53, we propose that acetylation of RPA may be resulting in a more 'open' conformation of the DNA binding domains on RPA1 providing more access to DNA. This could explain the increased affinity for binding ssDNA especially to shorter lengths of oligos as well as the 'tighter'/stronger binding to ssDNA binding as shown by the competitor assay. This has been observed for various other cellular proteins such as p53(150), E2F1(293), STAT3(232), GATA1 transcription factor(231), AP endonuclease (294), p50 and p65 (NF-κB) (295) amongst many others where acetylation improves their DNA binding properties. The increased and 'tighter' binding of Ac-RPA to ssDNA could also explain the increase in DNA melting and the decrease in ssDNA annealing to form dsDNA.

The number of sites acetylated on RPA1 subunit is proportional to the increase in ssDNA binding affinity as shown from our RPA1 mutant data. This suggests that acetylation of RPA1 at multiple lysine sites possibly causes a greater conformational change in the DBDs of RPA1 than at individual lysine acetylation sites. This further aids in our model of an 'open' conformation of acetylated RPA1 that results in better access to DNA. A crystal structure of Ac-RPA binding to ssDNA could shed some light on the 'open' conformation model, but this may be challenging given the dynamic nature of RPA complex on ssDNA.

Acetylation of non-histone proteins has been demonstrated to alter the stability of many proteins through competition between post-translational modifications such as acetylation and ubiquitination for the same lysine residues. Acetylation has been shown to increase stability and half-life of proteins such as p53(296), Smad7(297) and HNF-6(298), while it decreases protein stability of HIF-1α(299) and SV-40 large T-antigen(300). Under conditions of fork collapse such as UV damage (276), RPA1 has been reported to be ubiquitinated at sites K167 and K431, one of which is an acetylation site identified in this study. Ubiquitination at these sites by E3 ligase RFWD3 is a requirement for homologous recombination to proceed at stalled forks. However, unlike some proteins, RPA ubiquitination does not affect its stability or half-life. It is possible that these sites are subject to both acetylation and ubiquitination depending on the type of cellular stress the cells undergo. This then determines the specific repair pathways that need to be activated. Post-

translation modifications such as this could be a means of fine-tuning the activity of a multi-faceted protein such as RPA that has roles in multiple pathways.

Acetyltransferase p300 has been shown to acetylate both histones and non-histone proteins such as FEN1(53), Dna2(167), p53(301) and PCNA(302) amongst others, thereby regulating their function. Acetylation of PCNA prevents its excessive accumulation on chromatin(302) while p53 acetylation influences its activation and stability in the cell(301). During lagging strand synthesis, FEN1, Dna2 and RPA are required for Okazaki fragment processing and acetylation of these proteins affects their functionality. On acetylation, FEN1 activity is down regulated and this results in the creation of longer flaps of initiator RNA-DNA primers synthesized by the error prone DNA polymerase α (53). Ac-RPA then stably binds to the flap resulting in preferential processing through the long flap pathway, where proteins like Dna2 are recruited. Acetylation of Dna2 stimulates it endonuclease activity (167) allowing for RPA to be displaced and the flap cleaved. Following this, FEN1 can then cleave the remainder of the flap before ligation occurs. Taken together, this suggests that acetylation promotes genomic stability by processing Okazaki fragments through the long flap pathway, which would result in longer stretches of initiator RNA-DNA primer being removed.

Acetylation of proteins involved in DNA metabolism such as FEN1 and Dna2 have been previously reported to increase on UV-induced DNA damage(167). Similarly, we observed increase in acetylation of RPA1 upon DNA damage caused by UV damage despite no change in total levels of RPA. This suggested that acetylation of RPA1 does not affect RPA stability. Interestingly, we did observe basal level of RPA1 acetylation in these cells. This increase in acetylation of RPA could be attributed to various factors - increased HAT activity or decreased HDAC activity, either globally or specifically for RPA. While previous studies have shown both Gcn5 and PCAF as capable of acetylating RPA1, our studies now show that in addition to the reported KATs, p300 is also capable of acetylating RPA. Given that RPA interacts with a myriad of protein partners, we do not rule out that acetylation may be altering some of these interactions and further studies are needed to address it. In conclusion, RPA acetylation modulates its functions by increasing its ssDNA binding and dsDNA melting properties while reducing its ssDNA annealing property. These modifications in functions of RPA upon acetylation could have significant implications on various cellular pathways such as DNA replication, cell cycle checkpoint, DNA repair and recombination.

3.5 Materials and Methods

3.5.1 Recombinant Proteins

Full length hRPA was expressed in the E. coli expression strain BL21(DE3), and purified as previously described (303). The constructs for all hRPA1 DNA binding domains (DBDs) were generated using PCR in order to amplify specific regions of the RPA1 subunit. The PCR products were cloned into the pET28a vector, which introduced a six-histidine tag in frame at the C-terminus of each coding sequence. These constructs were expressed in E. coli BL21(DE3) cells and purified using Ni−NTA Superflow resin, as previously described (304). Catalytic subunit of p300 was expressed in E. coli expression strain BL21(DE3), and purified as previously described (194). Commercially available recombinant full length p300 (#31124), catalytic domain of p300 (#31205), were purchased from Active Motif, Carlsbad, CA.

3.5.2 Mass Spectroscopy Analysis

Tandem mass spectra from *in vitro* acetylated full-length RPA was collected in a data-dependent manner with an LTQ-Orbitrap Velos mass spectrometer running XCalibur 2.2 SP1 using a top-fifteen MS/MS method, a dynamic repeat count of one, and a repeat duration of 30 seconds. Enzyme specificity was set to endoproteinase Lys-C, with up to two missed cleavages permitted. High-scoring peptide identifications are those with cross-correlation (Xcorr) values of ≥1.5, delta CN values of ≥0.10, and precursor accuracy measurements within ±3 ppm in at least one injection. A mass accuracy of ±10 ppm was used for precursor ions and a mass accuracy of 0.8 Da was used for product ions. Carboxamidomethyl cysteine was specified as a fixed modification, with oxidized methionine and acetylation of lysine residues allowed for dynamic modifications. Acetylated peptides were classified according to gene ontology (GO) annotations by Uniprot.

3.5.3 Oligonucleotides

Synthetic oligonucleotides including those containing 5’ biotin conjugation or 5-TAMRA label were purchased from Integrated DNA Technologies (IDT), Coraville, IL. Biotinylated oligomers were used in BLItz assays to allow for binding to the streptavidin biosensors (Forte

Biosciences, CA). Oligomers used in biochemical assays were either labeled with radiolabeled (^{32}P) or fluorescently labeled (5-TAMRA). Radiolabeling was performed on the 5' end of oligonucleotides using [γ-^{32}P] ATP ([6000μCi/mmol] (Perkin Elmer) and polynucleotide kinase (Roche Applied Science) as previously described (305). Oligomer lengths and sequences (in the 5'-3' orientation) are provided in Table B-1.

3.5.4 In Vitro Acetylation

Recombinant human RPA was acetylated by incubating it in 1X histone acetyltransferase (HAT) buffer [50 mM Tris-HCl (pH 8.0), 10% (v/v) glycerol, 150 mM NaCl, 1mM dithiothreitol, 1mM phenylmethylsulfonyl fluoride, 10 mM sodium butyrate] with either the full length (or catalytic domain) of p300, full length GCN5, full length PCAF and acetyl CoA in a 1:1:10 ratio [RPA (full length or RPA1mutants) : acetyltransferase : acetyl CoA] for 30 mins at 37°C. The unmodified RPA (UM-RPA) control and the control with RPA and p300 (RPA+AT) were treated similar to the acetylated RPA (Ac-RPA). For autoradiography, *in vitro* acetylation reactions were performed using 0.1 μCi [^{14}C] acetyl coenzyme A (Perkin Elmer Life Sciences). The unmodified and acetylated forms of RPA were separated on a 4-15% SDS PAGE gel. After electrophoresis, the gels were stained with Coomassie brilliant blue (CBB), pictured and subsequently dried for autoradiography analysis.

3.5.5 Mammalian Cell Culture

Human embryonic kidney (HEK293T) cells (CRL-1573) was purchased from ATCC, USA and cultured in Minimum Essential Media (MEM) supplemented with 10% fetal bovine serum (FBS), 2 mM L-glutamine, 1% penicillin/streptomycin. HCT116 parent wild-type cells and HCT116 p300 knockout D10 clone was purchased from Cancer Research UK Cambridge Institute and cultured in McCoy's 5A medium supplemented with 10% FBS, 2mM L-glutamine and 1% penicillin/streptomycin. Cells were incubated at 37°C in a humidified 5% CO_2 environment and grown to approximately 80% confluency before the next passage or further experiments. The EP300 cDNA plasmid in pcDNA3.1- p300 was a gift from Warner Greene (Addgene plasmid # 23252). For transfection experiments, 0.7 x 10^6 cells (in 3 mL) of either HEK293 or HCT116 $p300^-$ in the respective media was seeded in a T-25 flask and 24 hours later was transfected with EP300

plasmid construct (1 µg or 2.5 µg) using Lipofectamine 3000 according to the manufacturer's protocol (Invitrogen). Following 24 hours of transfection, the cells were washed with 1X PBS, harvested and lysed in RIPA buffer containing 10mM sodium butyrate.

3.5.6 Cell Synchronization

HEK293T cells were arrested in different cell cycle phases using the following methods: For cells in G0/G1: cells were incubated in serum-free media for 72 hours before harvest; for cells in G1/S: cells were treated with 2.5mM thymidine for 17 hours, followed by washing the cells with 1X PBS, adding fresh media and further treatment with 2.5mM thymidine for 17 hours before harvest; for cells in S: cells were treated with 2.5mM thymidine for 17 hours before harvest and; for cells in M: cells were treated with 100 ng/mL Nocadozole (Sigma) for 18 hours before harvest. Following treatment all cells were processed as outlined above.

3.5.7 DNA Damaging Agent Treatment

For hydroxyurea (HU) treatment, cells were treated with 4 µM HU for 1, 3 and 6 hours. For methyl methanesulfonate (MMS) treatment, cells were treated with 2 mM MMS for 4, 8 and 12 hours. For ultraviolet (UV) treatment, cells were washed and maintained in warm 1X PBS during UV exposure. UV radiation of 10 J/m^2 was administered at 254 nm (UV-C) using a CL-1000 UV crosslinker (UVP, CA). Media was then replaced in the dishes and cells were incubated for 4, 8 and 12 hours before harvesting the cell lysate.

After specified hours of treatment, cells were washed thrice with 1X PBS and lysed in RIPA buffer containing 10mM sodium butyrate, lysated were quantified and further used in immunoprecipitation and western blot experiments. Dimethyl sulfoxide (DMSO) was used as the untreated control for HU, MMS and ETP experiments. For the UV experiment, untreated cells were handled in a similar manner as the treated cells with the exception of exposing cells to UV.

3.5.8 Isolation of proteins on nascent DNA (iPOND) Assay

HEK293T cells were subject to iPOND assay using a previously published protocol (306). Cell synchronization or treatment with different damaging agents were performed as outlined above. Synchronized or treated HEK293T cells (1 x 10^8) were labeled with 20 µM EdU for 15 min

alone or chased in the presence of 25 µM thymidine. Labeled cells were fixed and subjected to click-chemistry as described in the protocol. Replication proteins were eluted under reducing conditions by boiling in 2X SDS-sample buffer for 60 min. All buffers in the assay contained 10mM sodium butyrate to prevent KDAC activity and subsequent loss of acetylation signal from RPA1. Samples were then analyzed by western blotting as indicated in figure legend (Figure 3.2D and Figure 3.3C).

3.5.9 Immunoprecipitation

Immunoprecipitation was performed using the protocol described in the Dynabeads protein G manual (Thermo Fisher Scientific, MA) with minor modifications. Briefly, 20 µl of antibodies to acetyl-lysine or control IgG were prebound to 1 mg of HEK293 whole cell extract from different DNA damaging treatments and cell cycle phases with 200 µl of 1X PBST for 1 hour at room temperature with end-over mixing. Dynabeads (50 µl) were prepared by magnetic separation to remove the buffer and cell lysates were added to the beads and incubated with end-over mixing for 30 mins at room temperature. The Dynabeads-Ab-antigen complex was then washed thrice with 200 µls of washing buffer and separated on a magnet between washes. Elution was carried out using 20 µl Elution buffer and 20 µl of premixed 2X NuPAGE LDS sample buffer with NuPAGE sample reducing agent followed by heating the samples at 70°C for 10 mins. The immunoprecipitate was separated on the magnet and the supernatant was separated on precast 7.5% TGX gels (Bio-Rad). Western blot analysis was performed with anti-RPA1 antibody (Millipore # MS-692-P).

3.5.10 Western Blot Analysis

Synchronized or treated human embryonic kidney (HEK293T) cells were lysed in RIPA buffer (Thermo Fisher Scientific # 89901) containing 10mM of sodium butyrate. Protein concentration was determined using BCA Protein Assay (Pierce). Cell lysates (30 µg) were separated on precast 4-15% or 7.5% SDS-polyacrylamide Criterion gels (Bio-Rad, Hercules, CA) and transferred to polyvinylidene difluoride (PVDF) membranes (Bio-Rad). The following primary antibodies were used in overnight incubations at 4°C: RPA1, p-RPA2, RPA2, p-p53, p-Chk2, p-H2AX and GAPDH. Secondary antibody (HRP-conjugated anti-rabbit IgG, anti-goat IgG

or anti-mouse IgG) was added and incubated at room temperature for 1 hour. Blots were visualized using Amersham ECL western blotting detection reagent (GE Healthcare Life Sciences, Pittsburg, PA) and GE ImageQuant LAS4000 Imager. Blots were quantified by densitometry using LI-COR Image Studio Lite Ver 5.2.

3.5.11 Antibodies used in this study:

Anti-acetyl lysine (Cell Signaling, 9441), anti-RPA1 (Thermo Fisher Scientific, MS692P0), anti-RPA2 (Santa Cruz Biotechnology, sc-14692), anti-RPA3 (Santa Cruz Biotechnology, sc-30411) and anti-GAPDH (Santa Cruz Biotechnology sc-25778), anti-p300 (Millipore, 05257), anti-CBP (Cell Signaling, 7389), anti-acetyl $CBP_{K1499ac}$ (Cell Signaling, 4771), GCN5L2 (Cell Signaling, 3305), anti- p-RPA2 [phospho T21] (Abcam, ab109394) anti-p-Chk1 (Cell Signaling, 2348) anti-p-Chk2 (Cell Signaling, 2197), anti-p-H2AX (Cell Signaling, 9718), anti-p-p53 (Cell Signaling, 9286) and all secondary antibodies were purchased from Cell signaling.

3.5.12 Generation of RPAK163ac Antibody

The anti-RPAK163ac antibody was generated and purified Genmed Synthesis Inc., Texas. Briefly, two peptides were synthesized, one specifically for antibody production and affinity purification (C+AYGASK(ac)TFGKAAGP) and a control peptide for affinity purification (C+AYGASKTFGKAAGP). These peptides were purified to get >75% purity and were conjugated to keyhole limpet hemocyanin (KLH) carrier protein. This was then injected into 2 rabbits to generate the antibody. The antibody was subsequently purified using affinity columns and ELISA was performed to confirm specificity of the antibody.

3.5.13 BLItz Analysis

The BLItz binding system was equipped with a Dip and Read Streptavidin (SA) biosensors (ForteBio, CA, USA). BLItz binding assays were performed to measure binding between unmodified RPA (UM-RPA), RPA in presence of acetyltransferase p300 (RPA+AT) or acetylated RPA (Ac-RPA) with biotinylated ssDNA substrates. 10 μM of the biotinylated oligo was immobilized by the Streptavidin (SA) biosensor for 120 seconds. The Streptavidin (SA) biosensor immobilized by biotinylated oligo was dipped into 4 μl of RPA (UM or +AT or Ac) solution at

different concentrations (31.25, 62.5, 125 or 250 nM) for 150 second association, and 150 second dissociation in 1X HAT buffer. The real-time wavelength shift was recorded and analyzed by ForteBio software.

3.5.14 Electrophoretic Mobility Gel Shift Assays

Binding efficiency of Um-RPA, RPA+AT and Ac-RPA to 20, 25, 29 and 32 nt ssDNA were assessed using electrophoretic mobility gel shift assays. Five nanomolar of substrate was incubated with increasing concentrations (1, 2.5, and 5 nM) of either unmodified hRPA (Um-RPA) or acetylated hRPA (Ac-RPA) and incubated for 10 min at 37 °C in EMSA buffer consisting of 50mMTris-HCl (pH 8.0), 2 mM dithiothreitol, 30 mM NaCl, 0.1 mg/ml bovine serum albumin, and 5% glycerol. The reactions were loaded on pre-run 6% polyacrylamide gels in 1X Tris-borate EDTA (TBE) buffer. Gels were subjected to electrophoresis for 1 hour 45 mins at constant 180 V.

3.5.15 Competitor Assay

Similar to the electrophoretic mobility gel shift assay, the binding efficiency of Um-RPA and Ac-RPA to radiolabeled substrates (24 nt and 28 nt) in the presence of varying concentrations of a cold competitor 28 nt oligomer were assessed. Five nanomolar of radiolabeled substrate was pre-incubated with 100nM of hRPA (Um-RPA and Ac-RPA) at 37 °C for 2 minutes. To this reaction a competing non-radiolabeled oligomer (28 nt) was added at 100-, 250-, 500- and 1000-fold excess of radiolabeled primers and the reactions and further incubated for an additional 8 mins at 37 °C. Reactions were then loaded and electrophoresed similar to conditions described above.

3.5.16 Gel Analysis

Radioactive gels from all assays were dried, exposed to phosphor screen and analyzed using the Image Quant software as previously described (307). The percent of RPA bound to substrate is defined as [bound/(bound+unbound)]. Fold change is defined as [bound (Ac-RPA/bound (UM-RPA)]. Assays containing the TAMRA, labeled oligonucleotides were visualized on a Typhoon FLA9600 Imager (GE Biosciences) using the preset laser excitation and emission settings, with a photomultiplier gain of 200 V.

Figure 3.1 Acetylation of RPA1 Subunit.

(A) IP-western blot analysis of RPA1 acetylation in wtHCT116, HCT116 p300- and HCT116 p300^{-} cells rescued with EP300 expression. (B) In vitro acetylated RPA was subjected to SDS-PAGE analysis and stained using Coomassie brilliant blue (CBB). The same gel was subsequently analyzed by autoradiography (X-ray). (C) In vitro acetylation of RPA and full-length p300 was visualized by Western blot analysis using an anti-acetyl lysine antibody (D) Domains of Replication Protein A Subunit 1. Full length RPA was modified by in vitro acetylation using p300 and subject to MS/MS mass spectrometry. Acetylated lysine residues on RPA1 and their positions are denoted. Competing modifications on the same lysine residue previously reported by proteomic studies are indicated, ubiquitination (square), sumoylation (triangle) and methylation (circle). Data obtained by Sneha Surendrahan, PhD.

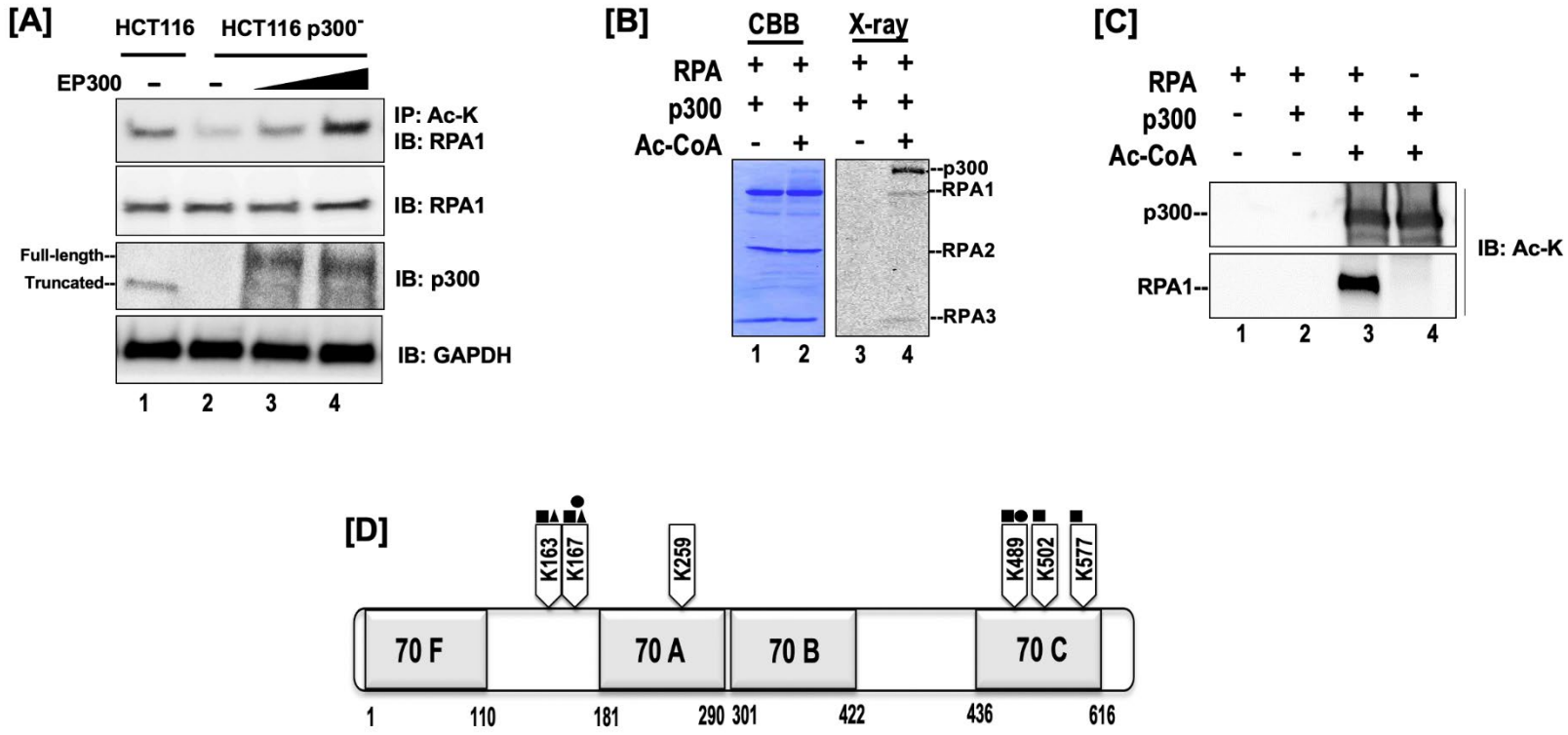
[A]
HCT116
HCT116 p300-
EP300 - - +
IP: Ac-K
IB: RPA1
IB: RPA1
Full-length--
Truncated--
IB: p300
IB: GAPDH
1 2 3 4
[B]
CBB
X-ray
RPA + + + +
p300 + + + +
Ac-CoA - + - +
--p300
--RPA1
--RPA2
--RPA3
1 2 3 4
[C]
RPA + + + -
p300 - + + +
Ac-CoA - - + +
p300--
RPA1--
IB: Ac-K
1 2 3 4
[D]
K163
K167
K259
K489
K502
K577
70 F
70 A
70 B
70 C
1 110 181 290 301 422 436 616

Figure 3.2 RPA1 Acetylation is Cell Cycle Dependent

(A) HEK293T cells were synchronized during different phases using either serum starvation or specific chemicals as described in the Materials and Methods. Cell lysates from different cell cycle phases were immunoprecipated using a pan acetyl-lysine antibody and immunoblotted using RPA1 specific antibody. (B) Graphical representation of change in levels of acetylated RPA1 during different cell cycle phases in HEK293T cells. * p-value < 0.05, *** p-value < 0.001; (C) HEK293 cells synchronized in various cell phases were subject to an iPOND assay. Lysates from the analysis were evaluated for the presence of acetylated RPA1 on the nascent replication strand. Figures A and C are representative gels, and the error bars in (B) are for the average of three independent experiments. Data obtained by Sneha Surendrahan, PhD (A and B) and Olivia Howald (C).

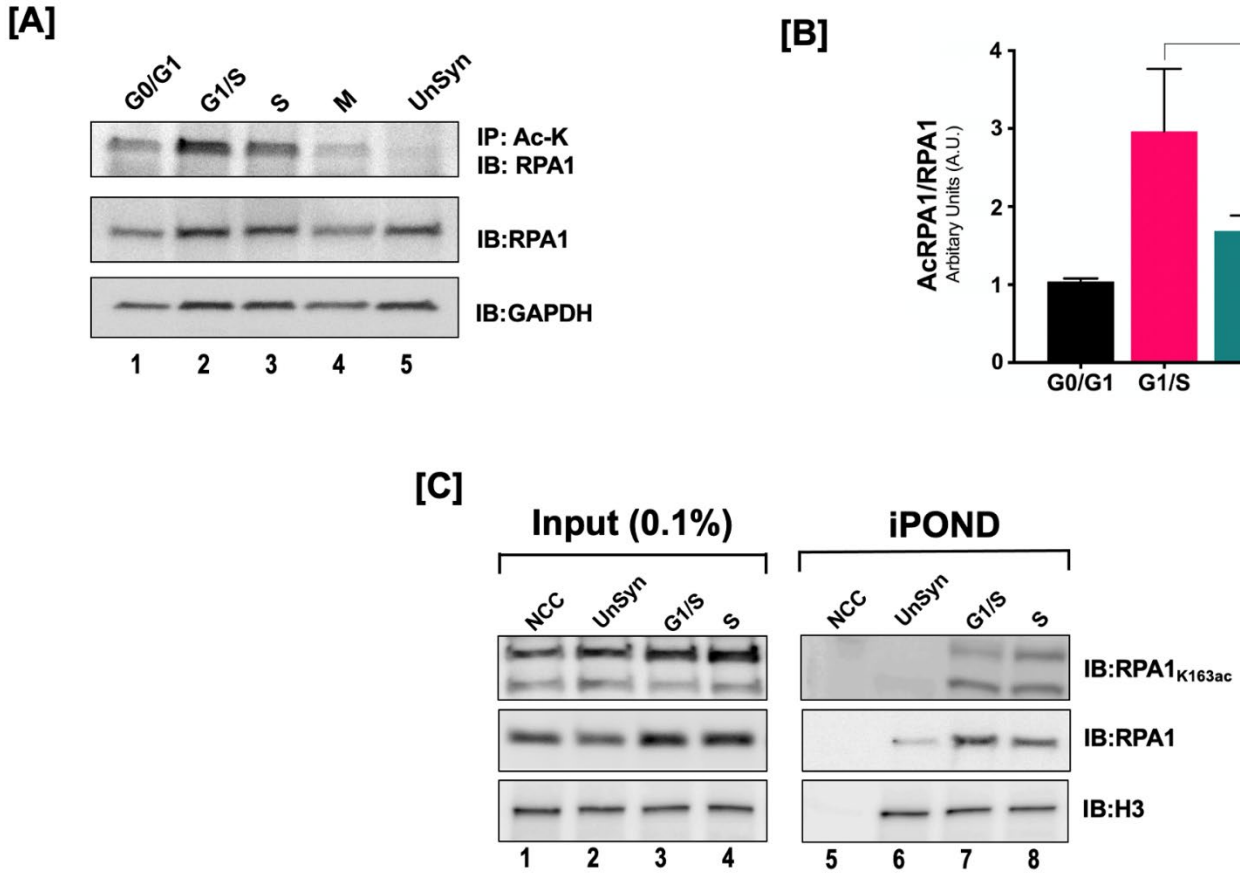
[A]
G0/G1
G1/S
S
M
UnSyn
IP: Ac-K
IB: RPA1
IB:RPA1
IB:GAPDH
1
2
3
4
5
[B]
AcRPA1/RPA1
Arbitary Units (A.U.)
***
*
0
1
2
3
4
G0/G1
G1/S
S
M
UnSyn
[C]
Input (0.1%)
iPOND
NCC
UnSyn
G1/S
S
IB:RPA1K163ac
IB:RPA1
IB:H3
1
2
3
4
5
6
7
8

Figure 3.3 Acetylation of RPA1 is Triggered on UV Damage to the Cells

(A) HEK293T cells were treated with different DNA damaging agents as described in the Materials and Methods. Cell lysates from the different treatments were immunoprecipitated using a pan acetyl-lysine antibody and immunoblotted using RPA1 specific antibody. Graphical representation of (B) change in levels of acetylated RPA1 and of (C) phospho-RPA2 on treatment with different DNA damaging agents in HEK293T cells (D) HEK293 cells treated with different DNA damaging agents (HU and ETP – 6 hours, MMS and UV – 12 hours), were subject to an iPOND assay. Lysates from the analysis were evaluated for the presence of acetylated RPA1 on the nascent replication strand. Figures A and D are representative gels, and the error bars in B and C are for the average of three independent experiments. * p-value ≤ 0.05,** p-value ≤ 0.01, **** p-value ≤ 0.0001. Data obtained by Sneha Surendrahan, PhD (A-C).

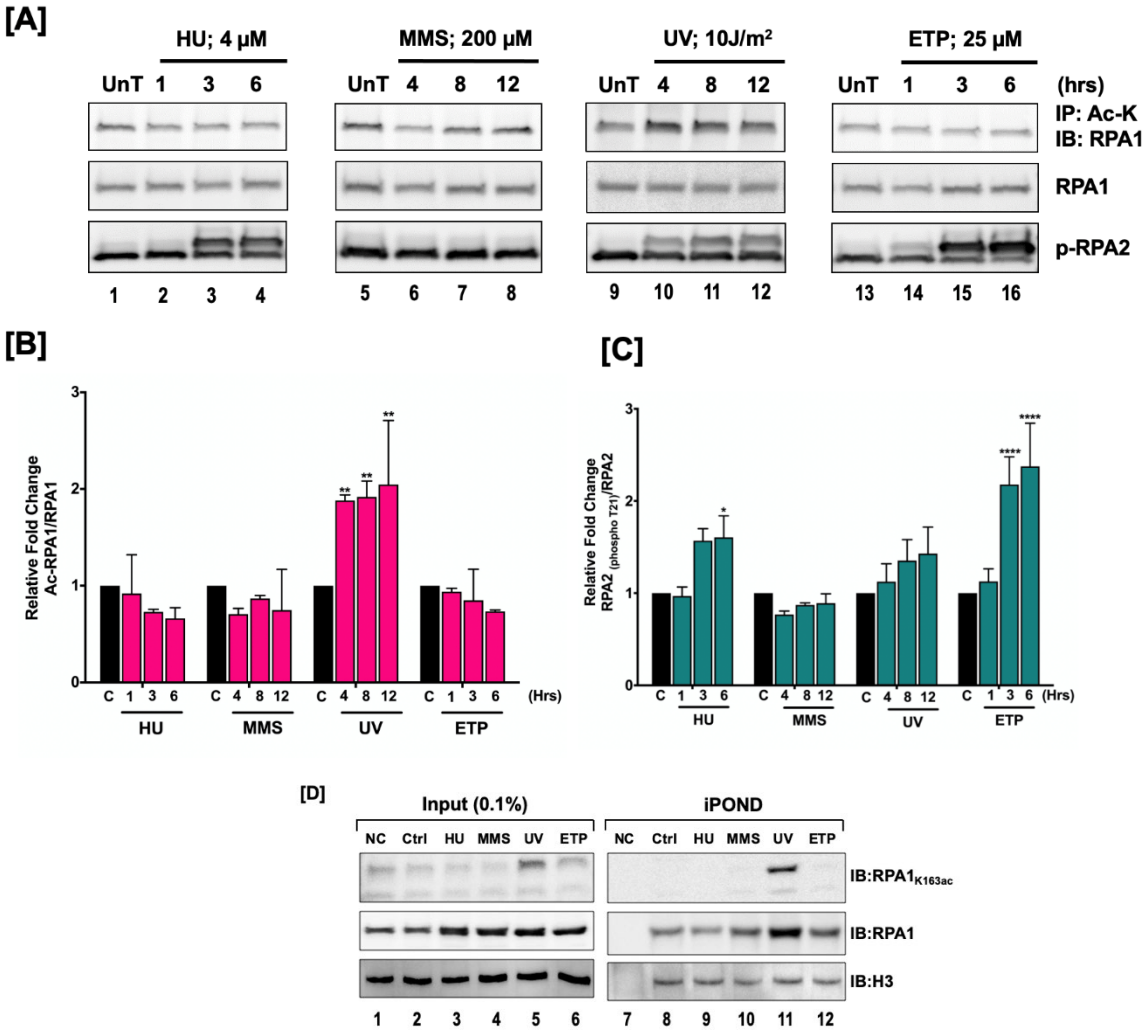
[A]
HU; 4 μM
MMS; 200 μM
UV; 10J/m2
ETP; 25 μM
UnT 1 3 6
UnT 4 8 12
UnT 4 8 12
UnT 1 3 6
(hrs)
IP: Ac-K
IB: RPA1
RPA1
p-RPA2
1 2 3 4 5 6 7 8 9 10 11 12 13 14 15 16
[B]
Relative Fold Change Ac-RPA1/RPA1
C 1 3 6 C 4 8 12 C 4 8 12 C 1 3 6 (Hrs)
HU MMS UV ETP
[C]
Relative Fold Change RPA2 (phospho T21)/RPA2
C 1 3 6 C 4 8 12 C 4 8 12 C 1 3 6 (Hrs)
HU MMS UV ETP
[D]
Input (0.1%)
iPOND
NC Ctrl HU MMS UV ETP NC Ctrl HU MMS UV ETP
IB:RPA1K163ac
IB:RPA1
IB:H3
1 2 3 4 5 6 7 8 9 10 11 12

Figure 3.4 Characterizing the Binding Property of Acetylated RPA

(A) Increase Binding Efficiency of Ac-RPA. Binding efficiency of unmodified and acetylated RPA was studies using EMSA. Five nanomolar of substrate of varying lengths (20, 24, 29 and 32nt) were incubated with increasing concentrations (5, 10, 25 nM) of Um-RPA or Ac-RPA, and the reactions were incubated for 10 min at 37°C and reactions were subsequently separated on a 6% polyacrylamide gel. The labeled substrate is depicted above the gel with the asterisk indicating 5' of the ^{32}P label. The substrate alone and the complexes containing RPA-bound substrate are indicated beside the gel at the right. Fold change in the binding of acetylated RPA compared to the unmodified RPA has been denoted below the lane numbers. (B) Sensorgram obtained using streptavidin biosensor coated with 10μM 28nt biotinylated oligonucleotide incubated with 160nM RPA, RPA+AT and Ac-RPA. The coating of the biosensor and the association and dissociation curves are shown in the sensorgram. (C) Fold change in binding affinity of RPA+AT and Ac-RPA compared to Um-RPA were calculated. The inverse fold change was then plotted graphically to show the stimulation in binding efficiencies of the Ac-RPA compared to Um-RPA and RPA+AT. (D) Data from the sensorgrams were fit globally to a 1:1 binding model to yield equilibrium dissociation constant (K_D). Values for K_D measurements for different length oligos are listed in the table.

[A]

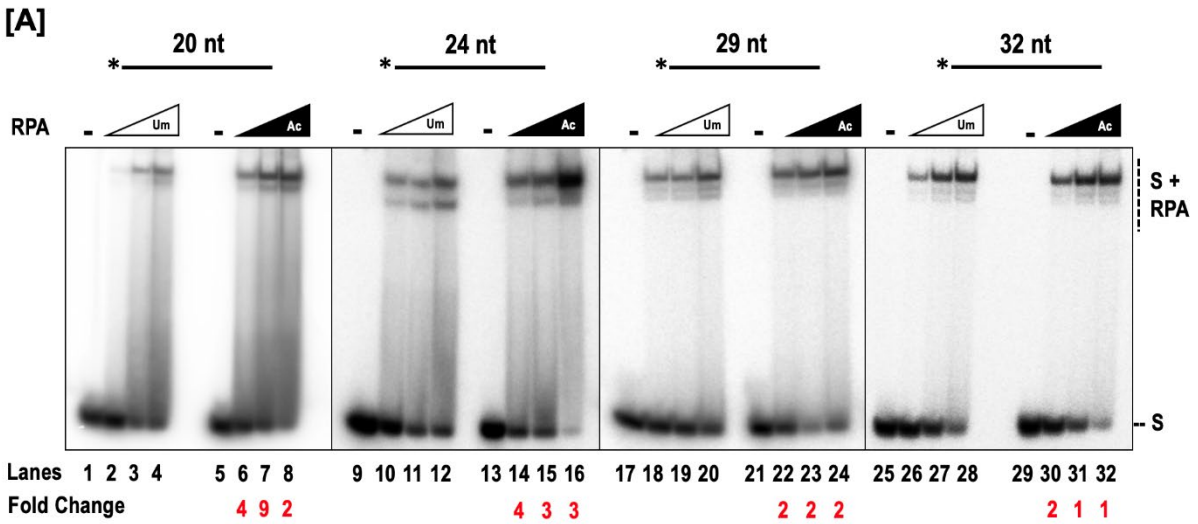

[B]

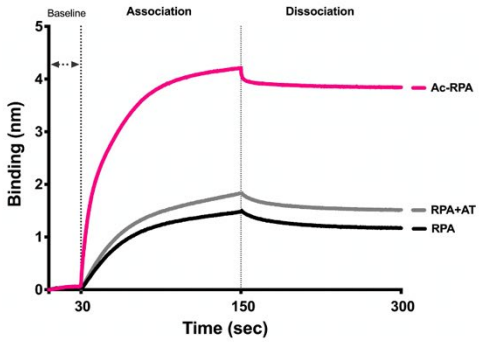

[C]

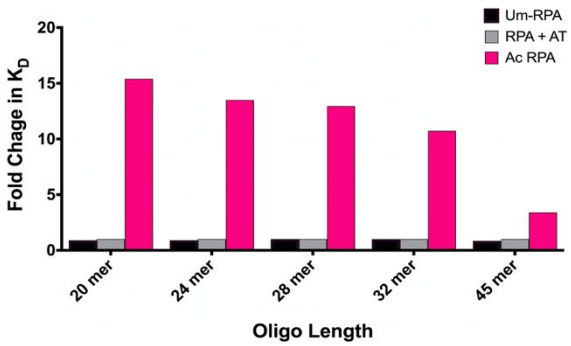

[D]

	K_D (in nM)		
Oligo	**RPA**	**RPA+AT**	**Ac-RPA**
20 nt	20	18	1.2
24 nt	14	13	0.9
28 nt	15	15	1.2
32 nt	13	13	1.2
45 nt	8.7	7.4	2.2

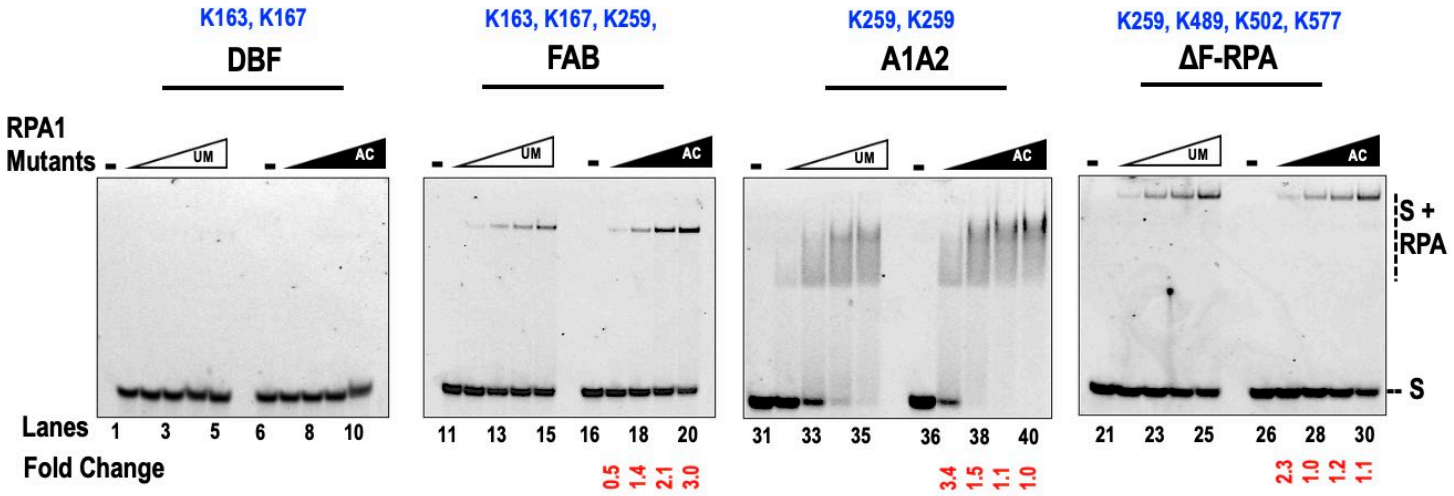

Figure 3.5 Correlating Number of Acetylated Lysine Sites to Increase in Binding Efficiency

Each lysine site acetylated on the mutant form of RPA1 are also indicated above every specific mutant RPA. Binding efficiency of unmodified (Um) and acetylated (Ac) forms of mutant RPA was studied using EMSA. Twenty five nanomolar 30 nt TAMRA-labeled ssDNA substrate was incubated in with increasing concentrations (25, 50, 125 nM) of RPA or Ac-RPA, and the and the reactions were incubated for 10 min at 37°C and separated on a 6% polyacrylamide gel. The substrate alone and the complexes containing RPA-bound substrate are indicated beside the gel at the right. Fold change in the binding of acetylated RPA compared to the unmodified RPA has been denoted below the lane numbers.

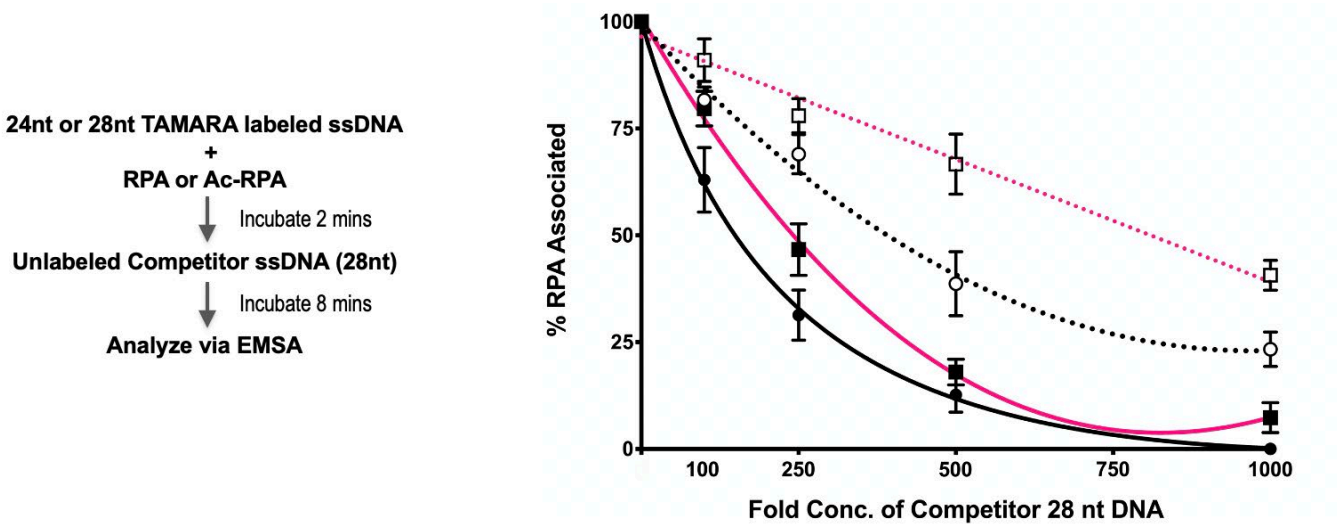

Figure 3.6 Assaying the Binding Efficiency of Acetylated RPA in Presence of Competing ssDNA.

One hundred nanomolar Um-RPA (straight line) or Ac-RPA (dotted line) was pre-incubated with either a 24 nt (black line, round bullet) or 28 nt (pink line, square bullet) TAMRA-labeled ssDNA substrate for a period of 2 minutes at 37°C. To this reaction 100, 250, 500, and 1000 - fold excess of cold competitor 28nt ssDNA was added and further incubated for 8 minutes at 37°C and separated on a 6% polyacrylamide gel. Percentage of protein dissociated from the substrate was calculated and graphically plotted to reveal the binding efficiency of RPA and Ac-RPA in the presence of an excess competitor ssDNA.

CHAPTER 4. ACETYLATED RPA HANDS-OFF OKAZAKI FRAGMENT PROCESSING OF SOME SHORT FLAPS TO THE LONG FLAP PATHWAY.

4.1 Abstract

In order to eliminate the RNA primer required for the initiation of lagging strand synthesis, two pathways have been proposed: the short flap and the long flap pathway. Previous studies have revealed that while the short flap pathway is processed by flap endonuclease 1 (FEN1) which cleaves Pol δ displaced primer flaps at their base, the long flap pathway utilizes a more concerted array of proteins including the activities of the single stranded DNA binding protein, RPA and Dna2, a sequentially cleaving endonuclease. In most cases, these primer flaps are processed through the short flap pathway, but in others, such as when FEN1 is disengaged from the replisome, they are lengthened enough to be stably bound by RPA promoting long flap processing. The presence of these redundant pathway suggests that a mode of regulation exists within the cell that can dictate the choice of one pathway over the other. Diversifying the proteome by post translationally modifying the enzymes involved in these pathways can serve as a form of regulation.

For over a decade, human replication proteins have been discovered to be post translationally modified by lysine acetylation. Coincidentally, the Okazaki fragment processing (OFP) proteins FEN1, RPA and Dna2 are all modified by p300, a lysine acetyl transferase. Acetylation variably modulates the biochemical properties of each protein. Upon lysine acetylation, FEN1 experiences an inhibition in its binding and cleavage activities whereas acetylation stimulates the binding and cleavage properties of Dna2. Given that this PTM impacts multiple proteins that function in OFP, we sought to decode its impact on their interactive properties. Our results show that lysine acetylation indeed promotes OFP through the long flap pathway.

4.2 Introduction

The accuracy of the replication process is highly dependent on the spatio-temporal arrangement, interaction and the precise activity of a multitude of proteins at the replication fork. Enzymes that are chosen for this process ensure that the DNA is duplicated with the highest fidelity in order to maintain genome stability. Due to the opposite polarity of the DNA duplex, the leading strand is synthesized continuously whereas the lagging strand is synthesized discontinuously in short stretches known as Okazaki fragments (OFs) (28,308). In a mammalian cell, approximately fifty million OFs are generated during one round of replication, each of which are initiated by DNA polymerase alpha (pol α) which synthesizes a short stretch of RNA (8-10nt), followed by 20-22 nucleotides of DNA (46,60,309). In order to complete replication, and create a fully functional lagging strand, these OFs need to be processed further to remove the RNA from the genome, resynthesize that region and ligate the strands in order to form a fully functional strand (263).

During lagging strand replication, pol α synthesized initiator primers are lengthened by DNA Pol δ, which during synthesis will frequently run into the downstream OF (310). At this point, pol δ switches from synthesis to strand displacement, wherein it displaces the 5' end of downstream OF to create a flap structure (37). The 5' flap is recognized and cleaved by flap endonuclease 1 (FEN1) creating a nick, which is then sealed by DNA ligase I (Lig I) (13,49,311). Experiments using recombinant replication proteins have identified this to be the primary method through which initiator ribonucleotides are removed from the lagging strand ensuring reduction of mutational load (48). This pathway is termed the "short flap pathway" of Okazaki fragment processing (OFP) (44).

Biochemical assays further showed that while the majority of the flaps are processed through the short flap pathway, a small minority of flaps are processed through an alternate pathway (55). This pathway is employed when FEN1 disengages from the replisome allowing for the possible formation of longer flaps to which the SSDBP, replication protein A (RPA) can bind (312). This alternative pathway can also be activated when the 5'-3' helicase, Pif1 is recruited ahead of the polymerase, lengthening the initiator primer region therefore allowing for high affinity binding of RPA (55). Flaps bound by RPA do not allow FEN1 to bind the substrate and thread through its active site, thereby inhibiting flap cleavage (57). Consequently, another protein, which functions both as a nuclease and a helicase, Dna2, is required to displace RPA. Displacement

of RPA is combined with flap cleavage by Dna2, which similar to FEN1, cleaves the flap by threading it through its active site. However, unlike FEN1, it makes multiple cuts on the flap and leaves behind a terminal 5-6nt product, which is small enough that it evades stable RPA binding (48,313). FEN1 is then able to displace Dna2 and cleave the flap allowing for subsequent ligation by Lig I (314). This alternate pathway is termed the "long flap pathway" or "two nuclease pathway" for OFP (44).

The presence of the two alternate pathways for OFP suggests existence of a regulatory mechanism through which the cell can dictate the processing of OFs. Previous work has indeed shown that at least two levels of regulation exist that can affect which pathway OFP proceeds through: the accumulation of RPA and the modulation of OFP proteins by lysine acetylation (167,315). The DNA replication process invariably generates and exposes single stranded DNA (ssDNA) requiring the substantial presence of RPA during the entirety of the process. Studies have shown that RPA plays a role in promoting the creation of long flaps by stimulating Pol δ synthesis and strand displacement activities (35). When these strands are lengthened either by stimulated Pol δ activities or Pif1 unwinding, more ssDNA is exposed to which RPA can stably bind thereby obstructing FEN1 cleavage (264). This inhibition single handedly promotes processing through the long flap pathway. Additionally, while RPA inhibits FEN1 cleavage on long flaps, it stimulates Dna2 cleavage (316). Taken together, one can surmise that the presence of RPA mediates the switch from the short flap to the long flap pathway for processing OFs (57).

For more than half a century, post translational modifications (PTMs) have been shown to regulate a myriad of biochemical pathways involved in numerous cellular processes. However, it is only in the past few decades that the importance of lysine acetylation as a PTM which impacts the function, localization and structure of non-histone proteins have gained popularity following the discovery of p53 as the first non-histone protein to be acetylated (150,155). As a result, our current understanding of this modification has since shifted from associating it solely with chromatin modifications to now recognizing acetylation as an important regulator of protein function. In 2009, Choudhary *et al* using an unbiased approach, identified over three thousand proteins to be acetylated in human cells (165). This study and other subsequent proteomic studies have identified a wide array of replication and repair associated proteins to be modified both in yeast and human cells (refs). Identification of lysine acetylation using proteomic analysis corroborated previous studies characterizing functional changes in acetylated OFP-associated

proteins, for e.g., FEN1 and PCNA (53,224). While biochemical analysis of individual acetylated proteins has been characterized, the impact of lysine acetylation on an entire biochemical pathway has thus far not been studied.

Lysine acetylation may act as one mode of regulation through which the cell dictates the choice of the OFP pathway. Upon lysine acetylation by p300, FEN1 exhibits a 90% inhibition in its binding and cleavage activities (53). Similar to the presence of RPA on long flaps, inhibition of FEN1's activities by lysine acetylation has been thought to promote long flap processing. The long flap pathway nuclease/helicase, Dna2, is also acetylated by p300, greatly stimulating its nuclease, helicase and binding activities (167). More recently, we have shown that in addition to PCAF and GCN5, RPA is also acetylated by p300 and similar to Dna2, it demonstrates an increased binding affinity to shorter length ssDNA. It has been proposed that processing *via* the long flap pathway would ensure complete removal of the Pol α synthesized initiator primer and resynthesis by the higher fidelity Pol δ (58,264,317)

In our current study, we have focused on RPA and determined how acetylation of this central protein can govern the switch between the short and long flap pathway. We show that lysine acetylation of RPA promotes long flap processing even in the presence of short DNA flaps by stably binding to it thereby inhibiting FEN1 binding and cleavage activities. Additionally, lysine acetylation of RPA further stimulates the formation of long flaps by stimulating Pol δ synthesis and strand displacement properties. Interestingly, we have observed that RPA acetylation impacts the cleavage properties of Dna2 which ultimately affects the maturation of OFs upon ligation. Our studies reemphasize the role of lysine acetylation as an important regulator of replication fidelity.

4.3 Results

4.3.1 Synthesis and Strand displacement by Polymerase delta (Pol δ) is stimulated in the presence of acetylated RPA

Although the core intrinsic function of RPA is ssDNA binding, it has also been shown that RPA exhibits some strand melting properties that aids in resolving secondary structures which limit the activity of some polymerases and helicases (257). Prior work in yeast and mammalian cells have revealed that the processivity of Pol δ is improved in the presence of certain accessory proteins including PCNA and RPA (318). This increased processivity ensures that each OF is

efficiently synthesized and that the preceding initiating primer is processed out of the genome preventing the incorporation of ribonucleotides and misincorporated deoxyribonucleotides (319). RPA binding to the parent strand helps melt most secondary structures that could serves as a barrier to synthesis. Work by our laboratory has shown that lysine acetylation of RPA promotes its strand melting properties (section 3.2.7). It is on this basis we sought to explore the impact of RPA acetylation on the processivity of Pol δ as measured by the amount of synthesis and strand displacement products formed from OFP like substrates as shown in Figure 4.1.

To assess polymerase synthesis, we pre-bound varying concentrations (100, 250, 500 and 750nM) of Um-RPA (lanes 3- 6) and Ac-RPA (lanes 7-10) to a synthesis substrate (44nt labeled upstream primer annealed to a 110 nt template) in the presence of a 150 nM of Pol δ. Our results revealed that Um-RPA was slightly able to stimulate the protein's processivity and gap filling activity at the tested concentrations. We detected a mild increase in the formation of a fully synthesized product compared to that formed by the activity of the polymerase alone (lane 2). Ac-RPA on the other hand, was seen to further stimulate Pol δ's processivity as the amount of fully synthesized product was ~2-fold higher than the product formed in the presence of Um-RPA. Using similar experimental conditions, the strand displacement activity of Pol δ was measured on a substrate containing a 60nt downstream oligonucleotide annealed to the 44+110 synthesis substrate thereby mirroring two OFs. Since the upstream substrate is radiolabeled, one can visualize strand displacement as synthesis that occurs beyond the 6nt gap separating both the upstream and downstream primers. In the presence of Um-RPA, there was slightly increased synthesis past the 6nt gap (lanes 13 – 16) when compared to the polymerase alone lane (lane 12). However, in the presence of Ac-RPA, ~ 2-fold stimulation to this strand displacement activity was detected.

4.3.2 Regulation of FEN1 activity by lysine acetylation promotes RPA binding to short flaps.

It has been demonstrated that OFP predominantly proceeds via the short flap pathway, wherein Pol δ and FEN1 function in a coordinated molecular handoff mechanism to ensure that relatively short flaps are created and removed allowing for ligation of upstream and downstream OFs (320). In some cases, however, FEN1 is unable to cleave these short flaps created by Pol δ opportunistically providing access to other proteins that could interact with the DNA such as

helicases or ssDBP such as RPA. There are a few instances where FEN1 cleavage is inhibited in the cell including the presence of structured substrates and modulation of the protein by lysine acetylation or phosphorylation (53,321,322). Given that lysine acetylation of FEN1 inhibits its binding by ~ 90%, we wanted to explore the impact of this modification on providing access to varying concentrations of RPA for DNA binding.

On a short 20 nt flap substrate, we expected to observe dynamic binding by RPA, with high on and off rates. This dynamic binding would offer FEN1 a chance to recognize and stably bind the flap base when RPA was not bound to the substrate. . Under these experimental conditions, we observed that although Um-FEN1 was mildly inhibited (~16%) by RPA at its highest concentration (150nM), Um-FEN1 bound to the substrate with higher affinity by either 2-3 fold (Lanes 3-5) or with a similar affinity (Lane 6) to RPA as highlighted in Figure 4.2. This shows that although FEN1 activity can be inhibited by RPA, the lower affinity for this ssDBP on a shorter length substrate can mildly regulate this interaction. The percentage of Um-FEN1 bound in the presence of increasing concentrations of RPA (50, 75, 100 and 150nM) were 55.3%, 53.3%,48.9% and 25.2% (lanes 3-6) compared to 60% (lane 2) bound in the absence of RPA as shown in Figure 2. However, when FEN1 was acetylated, there was a 2.4-fold decrease in the protein's ability to bind the flapped DNA substrate. Consequently, more RPA molecules (~ 2-fold) were able to accumulate on the flap as they didn't need to compete with FEN1 for binding. The percentage of FEN1 bound in the presence of equally varying concentrations of Ac-RPA was calculated to be 27.9%, 25.8%, 5.7% and 2.9%. These results show that when FEN1 is acetylated, it provides an opportunity for other protein players to alter the pathway for flap processing.

4.3.3 Lysine acetylation of RPA serves as the switch between the short flap and long flap pathway via inhibition of FEN1 cleavage on shorter flaps.

FEN1's preference for cleavage of double flaps has long been established (323-325). However, previous work has shown that its activity on these flap substrates is inhibited by RPA which accumulates as a result of the presence of single stranded DNA long enough for it to stably bind (54). This stability of RPA binding to DNA substrates is the basis upon which FEN1's nuclease activity is inhibited as the binding of the ssDBP does not allow FEN1 to thread the 5'end of the flap through it active site and make a precise cleavage at the flap base. RPA stably binds to DNA of approximately 28nt, but recent work from our laboratory shows that lysine acetylation of

the protein promotes higher binding affinity to even shorter substrates (Chapter 3). Therefore, we sought to determine the impact of RPA acetylation on FEN1's nuclease activity when bound to DNA substrates of varying lengths.

We observed that on the short flap substrate (20nt), UM-RPA does not stably bind thereby leading to minimal inhibition of FEN1 cleavage as shown in lanes 3-7 (4.9%, 6.2%, 9.1%, 13.6% and 23.2%) when compared to cleavage by FEN1 alone as shown in Figure 4.3. Conversely, AC-RPA which binds even shorter DNA flaps with higher affinity promoted increased inhibition of FEN1 cleavage (22.0%, 58.6%, 86.9%, 92.2% and 93.8%) represented by lanes 8-12. This shows that higher affinity binding of RPA even on short flaps prevents FEN1 from being able to thread through and cleave at the flap base. To further highlight that stable binding of RPA promotes inhibition of FEN1 cleavage, a 30nt flap was utilized in the same assay. At this length, it is believed that the dynamics of Um-RPA binding promotes more stable binding given the same concentration than on a short flap (data not shown.) Moreover, AC-RPA in all scenarios showed increased binding and increased inhibition of cleavage as shown in Figure 4.3. Although the fold change observed between the acetylated and unmodified forms of RPA was lower on the long 30nt flap compared to the short 20nt flap, our results highlight that acetylation of RPA is inhibitory to FEN1 cleavage both on short and long flaps.

4.3.4 Dna2 cleavage on short flaps is altered by acetylated RPA

Previous studies outlining the long flap pathway have shown that the endonuclease/helicase Dna2 is able to displace RPA while cleaving at multiple sites on the primer flap (57,326,327). Majority of the work done on this pathway have explored the interaction between Dna2 and RPA mostly on longer flapped substrates (~ over 30nt) because it has been shown that Dna2 can function more efficiently within the pathway when the primer flap length increases (265). In this experiment, we reasoned that if acetylation of RPA promoted more stable binding to shorter flaps, then this interaction would still necessitate cleavage by Dna2. Therefore, we evaluated the influence of RPA acetylation on Dna2 activity when acting on short flaps. In the presence and absence of a fixed concentration of Um-RPA and Ac-RPA prebound to a 20nt double flap, varying concentrations of Dna2 was titrated. The cleavage profile of Dna2 revealed that on short flaps, the presence of Um-RPA doesn't change its pattern of cleavage as has been previously reported to be the case for longer flaps (48). Instead, it mildly inhibits the amount of cleavage when Um-RPA is bound in

lanes 5-7 (57.5%, 68.6% and 71.0%) compared to the nuclease on its own, lanes 2-4 (64.8%, 71.9% and 72.2%). We rationalize that this could be due to steric reasons wherein the binding of RPA to the shorter substrate alters the binding pattern of Dna2 to it.

More significantly, while the amount of cleavage didn't greatly vary when Ac-RPA was present in the reaction, the pattern of cleavage differed possibly owing to the conformational change conferred upon the protein by its modification. We observed a 2-fold accumulation of cleavage products around the base of the flap showing that lysine acetylation of RPA directs Dna2 to cleave at the flap base accounting for 12% of all cleaved products when acting on a short flap. This pattern of base cleavage is usually associated with FEN1 (lane 11) which directly cleaves at the base of primer flaps.

4.4 Discussion

The discontinuous synthesis that arises owing to the polarity of the lagging strand creates a replication problem that the cell has to circumvent in order to ensure genomic stability. The collective amount of RNA and DNA primers synthesized by DNA polymerase alpha, the error prone polymerase during one round of the cell cycle presents deleterious consequences for the cell if left within the genome. As such, the sequential steps required for Okazaki fragment processing reveals a well-coordinated machinery that in many ways, is hinged on the availability and functions of RPA. Various studies have shown that RPA mediates a plethora of cellular transactions within the cell. More specifically, during lagging strand synthesis, RPA regulates the transition from primer initiation to strand elongation by interacting with a myriad of protein partners. While a lot of studies have elucidated the roles of these key protein players in silo or in tandem with other proteins, not much is known about how they function in tandem with one another when they are regulated by some PTMs (53,167,195,197). Lysine acetylation of different DNA replication proteins have been outlined and marked with varying impact on their biochemical properties. This study addresses how these biochemical changes affect the necessary protein-protein interactions required for OFP and provides more detailed understanding about the how this replicative process can be regulated.

While polymerases are integral to DNA replication on the basis of their synthesis activity, they require the aid of accessory proteins to processively carry out their functions (328,329). Across many organisms, polymerase activity is closely associated with the presence of single

stranded DNA binding proteins. In *E.coli*, it was discovered that the Pol III holoenzyme required SSB in order to replicate along ϕX174, G4 and M13 (328). Similarly in herpes simplex virus I (HSV1), the ssDBP, infected cell protein 8 (ICP8) stimulates the processivity of the herpes polymerase (330). Likewise, work done in eukaryotic cells has revealed that RPA is an important accessory factor for Pol δ (35). We rationalized that processivity is improved as a result of the strand melting properties of RPA which allows the polymerase duplicate DNA especially along hard to replicate regions such as those containing secondary structures including triplex and G-quadruplex DNA (331,332). Additionally, given that the DNA replication process accumulates single stranded DNA when the duplex is unwound, the presence of RPA prevents the reannealing of strands wherein $MgCl_2$ concentrations are greater than 2mM or salt concentrations are about 100mM NaCl (333,334). This further ensures that polymerase synthesis isn't prohibited. Furthermore, since Pol δ also contains strand displacement activities, the displaced downstream flap bound by RPA can also be melted improving the efficiency of synthesis as work by Treuner et al demonstrated that although not comparable to DNA helicases, RPA was able to "unwind" long double stranded regions (334). Recent work from our lab has shown that lysine acetylation of RPA regulates the melting properties of the protein creating a scenario where it could favor either the melting or annealing of duplex substrates. Therefore, we probed how this modification might impact Pol δ activities. Interestingly, our results revealed that under the experimental conditions, the presence of lysine acetylated RPA enhanced both synthesis and strand displacement activities possibly because the strand melting reaction was favored. Additional work is required to determine if this is the case by altering local NaCl and $MgCl_2$ concentrations. Likewise, we observed that in the presence of the modified protein, the exonuclease property of this B- family polymerase was highly stimulated. Mechanistically, the exonuclease proof reading activity of Pol δ occurs in the 3' – 5' direction and accounts for 10^1 or 10^2 fold mutational increase in cells lacking this domain (335). We rationalize that RPA stabilizes Pol δ thereby promoting its exonuclease activity similar to its yeast homolog where it stabilizes the 3'-5' endonuclease activity of Apn2 (336).

The displacement of the initiating RNA-DNA primer has long been shown to be regulated by PCNA mediated interactions between Pol δ and FEN1. In more recent times, the PTM, lysine acetylation has been shown to regulate this process too. While lysine acetylation of Pol δ has been outlined (unpublished work from our group), work by Hasan et al detailed the impact of this

modification on FEN1's biochemistry (53). Corroborating the results from our study, FEN1 acetylation exhibits decreased DNA binding which allows for the accumulation of RPA even on shorter length flaps to which it dynamically binds. Similarly, the binding of RPA to displaced flaps serves as a form of regulating OFP as described by Bae et al (57). In their work, RPA is described as the switch that governs the choice of what pathway OFP proceeds. Therefore, although FEN1 binding is required for processing short flaps, lysine acetylation inhibits this process in two ways: 1) it prevents FEN1 from being able to bind when modified and 2) it confers higher affinity binding to RPA in the presence of short flaps thereby activating the long flap processing proteins. This form of regulation possibly ensures that the RNA primer and erroneously incorporated DNA synthesized by Pol α are completely removed promoting higher fidelity synthesis. While the outcome of these interactions might have been hypothesized, this study clearly highlights that *in vitro*, lysine acetylation promotes favors the activation of long flap pathway proteins even in the presence of shorter flaps than was earlier perceived.

To further process these RPA bound flaps, the so-called long flap endonuclease, Dna2 is required to interact with and displace RPA, subsequently allowing for sequential flap cleavage. Following this, an ~5-6 nucleotide flap is retained which is then processed by FEN1. In enquiring about how lysine acetylated RPA might impact its interaction with Dna2, we discovered that while sequential cleavage above the flap base was observed, RPA was able to direct Dna2 to cleave at the flap base. This result was fascinating because it denoted that while majority of the time, Dna2 is unable to cleave at the flap base consequently requiring the action of FEN1 prior to ligation, Ac-RPA might sterically position Dna2 in such a manner that it cleaves the flap at its base 12% of the time even on short flaps. The two-nuclease pathway has always been believed to process long flaps. However, it seems that even short flaps can be processed in this manner. Seemingly, what determines if short flaps are also processed by long flap pathway proteins is lysine acetylation of FEN1 or RPA. We hypothesize that although this doesn't happen majority of the time, when there is UV induced p300 mediated acetylation of FEN1, this could occur (53). Concurrently, since RPA acetylation is also further increased upon DNA damage. It could be that case that a subset of these short flaps are processed through the long flap pathway.

4.5 Materials and Methods

4.5.1 Oligonucleotides

Synthetic oligonucleotides were designed and purchased from Integrated DNA Technologies (IDT.) For FEN1 cleavage and competition assays, the downstream flaps (20F and 30F) were 5' labelled with IR-700 and annealed to the template (T1) and upstream oligonucleotides (26U) in the ratio 1:3:6 using duplex buffer obtained from IDT to form a double flap structure. The upstream 44nt oligonucleotide (44U) used in the polymerase assays was radiolabeled with [γ-^{32}P] ATP from Perkin Elmer as previously described (194). The 5' labelled substrate was annealed to the 110 nt template (T2) in a 1:4 ratio and referred to as the synthesis substrate while the strand displacement substrate consisted of the upstream primer (44U) annealed to the downstream oligonucleotide (60D) and template (110T) in the ratio 1:3:6. In addition, the 20 nt downstream flap (20F) used in the Dna2 cleavage assay although similar in sequence to that of the FEN1 cleavage substrate was radiolabeled at the 3' end using [α-^{32}P] dCTP obtained from Perkin Elmer. This substrate was similarly annealed to T1 and 26U in a 1:3:6 ratio to form a 3' double flap.

4.5.2 In Vitro Acetylation

Recombinant proteins were acetylated in the presence of acetyl CoA and the catalytic domain of p300 in 1X HAT buffer [50 mM Tris-HCl (pH 8.0), 10% (v/v) glycerol, 150 mM NaCl, 1mM dithiothreitol, 1mM phenylmethylsulfonyl fluoride, 10 mM sodium butyrate]. RPA was acetylated in the ratio 1:1:10 (protein : p300 : Acetyl CoA) while FEN1 was acetylated in the ratio (1:0.1:10) as previously reported (194). The reactions were incubated at 37°C for 30 minutes and subsequently used in biochemical assays.

4.5.3 Polymerase delta Synthesis Assay

Polymerase activity by pol δ on a synthesis substrate (44U + 110T) and a strand-displacement substrate (44U + 60D + 110T) was performed in the presence of varying concentrations of unmodified and acetylated RPA. To a reaction buffer containing 50 mM Tris-HCl (pH 8.0), 2 mM DTT, 2 μg/uL BSA, 2mM ATP, 5mM MgCl2, 1 mM dNTP mix, and 1 mM

NaCl. Five nanomolar of each substrate was incubated with 150 nM of human Pol δ and RPA (100, 250, 500, and 750 nM) at 37 °C for 10 minutes to a final volume of 20 uL. Reactions were terminated by adding 20 uL of 2X Termination Dye (90% formamide (v/v), 10mM EDTA, 0.01% xylene cyanol and bromophenol blue) and boiled at 95 °C for 5 minutes. Samples were loaded onto a pre-run 12% polyacrylamide denaturation gel for 60 minutes at 80 W. The gels were exposed on a phosphor screen overnight and imaged using a Typhoon scanner. To quantify the relative difference in the amount of synthesis and strand displacement products observed, individual lanes representing the highest Pol δ concentration were quantified and graphed, using ImageQuant TL v8.1.

4.5.4 FEN1 and RPA Competition Assay

To assess the impact of FEN1 acetylation on the binding of RPA to short flaps (20nt), 200nM of both unmodified and acetylated forms of FEN1 together with increasing concentrations of RPA (50, 75, 100 and 150nM) were added to the reaction buffer (50mM Tris-HCl (pH 8.0), 2mM DTT, 20mM NaCl, 0.1mg/mL BSA, 5% (v/v) glycerol and 20μM EDTA.) To each reaction tube, 5nM of a 20nt IR-700 labelled flapped substrate was added, and the reaction was incubated at 37°C for 15 minutes. To an 8% pre-run native polyacrylamide gel, the samples were loaded and electrophoresed at 250V for 45 minutes. Gels were imaged using the previously outlined method. To determine the percentage of RPA or FEN1 bound flaps, the intensity of the RPA/FEN1 bound lanes were compared to the presence of unbound substrate and FEN1/RPA bound substrates. The formula used to quantify this was [(RPA or FEN1 bound product) / (RPA bound product + FEN1 bound product + unbound substrate *100.)]

4.5.5 FEN1 Cleavage Assay

The cleavage activity of FEN1 on two different flap substrates with varying length (20 and 30 nt) was assessed in the presence of varying concentrations of human RPA. To a reaction buffer containing 50mM Tris-HCl (pH 8.0), 2mM DTT, 20mM NaCl, 0.1mg/mL BSA, 5% (v/v) glycerol and 20μM EDTA, 5nM of flap substrate was incubated with 0.5nM hFEN1 and hRPA (100, 125, 150, 175 and 200nM) at 37°C for 15 minutes to a final volume of 20μL. Following this, 2mM $MgCl_2$ was added to the reaction and further incubated at 37°C for 10 minutes. Reactions were

terminated by the addition of 80mM EDTA, 50% formamide (final volume), and 0.08% SDS as previously described and then boiled at 95C for 5 minutes. Samples were loaded onto a pre-run 8% polyacrylamide native gel for 45 minutes at 250V. The gels were imaged using the Odyssey imaging system (700-nM filter) and quantified using the accompanying Image studio software. The intensity of each band was measured, and the amount of cleaved product was calculated using the equation [(cleaved product) / (cleaved product + uncleaved remnant) * 100]. Additionally, the percentage of cleavage inhibited by the presence of RPA was calculated by subtracting the number of cleaved products formed in the presence of RPA and FEN1 from the amount of product formed in the presence of FEN1 alone.

4.5.6 Dna2 Cleavage Assay

To visualize the cleavage products resulting from the activity of the nuclease Dna2, a 3' labelled 20nt flap was pre-incubated with or without of 50nM Um-RPA and Ac-RPA for 5 minutes at 37°C. Upon completion of incubation, varying concentrations of Dna2 (50, 100 and 200nM) were added to a final reaction volume of 20µl at 37°C for 10 minutes. Reactions were performed in a buffer containing 50mM Tris-HCl (pH 8.0), 2mM DTT, 20mM NaCl, 0.1mg/mL BSA, 5% (v/v) glycerol, 4mM ATP and 2mM MgCl2 and terminated by the addition of 80mM EDTA, 50% formamide (final volume), and 0.08% SDS. This was followed by boiling at 95C for 5 minutes. Samples were loaded onto a pre-run 12% polyacrylamide denaturing gel with 7M urea for 90 minutes at 80 W. The gels were exposed on a phosphor screen overnight and imaged using a Typhoon scanner. Using the Image studio software, the intensity of each band was measured and the amount of cleaved product was calculated using the equation [(cleaved product) / (cleaved product + uncleaved remnant) * 100]. Furthermore, the percentage of cleaved product present at the flap base was calculated using the equation [(product at flap base)/(total cleaved product)*100].

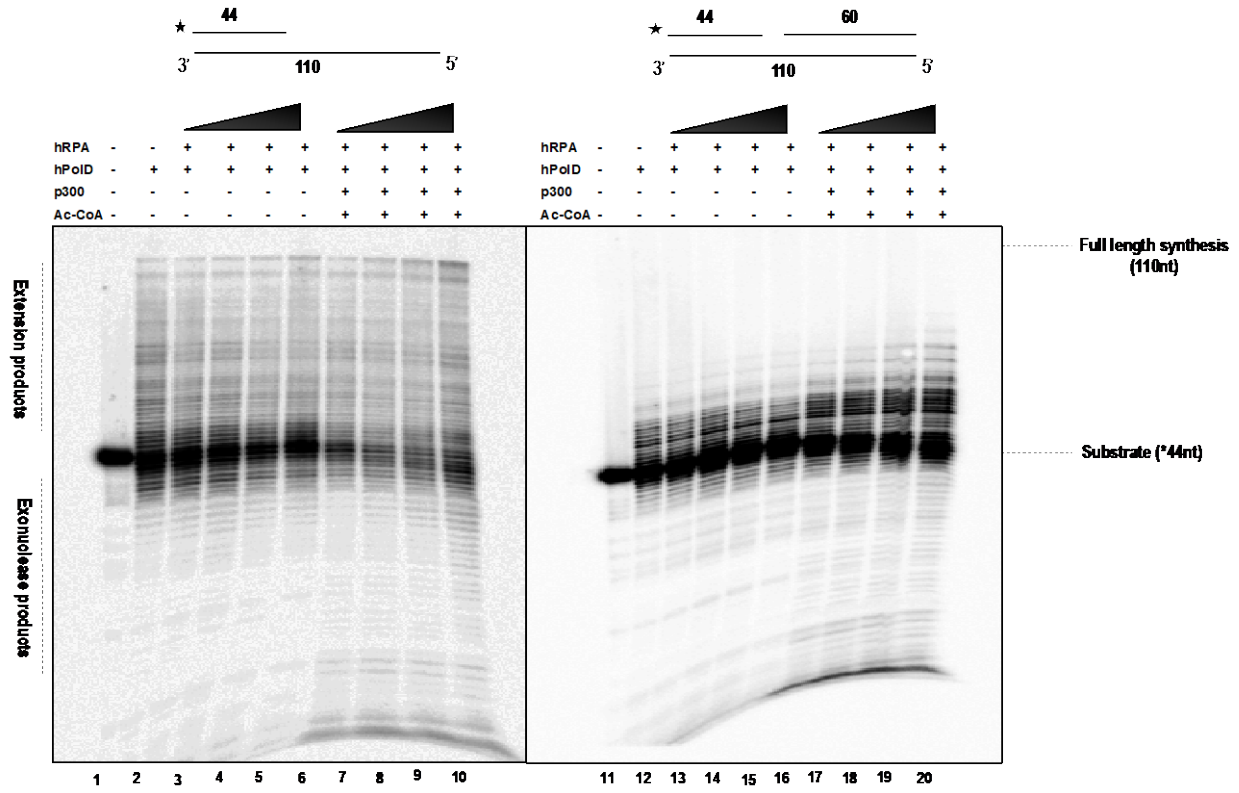

Figure 4.1 Polymerase delta (Pol δ) synthesis and strand displacement activities are stimulated by RPA acetylation.

A) Five nanomolar synthesis substrate (44U:110T) was bound to increasing concentrations of Um-RPA and Ac-RPA(100, 250, 500 and 750nM). Concurrently, 150nM of Pol δ was added to the reaction and loaded unto a pre-run 12% denaturing polyacrylamide gel. B) Similar concentrations were utilized on a strand displacement substrate (44U:60D:110T) and equally pre-run on a 12% denaturing polyacrylamide gel. ★ indicates site of 5'-32P label. Data obtained by Brandon Wysong, Balakrishnan Laboratory.

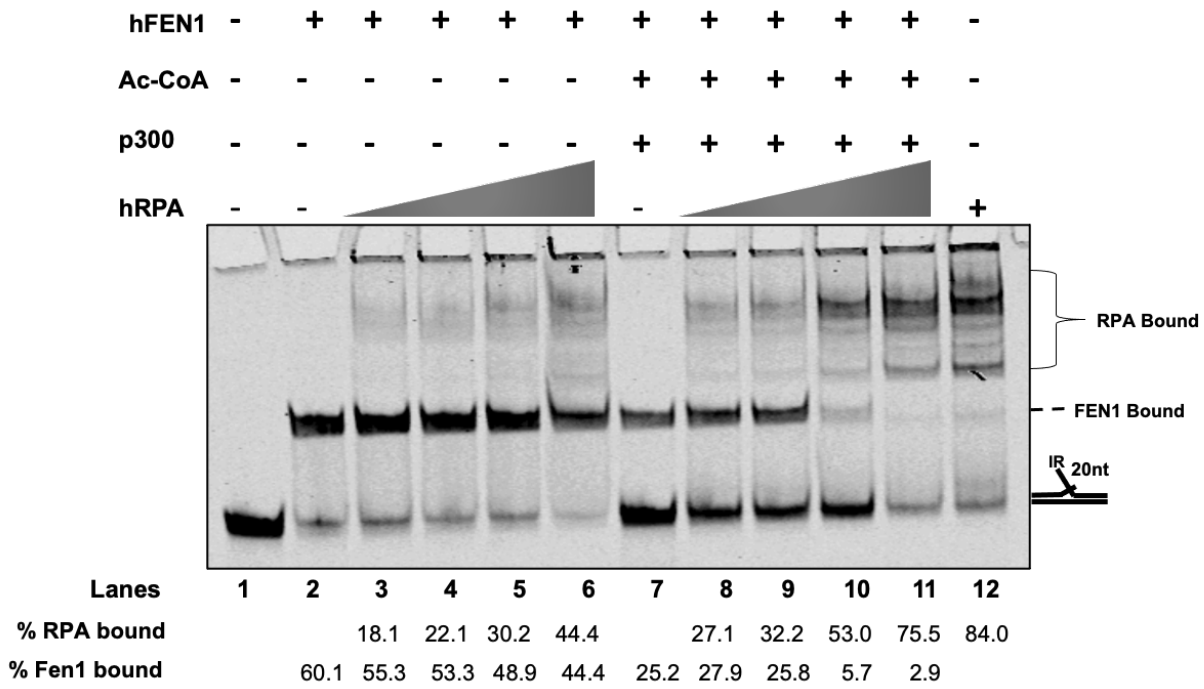

Figure 4.2 Binding of RPA to short flaps is regulated by lysine acetylation of FEN1.

The dynamic binding of RPA to 5nM of a short double flap (20nt) was assessed using an electro mobility gel shift assay (EMSA) wherein varying concentrations of Um-FEN1 (lanes 2- 6) and Ac-FEN1 (lanes 7-12) were incubated with it and electrophoresed on an 8% polyacrylamide native gel. Substrate alone control was loaded in lane 1 and RPA alone control in lane 12. IR indicates the site of fluorescent label.

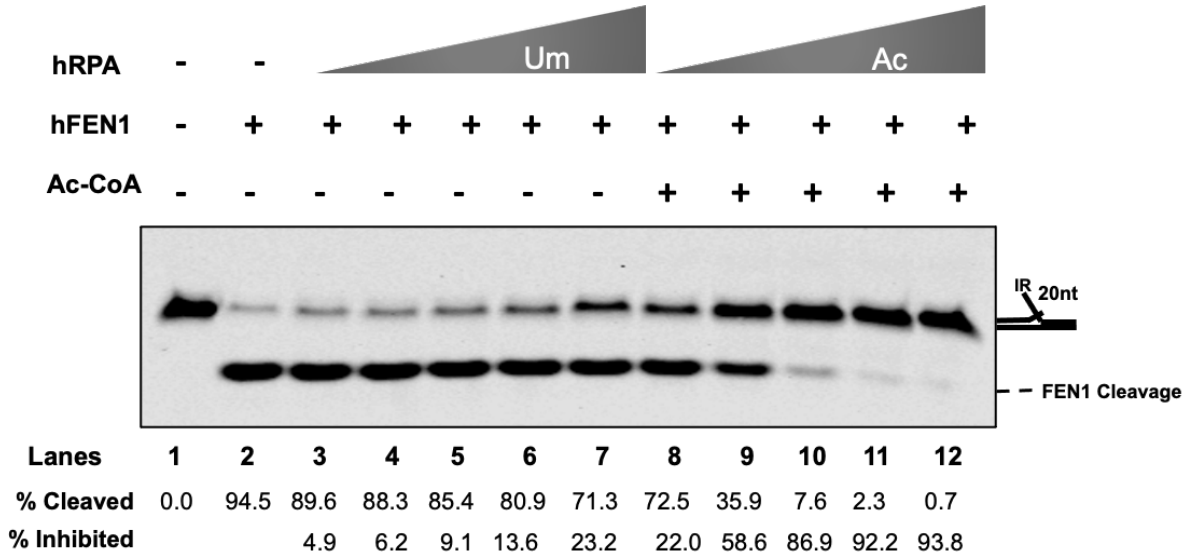

Figure 4.3 Lysine acetylation of RPA strongly inhibits FEN1 endonuclease activity.

Using an 8% polyacrylamide native gel, the cleavage activity of 0.5nM FEN1 on 5nM of a 20nt double flap was measured in the presence of increasing concentrations of both unmodified and acetylated RPA (100, 125, 175 and 200nM). Lane1 contains substrate alone, lane 2 shows FEN1 cleavage activity in the absence of RPA while lanes 3-7 represent cleavage in the presence of pre-bound Um-RPA and lanes 8-12 shows cleavage in the presence of pre-bound Ac-RPA. IR indicates the site of fluorescent label.

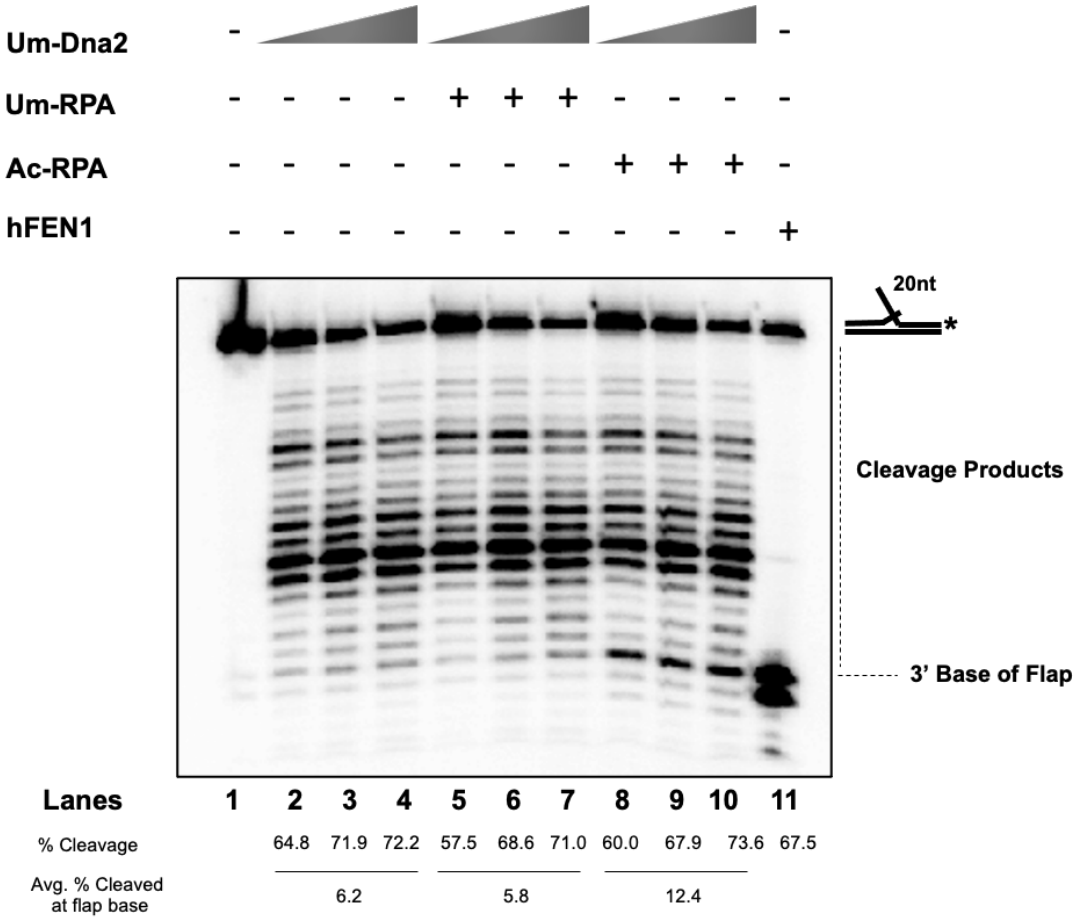

Figure 4.4 Dna2 cleavage pattern on a short flap is modified by RPA acetylation when bound to short flaps.

The sequential cleavage of increasing concentrations of Dna2 (50, 100 and 200nM) on 2.5nM of a 3'labelled 20nt short flap was electrophoresed on a 12% denaturing polyacrylamide gel. In the absence (lanes 2-4) or presence of 50nM Um-RPA (lanes 5-7) and 50nM Ac-RPA (lanes 8-10), the amount of products cleaved were compared. To determine the location of the flap base, 100fM FEN1 was incubated with the substrate (lane 11). Asterisk indicates the location of the 3' -32P label.

CHAPTER 5. CONCLUDING REMARKS

5.1 Overview

Replication fidelity describes the accuracy and precision with which the cell is able to duplicate its genome with the least amount of errors. Lagging strand replication utilizes a catalog of proteins and regulatory mechanisms to ensure that synthesis proceeds with the highest fidelity possible. The intricacy of the lagging strand replisome tows a fine line between creating necessary systems to circumvent naturally occurring hindrances (directionality of polymerases on a 5'-3'template) and ensuring that those same systems are efficiently regulated to keep up with the leading strand and prevent replication delay. Additionally, many of the proteins involved in replication, also function in other DNA transactions. Therefore, it is imperative to understand how these proteins are regulated within their various contexts. Lagging strand synthesis is one of those processes that implicates a variety of multifunctional proteins, with the minimal essential proteins including helicases (Pif1), polymerases (Pol α and δ), single stranded DNA binding proteins (RPA) and nucleases (FEN1 and Dna2) and DNA ligase I (Lig I). While the knowledge of the biochemical activities of individual protein players is important, more work is needed to outline how their activities and cellular interactions are impacted by different post translational modifications, including the focus of my studies, lysine acetylation. This is crucial as various studies have reported marked increases in the gene expression of KDACs across different cancers (337). This has led to the discovery and development of various KDAC inhibitors which regulate the acetylation profile of these cancer cells suggesting that this reversible modification has great impact on cellular growth and viability. This dissertation contributes valuable insight into how two additional replication proteins, Pif1 and RPA are post translationally modified by lysine acetylation. It also details how these individual modifications function to regulate an entire pathway.

5.2 Lysine Acetylation Regulates Lagging Strand Synthesis with Possible Caveats

Work done by our group and others has provided a framework for defining how lagging strand replication proteins are modified by lysine acetylation (167,197,338). While the short flap pathway is negatively regulated by this modification in that the binding and cleavage activities of

FEN1 are greatly hindered, the reverse is the case for proteins involved in the long flap pathway. Proteins like Pif1 helicase exhibit improved unwinding activity across numerous substrates while the binding affinity of the single stranded DNA binding protein, RPA, is equally increased even on shorter length substrates (<26nt) (338). Furthermore, the long flap endonuclease, Dna2 exhibits stimulated binding and cleavage activities (167). Understanding the direct impact of lysine acetylation on the individual biochemical properties of these proteins has allowed us to study the role of the PTM to directly regulate the function of the protein. The work presented in Chapter 4 of this dissertation is the first report that details how lysine acetylation of all the proteins in the lagging strand maturation pathway can influence the activities of its protein partners, thereby impacting the functional outcomes of the pathway. A caveat however is that we do not fully understand how the changes associated with the lysine acetylation signature of one protein impacts that of another either upstream or downstream from it. For example, we do not know if the replication proteins are acetylated in concert with one another or if there is a sequential approach to how they are modified. Similarly, we are unaware if the KAT mediating the acetylation reaction is recruited specifically to one protein, but opportunistically modifies the others surrounding it or if a specific lysine acetylation signature prevents other proteins from being modified serving as some form of regulation.

Yet another caveat to consider is how the lysine acetylation signature of these proteins can change in response to various cellular events. DNA damage has been shown to induce lysine acetylation of replication proteins such as FEN1, RPA and Dna2 (53,167,197). However, it is yet to be elucidated if this trigger contributes to changes in their acetylation signature which could impact how downstream effectors during repair are regulated. For instance, hydroxy urea (HU) induced RPA2 hyperphosphorylation leads to the recruitment of Rad51 for repair which wouldn't occur otherwise (339). Similarly, phosphorylation of Pif1 inhibits telomeres at sites of double strand breaks, but this modification is not required for inhibition at telomeric regions (182). We hypothesize that under different cellular conditions as highlighted in Figure 5.1, replication proteins such as Pif1 might function differently based on their acetylation signature. Concurrently, since it is known that there is a redundancy that exists in the cell whereby multiple KATs can mediate the same acetylation reaction given the cellular context, one must probe if this in itself can alter a protein's acetylation signature. One such protein that exemplifies this phenomenon is p53. Studies have revealed that similar to RPA, p53 can be acetylated by both p300 and PCAF and

these KATs modify the protein at different lysine residues (340). For RPA, the only site identified to be acetylated by PCAF was also identified to be acetylated by p300 (197). We also discovered using mass spectrometry that additional sites were modified when p300 mediated the reaction. This therefore suggests that the KAT responsible for mediating each protein modification can confer a different acetylation signature which possibly extends the functionality of the protein within a given pathway.

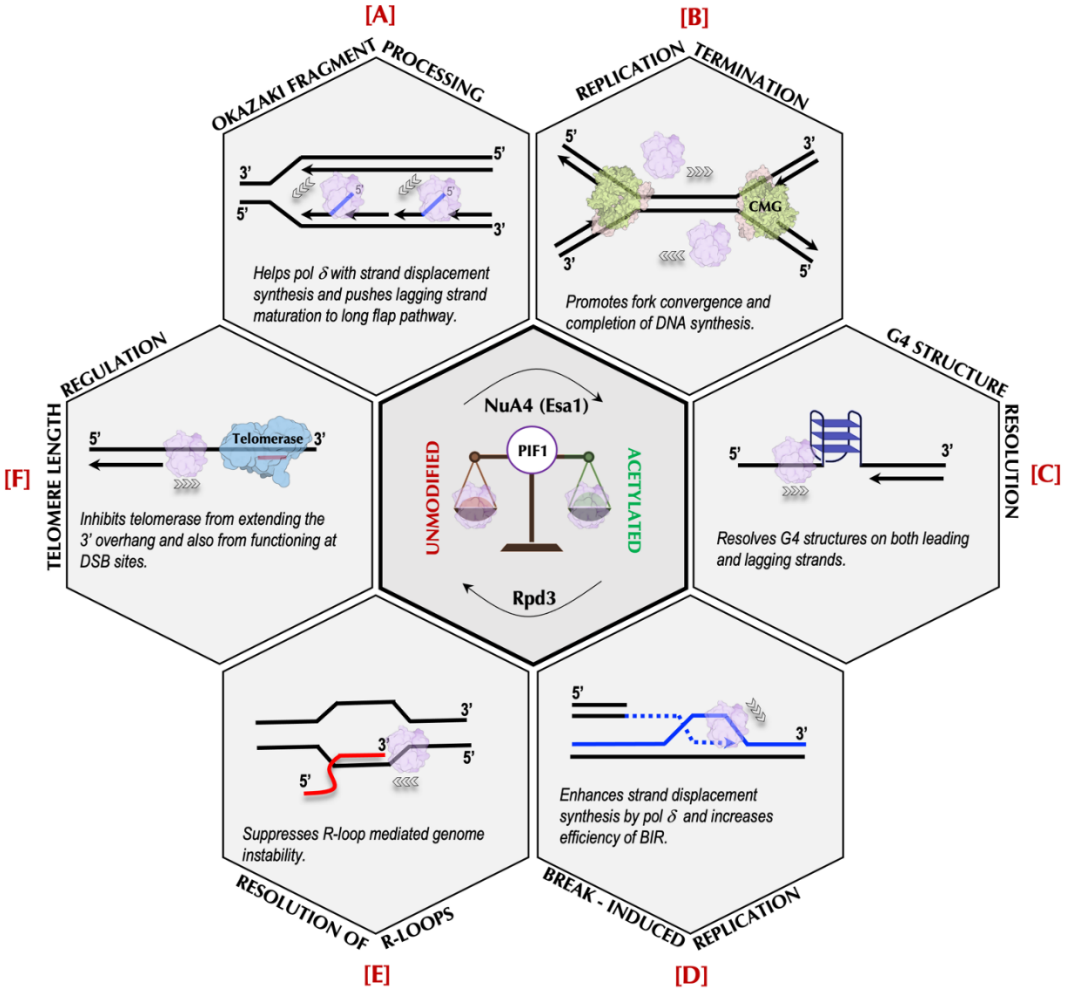

Figure 5.1 Possible cellular activities that can be mediated by lysine acetylation of Pif1 helicase.

Pif1's involvement in replication (A,B), repair (D), structure resolution (C,E)and telomere regulation (F) can be reversibly modified by the identified KAT (Esa1) and KDAC (Rpd3)[341].

5.3 Future Directions

To provide clarity on some of these unknowns, experiments such as isolation of proteins on nascent DNA accompanied by stable isotope labelling of amino acids in culture mass spectrometry (iPOND-SILAC MS) will be vital. Using these techniques outlined in Figure 5.2, one will be able to: i) determine if these proteins are modified at the replication fork ii) identify which KAT mediates the acetylation reaction and iii) outline a lysine acetylation signature as defined by normal replication events as well as during various cellular triggers including DNA damage and cell cycle perturbations.

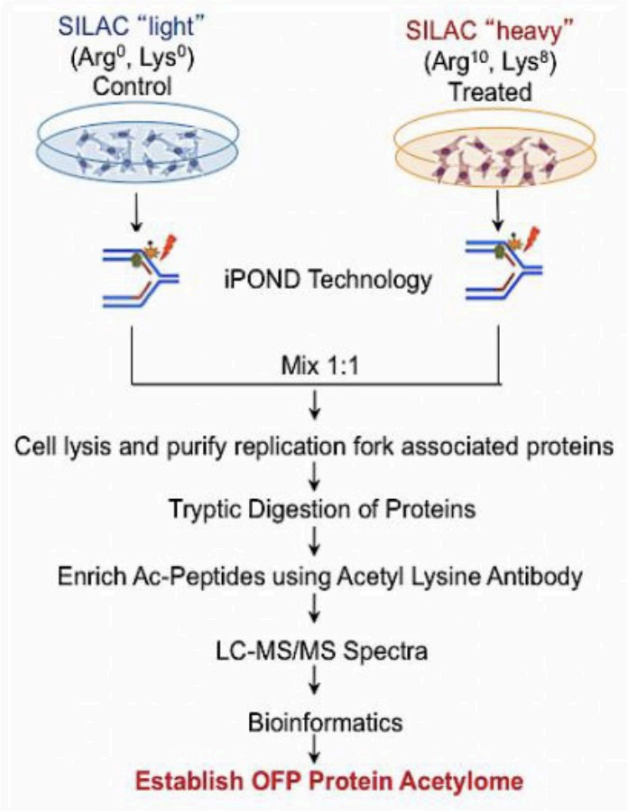

Figure 5.2 iPOND-SILAC MS technique for defining OFP protein acetylome.
Incorporation of labelled amino acids to determine acetylation signature under various cellular contexts.

Often times, in an attempt to further define the acetylation signature of a protein, a series of point mutations can be utilized wherein mutants are created to serve as phenocopies of an acetyl mimic (K- Q) or a non-acetylated residue (K- R). Unfortunately, while this approach is feasible in

theory, it poses some form of challenges of its own. Changing any residue especially if it resides within a functional domain can impact protein structure. Consequently, one cannot confidently attribute observed phenotypic or biochemical changes to a varied acetylation profile. To further detail the key players that make up the lagging strand acetylome, KAT and KDAC deletion and overexpression experiments can prove helpful, but not without some limitations. Lysine acetylation is an important regulator of cellular activities including chromatin assembly. Therefore, any change to the epigenetic environment can alter gene expression of a variety of proteins which could impact our understanding of the results and ultimately be deleterious for the cell.

So far, this dissertation has highlighted the importance of the acetylation of lysine residues in maintaining genome fidelity. However, there are other modifications including those that specifically target lysine residues such as methylation, SUMOylation, crotonylation and ubiquitination which play a role in ensuring these replication proteins are efficiently regulated. Only a little is known about the role of PTM cross talks in managing the DNA replication processes. One such cross talk is observed between methylation and phosphorylation of the short flap endonuclease, FEN1. It was reported that FEN1 methylation inhibits its phosphorylation activities promoting its engagement with the proliferating cell nuclear antigen, PCNA ensuring effective OFP (342). However, if FEN1 methylation was prohibited, the protein can then get phosphorylated preventing its interaction with PCNA. On this basis, experiments targeting cross talks on different replication proteins will aid in creating a network of PTMs and how they function together to maintain genome stability.

While many questions are yet to be addressed, this dissertation has filled three major knowledge gaps in the field: i) We identified acetylation of *S. cerevisiae* Pif1, the enzyme modifiers (Esa1 and Rpd3) and determined the impact of this modification on its biochemical properties showing a stimulation in binding, helicase and ATPase activities ii) We discovered that human RPA can be acetylated by p300 which peaks at G1/S phase of the cell cycle and exhibits a higher binding affinity state even to short oligonucleotides when modified iii) Lysine acetylation of human RPA activates long flap pathway proteins for OFP including the processing of a subset of short flaps.(343)

REFERENCES

1. Tsegay, P. S., Lai, Y., and Liu, Y. (2019) Replication Stress and Consequential Instability of the Genome and Epigenome. *Molecules* **24**
2. Reis, V. C., Torres, F. A., Pocas-Fonseca, M. J., De-Souza, M. T., Souza, D. P., Almeida, J. R., Marinho-Silva, C., Parachin, N. S., Dantas Ada, S., Mello-de-Sousa, T. M., and Moraes, L. M. (2005) Cell cycle, DNA replication, repair, and recombination in the dimorphic human pathogenic fungus Paracoccidioides brasiliensis. *Genet Mol Res* **4**, 232-250
3. Kelly, T., and Callegari, A. J. (2019) Dynamics of DNA replication in a eukaryotic cell. *Proc Natl Acad Sci U S A* **116**, 4973-4982
4. Cooper, G. M. (2000) The Events of M Phase. in *The Cell: A Molecular Approach* (Sunderland ed.), 2nd Ed., Sinauer Associates, MA. pp
5. Neil A. Campbell, J. B. R. Cell Cycle. in *Biology*, Benjamin Cummins. pp
6. Barr, A. R., Heldt, F. S., Zhang, T., Bakal, C., and Novak, B. (2016) A Dynamical Framework for the All-or-None G1/S Transition. *Cell Syst* **2**, 27-37
7. Moser, J., Miller, I., Carter, D., and Spencer, S. L. (2018) Control of the Restriction Point by Rb and p21. *Proc Natl Acad Sci U S A* **115**, E8219-E8227
8. Foster, D. A., Yellen, P., Xu, L., and Saqcena, M. (2010) Regulation of G1 Cell Cycle Progression: Distinguishing the Restriction Point from a Nutrient-Sensing Cell Growth Checkpoint(s). *Genes Cancer* **1**, 1124-1131
9. Ho, A., and Dowdy, S. F. (2002) Regulation of G(1) cell-cycle progression by oncogenes and tumor suppressor genes. *Curr Opin Genet Dev* **12**, 47-52
10. Elledge, S. J. (1996) Cell cycle checkpoints: preventing an identity crisis. *Science* **274**, 1664-1672
11. Golubnitschaja, O. (2007) Cell cycle checkpoints: the role and evaluation for early diagnosis of senescence, cardiovascular, cancer, and neurodegenerative diseases. *Amino Acids* **32**, 359-371
12. Meselson, M., and Stahl, F. W. (1958) The Replication of DNA in Escherichia Coli. *Proc Natl Acad Sci U S A* **44**, 671-682
13. Okazaki, R., Okazaki, T., Sakabe, K., Sugimoto, K., and Sugino, A. (1968) Mechanism of DNA chain growth. I. Possible discontinuity and unusual secondary structure of newly synthesized chains. *Proc Natl Acad Sci U S A* **59**, 598-605
14. Fijalkowska, I. J., Jonczyk, P., Tkaczyk, M. M., Bialoskorska, M., and Schaaper, R. M. (1998) Unequal fidelity of leading strand and lagging strand DNA replication on the Escherichia coli chromosome. *Proc Natl Acad Sci U S A* **95**, 10020-10025
15. Dewar, J. M., and Walter, J. C. (2017) Mechanisms of DNA replication termination. *Nat Rev Mol Cell Biol* **18**, 507-516

16. Reusswig, K. U., and Pfander, B. (2019) Control of Eukaryotic DNA Replication Initiation-Mechanisms to Ensure Smooth Transitions. *Genes (Basel)* **10**

17. Gao, F. (2015) Bacteria may have multiple replication origins. *Front Microbiol* **6**, 324

18. Mechali, M. (2010) Eukaryotic DNA replication origins: many choices for appropriate answers. *Nat Rev Mol Cell Biol* **11**, 728-738

19. Siddiqui, K., On, K. F., and Diffley, J. F. (2013) Regulating DNA replication in eukarya. *Cold Spring Harb Perspect Biol* **5**

20. Lujan, S. A., Williams, J. S., and Kunkel, T. A. (2016) DNA Polymerases Divide the Labor of Genome Replication. *Trends Cell Biol* **26**, 640-654

21. Mitra, S., and Kornberg, A. (1966) Enzymatic mechanisms of DNA replication. *J Gen Physiol* **49**, 59-79

22. Muzi-Falconi, M., Giannattasio, M., Foiani, M., and Plevani, P. (2003) The DNA polymerase alpha-primase complex: multiple functions and interactions. *ScientificWorldJournal* **3**, 21-33

23. Deshmukh, A. L., Kumar, C., Singh, D. K., Maurya, P., and Banerjee, D. (2016) Dynamics of replication proteins during lagging strand synthesis: A crossroads for genomic instability and cancer. *DNA Repair (Amst)* **42**, 72-81

24. Yamaguchi, M., Hendrickson, E. A., and DePamphilis, M. L. (1985) DNA primase-DNA polymerase alpha from simian cells. Modulation of RNA primer synthesis by ribonucleoside triphosphates. *J Biol Chem* **260**, 6254-6263

25. Tseng, B. Y., and Goulian, M. (1977) Initiator RNA of discontinuous DNA synthesis in human lymphocytes. *Cell* **12**, 483-489

26. Kozu, T., Yagura, T., and Seno, T. (1982) De novo DNA synthesis by a novel mouse DNA polymerase associated with primase activity. *Nature* **298**, 180-182

27. Baranovskiy, A. G., Babayeva, N. D., Zhang, Y., Gu, J., Suwa, Y., Pavlov, Y. I., and Tahirov, T. H. (2016) Mechanism of Concerted RNA-DNA Primer Synthesis by the Human Primosome. *J Biol Chem* **291**, 10006-10020

28. Burgers, P. M. J., and Kunkel, T. A. (2017) Eukaryotic DNA Replication Fork. *Annu Rev Biochem* **86**, 417-438

29. Waisertreiger, I. S., Liston, V. G., Menezes, M. R., Kim, H. M., Lobachev, K. S., Stepchenkova, E. I., Tahirov, T. H., Rogozin, I. B., and Pavlov, Y. I. (2012) Modulation of mutagenesis in eukaryotes by DNA replication fork dynamics and quality of nucleotide pools. *Environ Mol Mutagen* **53**, 699-724

30. Reijns, M. A. M., Kemp, H., Ding, J., de Proce, S. M., Jackson, A. P., and Taylor, M. S. (2015) Lagging-strand replication shapes the mutational landscape of the genome. *Nature* **518**, 502-506

31. Baranovskiy, A. G., Duong, V. N., Babayeva, N. D., Zhang, Y., Pavlov, Y. I., Anderson, K. S., and Tahirov, T. H. (2018) Activity and fidelity of human DNA polymerase alpha depend on primer structure. *J Biol Chem* **293**, 6824-6843

32. Tsurimoto, T., Melendy, T., and Stillman, B. (1990) Sequential initiation of lagging and leading strand synthesis by two different polymerase complexes at the SV40 DNA replication origin. *Nature* **346**, 534-539

33. Brill, S. J., and Stillman, B. (1991) Replication factor-A from Saccharomyces cerevisiae is encoded by three essential genes coordinately expressed at S phase. *Genes Dev* **5**, 1589-1600

34. Dornreiter, I., Erdile, L. F., Gilbert, I. U., von Winkler, D., Kelly, T. J., and Fanning, E. (1992) Interaction of DNA polymerase alpha-primase with cellular replication protein A and SV40 T antigen. *EMBO J* **11**, 769-776

35. Yuzhakov, A., Kelman, Z., Hurwitz, J., and O'Donnell, M. (1999) Multiple competition reactions for RPA order the assembly of the DNA polymerase delta holoenzyme. *EMBO J* **18**, 6189-6199

36. Nick McElhinny, S. A., Gordenin, D. A., Stith, C. M., Burgers, P. M., and Kunkel, T. A. (2008) Division of labor at the eukaryotic replication fork. *Mol Cell* **30**, 137-144

37. Maga, G., Villani, G., Tillement, V., Stucki, M., Locatelli, G. A., Frouin, I., Spadari, S., and Hubscher, U. (2001) Okazaki fragment processing: modulation of the strand displacement activity of DNA polymerase delta by the concerted action of replication protein A, proliferating cell nuclear antigen, and flap endonuclease-1. *Proc Natl Acad Sci U S A* **98**, 14298-14303

38. Mozzherin, D. J., Tan, C. K., Downey, K. M., and Fisher, P. A. (1999) Architecture of the active DNA polymerase delta.proliferating cell nuclear antigen.template-primer complex. *J Biol Chem* **274**, 19862-19867

39. Chilkova, O., Stenlund, P., Isoz, I., Stith, C. M., Grabowski, P., Lundstrom, E. B., Burgers, P. M., and Johansson, E. (2007) The eukaryotic leading and lagging strand DNA polymerases are loaded onto primer-ends via separate mechanisms but have comparable processivity in the presence of PCNA. *Nucleic Acids Res* **35**, 6588-6597

40. Balakrishnan, L., and Bambara, R. A. (2013) Okazaki fragment metabolism. *Cold Spring Harb Perspect Biol* **5**

41. Meroni, A., Mentegari, E., Crespan, E., Muzi-Falconi, M., Lazzaro, F., and Podesta, A. (2017) The Incorporation of Ribonucleotides Induces Structural and Conformational Changes in DNA. *Biophys J* **113**, 1373-1382

42. Podust, V. N., Podust, L. M., Muller, F., and Hubscher, U. (1995) DNA polymerase delta holoenzyme: action on single-stranded DNA and on double-stranded DNA in the presence of replicative DNA helicases. *Biochemistry* **34**, 5003-5010

43. Kao, H. I., Henricksen, L. A., Liu, Y., and Bambara, R. A. (2002) Cleavage specificity of Saccharomyces cerevisiae flap endonuclease 1 suggests a double-flap structure as the cellular substrate. *J Biol Chem* **277**, 14379-14389

44. Balakrishnan, L., and Bambara, R. A. (2011) Eukaryotic lagging strand DNA replication employs a multi-pathway mechanism that protects genome integrity. *J Biol Chem* **286**, 6865-6870

45. Li, X., Li, J., Harrington, J., Lieber, M. R., and Burgers, P. M. (1995) Lagging strand DNA synthesis at the eukaryotic replication fork involves binding and stimulation of FEN-1 by proliferating cell nuclear antigen. *J Biol Chem* **270**, 22109-22112

46. Bambara, R. A., Murante, R. S., and Henricksen, L. A. (1997) Enzymes and reactions at the eukaryotic DNA replication fork. *J Biol Chem* **272**, 4647-4650

47. Tsutakawa, S. E., Classen, S., Chapados, B. R., Arvai, A. S., Finger, L. D., Guenther, G., Tomlinson, C. G., Thompson, P., Sarker, A. H., Shen, B., Cooper, P. K., Grasby, J. A., and Tainer, J. A. (2011) Human flap endonuclease structures, DNA double-base flipping, and a unified understanding of the FEN1 superfamily. *Cell* **145**, 198-211

48. Stewart, J. A., Miller, A. S., Campbell, J. L., and Bambara, R. A. (2008) Dynamic removal of replication protein A by Dna2 facilitates primer cleavage during Okazaki fragment processing in Saccharomyces cerevisiae. *J Biol Chem* **283**, 31356-31365

49. Balakrishnan, L., and Bambara, R. A. (2013) Flap endonuclease 1. *Annu Rev Biochem* **82**, 119-138

50. Howes, T. R., and Tomkinson, A. E. (2012) DNA ligase I, the replicative DNA ligase. *Subcell Biochem* **62**, 327-341

51. Levin, D. S., Bai, W., Yao, N., O'Donnell, M., and Tomkinson, A. E. (1997) An interaction between DNA ligase I and proliferating cell nuclear antigen: implications for Okazaki fragment synthesis and joining. *Proc Natl Acad Sci U S A* **94**, 12863-12868

52. Rossi, M. L., and Bambara, R. A. (2006) Reconstituted Okazaki fragment processing indicates two pathways of primer removal. *J Biol Chem* **281**, 26051-26061

53. Hasan, S., Stucki, M., Hassa, P. O., Imhof, R., Gehrig, P., Hunziker, P., Hubscher, U., and Hottiger, M. O. (2001) Regulation of human flap endonuclease-1 activity by acetylation through the transcriptional coactivator p300. *Mol Cell* **7**, 1221-1231

54. Ayyagari, R., Gomes, X. V., Gordenin, D. A., and Burgers, P. M. (2003) Okazaki fragment maturation in yeast. I. Distribution of functions between FEN1 AND DNA2. *J Biol Chem* **278**, 1618-1625

55. Pike, J. E., Burgers, P. M., Campbell, J. L., and Bambara, R. A. (2009) Pif1 helicase lengthens some Okazaki fragment flaps necessitating Dna2 nuclease/helicase action in the two-nuclease processing pathway. *J Biol Chem* **284**, 25170-25180

56. Rossi, M. L., Pike, J. E., Wang, W., Burgers, P. M., Campbell, J. L., and Bambara, R. A. (2008) Pif1 helicase directs eukaryotic Okazaki fragments toward the two-nuclease cleavage pathway for primer removal. *J Biol Chem* **283**, 27483-27493

57. Bae, S. H., Bae, K. H., Kim, J. A., and Seo, Y. S. (2001) RPA governs endonuclease switching during processing of Okazaki fragments in eukaryotes. *Nature* **412**, 456-461

58. Bae, S. H., and Seo, Y. S. (2000) Characterization of the enzymatic properties of the yeast dna2 Helicase/endonuclease suggests a new model for Okazaki fragment processing. *J Biol Chem* **275**, 38022-38031

59. Henry, R. A., Balakrishnan, L., Ying-Lin, S. T., Campbell, J. L., and Bambara, R. A. (2010) Components of the secondary pathway stimulate the primary pathway of eukaryotic Okazaki fragment processing. *J Biol Chem* **285**, 28496-28505

60. Zheng, L., and Shen, B. (2011) Okazaki fragment maturation: nucleases take centre stage. *J Mol Cell Biol* **3**, 23-30

61. Smith, D. J., and Whitehouse, I. (2012) Intrinsic coupling of lagging-strand synthesis to chromatin assembly. *Nature* **483**, 434-438

62. Hoek, M., and Stillman, B. (2003) Chromatin assembly factor 1 is essential and couples chromatin assembly to DNA replication in vivo. *Proc Natl Acad Sci U S A* **100**, 12183-12188

63. Tyagi, M., Imam, N., Verma, K., and Patel, A. K. (2016) Chromatin remodelers: We are the drivers!! *Nucleus* **7**, 388-404

64. McCullough, S. D., and Grant, P. A. (2010) Histone acetylation, acetyltransferases, and ataxia--alteration of histone acetylation and chromatin dynamics is implicated in the pathogenesis of polyglutamine-expansion disorders. *Adv Protein Chem Struct Biol* **79**, 165-203

65. Krude, T. (1995) Chromatin. Nucleosome assembly during DNA replication. *Curr Biol* **5**, 1232-1234

66. Tagami, H., Ray-Gallet, D., Almouzni, G., and Nakatani, Y. (2004) Histone H3.1 and H3.3 complexes mediate nucleosome assembly pathways dependent or independent of DNA synthesis. *Cell* **116**, 51-61

67. Ransom, M., Dennehey, B. K., and Tyler, J. K. (2010) Chaperoning histones during DNA replication and repair. *Cell* **140**, 183-195

68. Jiang, J., Lu, J., Lu, D., Liang, Z., Li, L., Ouyang, S., Kong, X., Jiang, H., Shen, B., and Luo, C. (2012) Investigation of the acetylation mechanism by GCN5 histone acetyltransferase. *PLoS One* **7**, e36660

69. Marzluff, W. F., Wagner, E. J., and Duronio, R. J. (2008) Metabolism and regulation of canonical histone mRNAs: life without a poly(A) tail. *Nat Rev Genet* **9**, 843-854

70. Alabert, C., and Groth, A. (2012) Chromatin replication and epigenome maintenance. *Nat Rev Mol Cell Biol* **13**, 153-167

71. Gunesdogan, U., Jackle, H., and Herzig, A. (2014) Histone supply regulates S phase timing and cell cycle progression. *Elife* **3**, e02443

72. Rothbart, S. B., and Strahl, B. D. (2014) Interpreting the language of histone and DNA modifications. *Biochim Biophys Acta* **1839**, 627-643

73. Larsen, M. R., Trelle, M. B., Thingholm, T. E., and Jensen, O. N. (2006) Analysis of posttranslational modifications of proteins by tandem mass spectrometry. *Biotechniques* **40**, 790-798

74. Darling, A. L., and Uversky, V. N. (2018) Intrinsic Disorder and Posttranslational Modifications: The Darker Side of the Biological Dark Matter. *Front Genet* **9**, 158

75. Murray, K. (1964) The Occurrence of Epsilon-N-Methyl Lysine in Histones. *Biochemistry* **3**, 10-15

76. Mersfelder, E. L., and Parthun, M. R. (2006) The tale beyond the tail: histone core domain modifications and the regulation of chromatin structure. *Nucleic Acids Res* **34**, 2653-2662

77. Arnaudo, A. M., and Garcia, B. A. (2013) Proteomic characterization of novel histone post-translational modifications. *Epigenetics Chromatin* **6**, 24

78. Allfrey, V. G., Faulkner, R., and Mirsky, A. E. (1964) Acetylation and Methylation of Histones and Their Possible Role in the Regulation of Rna Synthesis. *Proc Natl Acad Sci U S A* **51**, 786-794

79. Kouzarides, T. (2000) Acetylation: a regulatory modification to rival phosphorylation? *EMBO J* **19**, 1176-1179

80. Ali, I., Conrad, R. J., Verdin, E., and Ott, M. (2018) Lysine Acetylation Goes Global: From Epigenetics to Metabolism and Therapeutics. *Chem Rev* **118**, 1216-1252

81. Dhalluin, C., Carlson, J. E., Zeng, L., He, C., Aggarwal, A. K., and Zhou, M. M. (1999) Structure and ligand of a histone acetyltransferase bromodomain. *Nature* **399**, 491-496

82. Bannister, A. J., and Kouzarides, T. (2011) Regulation of chromatin by histone modifications. *Cell Res* **21**, 381-395

83. Brownell, J. E., and Allis, C. D. (1996) Special HATs for special occasions: linking histone acetylation to chromatin assembly and gene activation. *Curr Opin Genet Dev* **6**, 176-184

84. Marmorstein, R. (2001) Structure and function of histone acetyltransferases. *Cell Mol Life Sci* **58**, 693-703

85. Allis, C. D., Berger, S. L., Cote, J., Dent, S., Jenuwien, T., Kouzarides, T., Pillus, L., Reinberg, D., Shi, Y., Shiekhattar, R., Shilatifard, A., Workman, J., and Zhang, Y. (2007) New nomenclature for chromatin-modifying enzymes. *Cell* **131**, 633-636

86. Kim, G. W., and Yang, X. J. (2011) Comprehensive lysine acetylomes emerging from bacteria to humans. *Trends Biochem Sci* **36**, 211-220

87. Downey, M., and Baetz, K. (2016) Building a KATalogue of acetyllysine targeting and function. *Brief Funct Genomics* **15**, 109-118

88. Sun, X. J., Man, N., Tan, Y., Nimer, S. D., and Wang, L. (2015) The Role of Histone Acetyltransferases in Normal and Malignant Hematopoiesis. *Front Oncol* **5**, 108

89. Lu, L., Berkey, K. A., and Casero, R. A., Jr. (1996) RGFGIGS is an amino acid sequence required for acetyl coenzyme A binding and activity of human spermidine/spermine N1acetyltransferase. *J Biol Chem* **271**, 18920-18924

90. Grant, P. A., Eberharter, A., John, S., Cook, R. G., Turner, B. M., and Workman, J. L. (1999) Expanded lysine acetylation specificity of Gcn5 in native complexes. *J Biol Chem* **274**, 5895-5900

91. Li, S., and Shogren-Knaak, M. A. (2009) The Gcn5 bromodomain of the SAGA complex facilitates cooperative and cross-tail acetylation of nucleosomes. *J Biol Chem* **284**, 9411-9417

92. Zhang, W., Bone, J. R., Edmondson, D. G., Turner, B. M., and Roth, S. Y. (1998) Essential and redundant functions of histone acetylation revealed by mutation of target lysines and loss of the Gcn5p acetyltransferase. *EMBO J* **17**, 3155-3167

93. Burgess, R. J., Zhou, H., Han, J., and Zhang, Z. (2010) A role for Gcn5 in replication-coupled nucleosome assembly. *Mol Cell* **37**, 469-480

94. Yang, X. J., Ogryzko, V. V., Nishikawa, J., Howard, B. H., and Nakatani, Y. (1996) A p300/CBP-associated factor that competes with the adenoviral oncoprotein E1A. *Nature* **382**, 319-324

95. Yee, S. P., and Branton, P. E. (1985) Detection of cellular proteins associated with human adenovirus type 5 early region 1A polypeptides. *Virology* **147**, 142-153

96. Bannister, A. J., and Kouzarides, T. (1996) The CBP co-activator is a histone acetyltransferase. *Nature* **384**, 641-643

97. Ogryzko, V. V., Schiltz, R. L., Russanova, V., Howard, B. H., and Nakatani, Y. (1996) The transcriptional coactivators p300 and CBP are histone acetyltransferases. *Cell* **87**, 953-959

98. Yuan, H., and Marmorstein, R. (2013) Histone acetyltransferases: Rising ancient counterparts to protein kinases. *Biopolymers* **99**, 98-111

99. Zhang, X., Ouyang, S., Kong, X., Liang, Z., Lu, J., Zhu, K., Zhao, D., Zheng, M., Jiang, H., Liu, X., Marmorstein, R., and Luo, C. (2014) Catalytic mechanism of histone acetyltransferase p300: from the proton transfer to acetylation reaction. *J Phys Chem B* **118**, 2009-2019

100. Marmorstein, R. (2001) Structure of histone acetyltransferases. *J Mol Biol* **311**, 433-444

101. Avvakumov, N., and Cote, J. (2007) The MYST family of histone acetyltransferases and their intimate links to cancer. *Oncogene* **26**, 5395-5407

102. Doyon, Y., Selleck, W., Lane, W. S., Tan, S., and Cote, J. (2004) Structural and functional conservation of the NuA4 histone acetyltransferase complex from yeast to humans. *Mol Cell Biol* **24**, 1884-1896

103. Clarke, A. S., Lowell, J. E., Jacobson, S. J., and Pillus, L. (1999) Esa1p is an essential histone acetyltransferase required for cell cycle progression. *Mol Cell Biol* **19**, 2515-2526

104. Bird, A. W., Yu, D. Y., Pray-Grant, M. G., Qiu, Q., Harmon, K. E., Megee, P. C., Grant, P. A., Smith, M. M., and Christman, M. F. (2002) Acetylation of histone H4 by Esa1 is required for DNA double-strand break repair. *Nature* **419**, 411-415

105. Yan, Y., Harper, S., Speicher, D. W., and Marmorstein, R. (2002) The catalytic mechanism of the ESA1 histone acetyltransferase involves a self-acetylated intermediate. *Nat Struct Biol* **9**, 862-869

106. Gregoretti, I. V., Lee, Y. M., and Goodson, H. V. (2004) Molecular evolution of the histone deacetylase family: functional implications of phylogenetic analysis. *J Mol Biol* **338**, 17-31

107. Taunton, J., Hassig, C. A., and Schreiber, S. L. (1996) A mammalian histone deacetylase related to the yeast transcriptional regulator Rpd3p. *Science* **272**, 408-411

108. Riggs, M. G., Whittaker, R. G., Neumann, J. R., and Ingram, V. M. (1977) n-Butyrate causes histone modification in HeLa and Friend erythroleukaemia cells. *Nature* **268**, 462-464

109. Milazzo, G., Mercatelli, D., Di Muzio, G., Triboli, L., De Rosa, P., Perini, G., and Giorgi, F. M. (2020) Histone Deacetylases (HDACs): Evolution, Specificity, Role in Transcriptional Complexes, and Pharmacological Actionability. *Genes (Basel)* **11**

110. Sauve, A. A., Celic, I., Avalos, J., Deng, H., Boeke, J. D., and Schramm, V. L. (2001) Chemistry of gene silencing: the mechanism of NAD+-dependent deacetylation reactions. *Biochemistry* **40**, 15456-15463

111. Yoshida, M., Kudo, N., Kosono, S., and Ito, A. (2017) Chemical and structural biology of protein lysine deacetylases. *Proc Jpn Acad Ser B Phys Biol Sci* **93**, 297-321

112. Alonso, W. R., and Nelson, D. A. (1986) A novel yeast histone deacetylase: partial characterization and development of an activity assay. *Biochim Biophys Acta* **866**, 161-169

113. Kouzarides, T. (2007) Chromatin modifications and their function. *Cell* **128**, 693-705

114. Allen, H. F., Wade, P. A., and Kutateladze, T. G. (2013) The NuRD architecture. *Cell Mol Life Sci* **70**, 3513-3524

115. Heinzel, T., Lavinsky, R. M., Mullen, T. M., Soderstrom, M., Laherty, C. D., Torchia, J., Yang, W. M., Brard, G., Ngo, S. D., Davie, J. R., Seto, E., Eisenman, R. N., Rose, D. W., Glass, C. K., and Rosenfeld, M. G. (1997) A complex containing N-CoR, mSin3 and histone deacetylase mediates transcriptional repression. *Nature* **387**, 43-48

116. Hodawadekar, S. C., and Marmorstein, R. (2007) Chemistry of acetyl transfer by histone modifying enzymes: structure, mechanism and implications for effector design. *Oncogene* **26**, 5528-5540

117. Kim, Y. B., Ki, S. W., Yoshida, M., and Horinouchi, S. (2000) Mechanism of cell cycle arrest caused by histone deacetylase inhibitors in human carcinoma cells. *J Antibiot (Tokyo)* **53**, 1191-1200

118. Montgomery, R. L., Davis, C. A., Potthoff, M. J., Haberland, M., Fielitz, J., Qi, X., Hill, J. A., Richardson, J. A., and Olson, E. N. (2007) Histone deacetylases 1 and 2 redundantly regulate cardiac morphogenesis, growth, and contractility. *Genes Dev* **21**, 1790-1802

119. de Ruijter, A. J., van Gennip, A. H., Caron, H. N., Kemp, S., and van Kuilenburg, A. B. (2003) Histone deacetylases (HDACs): characterization of the classical HDAC family. *Biochem J* **370**, 737-749

120. Haberland, M., Mokalled, M. H., Montgomery, R. L., and Olson, E. N. (2009) Epigenetic control of skull morphogenesis by histone deacetylase 8. *Genes Dev* **23**, 1625-1630

121. Boyault, C., Sadoul, K., Pabion, M., and Khochbin, S. (2007) HDAC6, at the crossroads between cytoskeleton and cell signaling by acetylation and ubiquitination. *Oncogene* **26**, 5468-5476

122. Chawla, S., Vanhoutte, P., Arnold, F. J., Huang, C. L., and Bading, H. (2003) Neuronal activity-dependent nucleocytoplasmic shuttling of HDAC4 and HDAC5. *J Neurochem* **85**, 151-159

123. Wu, J., Carmen, A. A., Kobayashi, R., Suka, N., and Grunstein, M. (2001) HDA2 and HDA3 are related proteins that interact with and are essential for the activity of the yeast histone deacetylase HDA1. *Proc Natl Acad Sci U S A* **98**, 4391-4396

124. Carmen, A. A., Rundlett, S. E., and Grunstein, M. (1996) HDA1 and HDA3 are components of a yeast histone deacetylase (HDA) complex. *J Biol Chem* **271**, 15837-15844

125. Fischle, W., Emiliani, S., Hendzel, M. J., Nagase, T., Nomura, N., Voelter, W., and Verdin, E. (1999) A new family of human histone deacetylases related to Saccharomyces cerevisiae HDA1p. *J Biol Chem* **274**, 11713-11720

126. Kao, H. Y., Downes, M., Ordentlich, P., and Evans, R. M. (2000) Isolation of a novel histone deacetylase reveals that class I and class II deacetylases promote SMRT-mediated repression. *Genes Dev* **14**, 55-66

127. Verdin, E., Dequiedt, F., and Kasler, H. G. (2003) Class II histone deacetylases: versatile regulators. *Trends Genet* **19**, 286-293

128. Emionite, L., Galmozzi, F., Grattarola, M., Boccardo, F., Vergani, L., and Toma, S. (2004) Histone deacetylase inhibitors enhance retinoid response in human breast cancer cell lines. *Anticancer Res* **24**, 4019-4024

129. Chang, S., McKinsey, T. A., Zhang, C. L., Richardson, J. A., Hill, J. A., and Olson, E. N. (2004) Histone deacetylases 5 and 9 govern responsiveness of the heart to a subset of stress signals and play redundant roles in heart development. *Mol Cell Biol* **24**, 8467-8476

130. Seigneurin-Berny, D., Verdel, A., Curtet, S., Lemercier, C., Garin, J., Rousseaux, S., and Khochbin, S. (2001) Identification of components of the murine histone deacetylase 6 complex: link between acetylation and ubiquitination signaling pathways. *Mol Cell Biol* **21**, 8035-8044

131. Hai, Y., Shinsky, S. A., Porter, N. J., and Christianson, D. W. (2017) Histone deacetylase 10 structure and molecular function as a polyamine deacetylase. *Nat Commun* **8**, 15368

132. Zhang, Y., Kwon, S., Yamaguchi, T., Cubizolles, F., Rousseaux, S., Kneissel, M., Cao, C., Li, N., Cheng, H. L., Chua, K., Lombard, D., Mizeracki, A., Matthias, G., Alt, F. W., Khochbin, S., and Matthias, P. (2008) Mice lacking histone deacetylase 6 have hyperacetylated tubulin but are viable and develop normally. *Mol Cell Biol* **28**, 1688-1701

133. Sinclair, D. A., and Guarente, L. (1997) Extrachromosomal rDNA circles--a cause of aging in yeast. *Cell* **91**, 1033-1042

134. Kaeberlein, M., McVey, M., and Guarente, L. (1999) The SIR2/3/4 complex and SIR2 alone promote longevity in Saccharomyces cerevisiae by two different mechanisms. *Genes Dev* **13**, 2570-2580

135. Imai, S., Johnson, F. B., Marciniak, R. A., McVey, M., Park, P. U., and Guarente, L. (2000) Sir2: an NAD-dependent histone deacetylase that connects chromatin silencing, metabolism, and aging. *Cold Spring Harb Symp Quant Biol* **65**, 297-302

136. Kane, A. E., and Sinclair, D. A. (2018) Sirtuins and NAD(+) in the Development and Treatment of Metabolic and Cardiovascular Diseases. *Circ Res* **123**, 868-885

137. Frye, R. A. (2000) Phylogenetic classification of prokaryotic and eukaryotic Sir2-like proteins. *Biochem Biophys Res Commun* **273**, 793-798

138. North, B. J., Marshall, B. L., Borra, M. T., Denu, J. M., and Verdin, E. (2003) The human Sir2 ortholog, SIRT2, is an NAD+-dependent tubulin deacetylase. *Mol Cell* **11**, 437-444

139. Vaziri, H., Dessain, S. K., Ng Eaton, E., Imai, S. I., Frye, R. A., Pandita, T. K., Guarente, L., and Weinberg, R. A. (2001) hSIR2(SIRT1) functions as an NAD-dependent p53 deacetylase. *Cell* **107**, 149-159

140. Mostoslavsky, R., Chua, K. F., Lombard, D. B., Pang, W. W., Fischer, M. R., Gellon, L., Liu, P., Mostoslavsky, G., Franco, S., Murphy, M. M., Mills, K. D., Patel, P., Hsu, J. T., Hong, A. L., Ford, E., Cheng, H. L., Kennedy, C., Nunez, N., Bronson, R., Frendewey, D., Auerbach, W., Valenzuela, D., Karow, M., Hottiger, M. O., Hursting, S., Barrett, J. C., Guarente, L., Mulligan, R., Demple, B., Yancopoulos, G. D., and Alt, F. W. (2006) Genomic instability and aging-like phenotype in the absence of mammalian SIRT6. *Cell* **124**, 315-329

141. Verdin, E., Hirschey, M. D., Finley, L. W., and Haigis, M. C. (2010) Sirtuin regulation of mitochondria: energy production, apoptosis, and signaling. *Trends Biochem Sci* **35**, 669-675

142. Nakagawa, T., Lomb, D. J., Haigis, M. C., and Guarente, L. (2009) SIRT5 Deacetylates carbamoyl phosphate synthetase 1 and regulates the urea cycle. *Cell* **137**, 560-570

143. Haigis, M. C., Mostoslavsky, R., Haigis, K. M., Fahie, K., Christodoulou, D. C., Murphy, A. J., Valenzuela, D. M., Yancopoulos, G. D., Karow, M., Blander, G., Wolberger, C., Prolla, T. A., Weindruch, R., Alt, F. W., and Guarente, L. (2006) SIRT4 inhibits glutamate dehydrogenase and opposes the effects of calorie restriction in pancreatic beta cells. *Cell* **126**, 941-954

144. Vakhrusheva, O., Smolka, C., Gajawada, P., Kostin, S., Boettger, T., Kubin, T., Braun, T., and Bober, E. (2008) Sirt7 increases stress resistance of cardiomyocytes and prevents apoptosis and inflammatory cardiomyopathy in mice. *Circ Res* **102**, 703-710

145. Gao, L., Cueto, M. A., Asselbergs, F., and Atadja, P. (2002) Cloning and functional characterization of HDAC11, a novel member of the human histone deacetylase family. *J Biol Chem* **277**, 25748-25755

146. Cao, J., Sun, L., Aramsangtienchai, P., Spiegelman, N. A., Zhang, X., Huang, W., Seto, E., and Lin, H. (2019) HDAC11 regulates type I interferon signaling through defatty-acylation of SHMT2. *Proc Natl Acad Sci U S A* **116**, 5487-5492

147. Kutil, Z., Novakova, Z., Meleshin, M., Mikesova, J., Schutkowski, M., and Barinka, C. (2018) Histone Deacetylase 11 Is a Fatty-Acid Deacylase. *ACS Chem Biol* **13**, 685-693

148. Brown, J. L., and Roberts, W. K. (1976) Evidence that approximately eighty per cent of the soluble proteins from Ehrlich ascites cells are Nalpha-acetylated. *J Biol Chem* **251**, 1009-1014

149. Narita, T., Weinert, B. T., and Choudhary, C. (2019) Author Correction: Functions and mechanisms of non-histone protein acetylation. *Nat Rev Mol Cell Biol* **20**, 508

150. Gu, W., and Roeder, R. G. (1997) Activation of p53 sequence-specific DNA binding by acetylation of the p53 C-terminal domain. *Cell* **90**, 595-606

151. Tang, Y., Zhao, W., Chen, Y., Zhao, Y., and Gu, W. (2008) Acetylation is indispensable for p53 activation. *Cell* **133**, 612-626

152. Sykes, S. M., Mellert, H. S., Holbert, M. A., Li, K., Marmorstein, R., Lane, W. S., and McMahon, S. B. (2006) Acetylation of the p53 DNA-binding domain regulates apoptosis induction. *Mol Cell* **24**, 841-851

153. Nihira, N. T., Ogura, K., Shimizu, K., North, B. J., Zhang, J., Gao, D., Inuzuka, H., and Wei, W. (2017) Acetylation-dependent regulation of MDM2 E3 ligase activity dictates its oncogenic function. *Sci Signal* **10**

154. Quivy, V., and Van Lint, C. (2004) Regulation at multiple levels of NF-kappaB-mediated transactivation by protein acetylation. *Biochem Pharmacol* **68**, 1221-1229

155. Kim, S. C., Sprung, R., Chen, Y., Xu, Y., Ball, H., Pei, J., Cheng, T., Kho, Y., Xiao, H., Xiao, L., Grishin, N. V., White, M., Yang, X. J., and Zhao, Y. (2006) Substrate and functional diversity of lysine acetylation revealed by a proteomics survey. *Mol Cell* **23**, 607-618

156. Wu, H., and Parsons, J. T. (1993) Cortactin, an 80/85-kilodalton pp60src substrate, is a filamentous actin-binding protein enriched in the cell cortex. *J Cell Biol* **120**, 1417-1426

157. Chu, C. W., Hou, F., Zhang, J., Phu, L., Loktev, A. V., Kirkpatrick, D. S., Jackson, P. K., Zhao, Y., and Zou, H. (2011) A novel acetylation of beta-tubulin by San modulates microtubule polymerization via down-regulating tubulin incorporation. *Mol Biol Cell* **22**, 448-456

158. Lippens, G., Sillen, A., Landrieu, I., Amniai, L., Sibille, N., Barbier, P., Leroy, A., Hanoulle, X., and Wieruszeski, J. M. (2007) Tau aggregation in Alzheimer's disease: what role for phosphorylation? *Prion* **1**, 21-25

159. Cohen, T. J., Guo, J. L., Hurtado, D. E., Kwong, L. K., Mills, I. P., Trojanowski, J. Q., and Lee, V. M. (2011) The acetylation of tau inhibits its function and promotes pathological tau aggregation. *Nat Commun* **2**, 252

160. Andreadis, A., Brown, W. M., and Kosik, K. S. (1992) Structure and novel exons of the human tau gene. *Biochemistry* **31**, 10626-10633

161. Min, S. W., Cho, S. H., Zhou, Y., Schroeder, S., Haroutunian, V., Seeley, W. W., Huang, E. J., Shen, Y., Masliah, E., Mukherjee, C., Meyers, D., Cole, P. A., Ott, M., and Gan, L. (2010) Acetylation of tau inhibits its degradation and contributes to tauopathy. *Neuron* **67**, 953-966

162. Min, S. W., Chen, X., Tracy, T. E., Li, Y., Zhou, Y., Wang, C., Shirakawa, K., Minami, S. S., Defensor, E., Mok, S. A., Sohn, P. D., Schilling, B., Cong, X., Ellerby, L., Gibson, B. W., Johnson, J., Krogan, N., Shamloo, M., Gestwicki, J., Masliah, E., Verdin, E., and Gan, L. (2015) Critical role of acetylation in tau-mediated neurodegeneration and cognitive deficits. *Nat Med* **21**, 1154-1162

163. Dietschy, T., Shevelev, I., Pena-Diaz, J., Huhn, D., Kuenzle, S., Mak, R., Miah, M. F., Hess, D., Fey, M., Hottiger, M. O., Janscak, P., and Stagljar, I. (2009) p300-mediated acetylation of the Rothmund-Thomson-syndrome gene product RECQL4 regulates its subcellular localization. *J Cell Sci* **122**, 1258-1267

164. Bannister, A. J., Miska, E. A., Gorlich, D., and Kouzarides, T. (2000) Acetylation of importin-alpha nuclear import factors by CBP/p300. *Curr Biol* **10**, 467-470

165. Choudhary, C., Kumar, C., Gnad, F., Nielsen, M. L., Rehman, M., Walther, T. C., Olsen, J. V., and Mann, M. (2009) Lysine acetylation targets protein complexes and co-regulates major cellular functions. *Science* **325**, 834-840

166. Glozak, M. A., and Seto, E. (2009) Acetylation/deacetylation modulates the stability of DNA replication licensing factor Cdt1. *J Biol Chem* **284**, 11446-11453

167. Balakrishnan, L., Stewart, J., Polaczek, P., Campbell, J. L., and Bambara, R. A. (2010) Acetylation of Dna2 endonuclease/helicase and flap endonuclease 1 by p300 promotes DNA stability by creating long flap intermediates. *J Biol Chem* **285**, 4398-4404

168. Raney, K. D., Byrd, A. K., and Aarattuthodiyil, S. (2013) Structure and Mechanisms of SF1 DNA Helicases. *Adv Exp Med Biol* **973**, E1

169. Brosh, R. M., Jr. (2013) DNA helicases involved in DNA repair and their roles in cancer. *Nat Rev Cancer* **13**, 542-558

170. Zhou, R., Zhang, J., Bochman, M. L., Zakian, V. A., and Ha, T. (2014) Periodic DNA patrolling underlies diverse functions of Pif1 on R-loops and G-rich DNA. *Elife* **3**, e02190

171. Lahaye, A., Stahl, H., Thines-Sempoux, D., and Foury, F. (1991) PIF1: a DNA helicase in yeast mitochondria. *Embo J* **10**, 997-1007

172. Singleton, M. R., Dillingham, M. S., and Wigley, D. B. (2007) Structure and mechanism of helicases and nucleic acid translocases. *Annu Rev Biochem* **76**, 23-50

173. Chung, W. H. (2014) To Peep into Pif1 Helicase: Multifaceted All the Way from Genome Stability to Repair-Associated DNA Synthesis. *Journal of Microbiology* **52**, 89-98

174. Ribeyre, C., Lopes, J., Boule, J. B., Piazza, A., Guedin, A., Zakian, V. A., Mergny, J. L., and Nicolas, A. (2009) The Yeast Pif1 Helicase Prevents Genomic Instability Caused by G-Quadruplex-Forming CEB1 Sequences In Vivo. *Plos Genetics* **5**

175. Tran, P. L. T., Pohl, T. J., Chen, C. F., Chan, A., Pott, S., and Zakian, V. A. (2017) PIF1 family DNA helicases suppress R-loop mediated genome instability at tRNA genes. *Nat Commun* **8**, 15025

176. Nickens, D. G., Sausen, C. W., and Bochman, M. L. (2019) The Biochemical Activities of the Saccharomyces cerevisiae Pif1 Helicase Are Regulated by Its N-Terminal Domain. *Genes (Basel)* **10**

177. Paeschke, K., Bochman, M. L., Garcia, P. D., Cejka, P., Friedman, K. L., Kowalczykowski, S. C., and Zakian, V. A. (2013) Pif1 family helicases suppress genome instability at G-quadruplex motifs. *Nature* **497**, 458-+

178. Dahan, D., Tsirkas, I., Dovrat, D., Sparks, M. A., Singh, S. P., Galletto, R., and Aharoni, A. (2018) Pif1 is essential for efficient replisome progression through lagging strand G-quadruplex DNA secondary structures. *Nucleic Acids Res* **46**, 11847-11857

179. Wilson, M. A., Kwon, Y., Xu, Y., Chung, W. H., Chi, P., Niu, H., Mayle, R., Chen, X., Malkova, A., Sung, P., and Ira, G. (2013) Pif1 helicase and Poldelta promote recombination-coupled DNA synthesis via bubble migration. *Nature* **502**, 393-396

180. Ivessa, A. S., Zhou, J. Q., and Zakian, V. A. (2000) The Saccharomyces Pif1p DNA helicase and the highly related Rrm3p have opposite effects on replication fork progression in ribosomal DNA. *Cell* **100**, 479-489

181. Boule, J. B., Vega, L. R., and Zakian, V. A. (2005) The yeast Pif1p helicase removes telomerase from telomeric DNA. *Nature* **438**, 57-61

182. Makovets, S., and Blackburn, E. H. (2009) DNA damage signalling prevents deleterious telomere addition at DNA breaks. *Nat Cell Biol* **11**, 1383-1386

183. Bochman, M. L., Paeschke, K., Chan, A., and Zakian, V. A. (2014) Hrq1, a homolog of the human RecQ4 helicase, acts catalytically and structurally to promote genome integrity. *Cell Rep* **6**, 346-356

184. Nickens, D. G., Rogers, C. M., and Bochman, M. L. (2018) The Saccharomyces cerevisiae Hrq1 and Pif1 DNA helicases synergistically modulate telomerase activity in vitro. *J Biol Chem* **293**, 14481-14496

185. Singleton, M. R., and Wigley, D. B. (2002) Modularity and specialization in superfamily 1 and 2 helicases. *J Bacteriol* **184**, 1819-1826

186. Andis, N. M., Sausen, C. W., Alladin, A., and Bochman, M. L. (2018) The WYL Domain of the PIF1 Helicase from the Thermophilic Bacterium Thermotoga elfii is an Accessory Single-Stranded DNA Binding Module. *Biochemistry* **57**, 1108-1118

187. Fairman-Williams, M. E., Guenther, U. P., and Jankowsky, E. (2010) SF1 and SF2 helicases: family matters. *Curr Opin Struct Biol* **20**, 313-324

188. Deribe, Y. L., Pawson, T., and Dikic, I. (2010) Post-translational modifications in signal integration. *Nat Struct Mol Biol* **17**, 666-672

189. Allfrey, V. G., Faulkner, R., and Mirsky, A. E. (1964) Acetylation and methylation of histones and their possible role in the regulation of RNA synthesis. *Proc. Natl. Acad. Sci. U.S.A.* **51**, 786-794

190. Belyaev, N., Keohane, A. M., and Turner, B. M. (1996) Differential underacetylation of histones H2A, H3 and H4 on the inactive X chromosome in human female cells. *Hum. Genet.* **97**, 573-578

191. Chicoine, L. G., Richman, R., Cook, R. G., Gorovsky, M. A., and Allis, C. D. (1987) A single histone acetyltransferase from Tetrahymena macronuclei catalyzes deposition-related acetylation of free histones and transcription-related acetylation of nucleosomal histones. *J. Cell. Biol.* **105**, 127-135

192. Wang, Y., and Luo, J. (2017) Acetylation of BLM protein regulates its function in response to DNA damage. *RSC Advances* **7**, 55301-55308

193. Li, K., Wang, R., Lozada, E., Fan, W., Orren, D. K., and Luo, J. (2010) Acetylation of WRN protein regulates its stability by inhibiting ubiquitination. *PLoS One* **5**, e10341

194. Ononye, O. E., Njeri, C. W., and Balakrishnan, L. (2019) Analysis of DNA Processing Enzyme FEN1 and Its Regulation by Protein Lysine Acetylation. *Methods Mol Biol* **1983**, 207-224

195. Billon, P., and Cote, J. (2017) Novel mechanism of PCNA control through acetylation of its sliding surface. *Mol Cell Oncol* **4**, e1279724

196. Zhao, M., Geng, R., Guo, X., Yuan, R., Zhou, X., Zhong, Y., Huo, Y., Zhou, M., Shen, Q., Li, Y., Zhu, W., and Wang, J. (2017) PCAF/GCN5-Mediated Acetylation of RPA1 Promotes Nucleotide Excision Repair. *Cell Rep* **20**, 1997-2009

197. He, H., Wang, J., and Liu, T. (2017) UV-Induced RPA1 Acetylation Promotes Nucleotide Excision Repair. *Cell Rep* **20**, 2010-2025

198. Peng, W., Togawa, C., Zhang, K., and Kurdistani, S. K. (2008) Regulators of cellular levels of histone acetylation in Saccharomyces cerevisiae. *Genetics* **179**, 277-289

199. Spange, S., Wagner, T., Heinzel, T., and Kramer, O. H. (2009) Acetylation of non-histone proteins modulates cellular signalling at multiple levels. *Int J Biochem Cell Biol* **41**, 185-198

200. Chang, M., Luke, B., Kraft, C., Li, Z., Peter, M., Lingner, J., and Rothstein, R. (2009) Telomerase is essential to alleviate pif1-induced replication stress at telomeres. *Genetics* **183**, 779-791

201. Nickens, D. G., Sausen, C. W., and Bochman, M. L. (2019) The biochemical activities of the Saccharomyces cerevisiae Pif1 helicase are regulated by its N-terminal domain. *bioRxiv*, 596098

202. Yoshikawa, K., Tanaka, T., Ida, Y., Furusawa, C., Hirasawa, T., and Shimizu, H. (2011) Comprehensive phenotypic analysis of single-gene deletion and overexpression strains of Saccharomyces cerevisiae. *Yeast* **28**, 349-361

203. Ngo, M., Wechter, N., Tsai, E., Shun, T. Y., Gough, A., Schurdak, M. E., Schwacha, A., and Vogt, A. (2019) A High-Throughput Assay for DNA Replication Inhibitors Based upon Multivariate Analysis of Yeast Growth Kinetics. *SLAS Discovery* **24**, 669-681

204. Roth, S. Y., Denu, J. M., and Allis, C. D. (2001) Histone acetyltransferases. *Annu Rev Biochem* **70**, 81-120

205. Smith, E. R., Eisen, A., Gu, W., Sattah, M., Pannuti, A., Zhou, J., Cook, R. G., Lucchesi, J. C., and Allis, C. D. (1998) ESA1 is a histone acetyltransferase that is essential for growth in yeast. *Proceedings of the National Academy of Sciences of the United States of America* **95**, 3561-3565

206. Clarke, A. S., Lowell, J. E., Jacobson, S. J., and Pillus, L. (1999) Esa1p is an essential histone acetyltransferase required for cell cycle progression. *Molecular and cellular biology* **19**, 2515-2526

207. Chang, C. S., and Pillus, L. (2009) Collaboration between the essential Esa1 acetyltransferase and the Rpd3 deacetylase is mediated by H4K12 histone acetylation in Saccharomyces cerevisiae. *Genetics* **183**, 149-160

208. Chib, S., Byrd, A. K., and Raney, K. D. (2016) Yeast Helicase Pif1 Unwinds RNA:DNA Hybrids with Higher Processivity than DNA:DNA Duplexes. *J Biol Chem* **291**, 5889-5901

209. Sparks, M. A., Singh, S. P., Burgers, P. M., and Galletto, R. (2019) Complementary roles of Pif1 helicase and single stranded DNA binding proteins in stimulating DNA replication through G-quadruplexes. *Nucleic Acids Res* **47**, 8595-8605

210. Boule, J. B., and Zakian, V. A. (2007) The yeast Pif1p DNA helicase preferentially unwinds RNA DNA substrates. *Nucleic Acids Res* **35**, 5809-5818

211. Sausen, C. W., Rogers, C. M., and Bochman, M. L. (2019) Thin-Layer Chromatography and Real-Time Coupled Assays to Measure ATP Hydrolysis. *Methods Mol Biol* **1999**, 245-253

212. Byrd, A. K., and Raney, K. D. (2017) Structure and function of Pif1 helicase. *Biochem Soc Trans* **45**, 1159-1171

213. Lu, K.-Y., Chen, W.-F., Rety, S., Liu, N.-N., Wu, W.-Q., Dai, Y.-X., Li, D., Ma, H.-Y., Dou, S.-X., and Xi, X.-G. (2018) Insights into the structural and mechanistic basis of multifunctional S. cerevisiae Pif1p helicase. *Nucleic acids research* **46**, 1486-1500

214. Dehghani-Tafti, S., Levdikov, V., Antson, A. A., Bax, B., and Sanders, C. M. (2019) Structural and functional analysis of the nucleotide and DNA binding activities of the human PIF1 helicase. *Nucleic Acids Research* **47**, 3208-3222

215. Chib, S., Byrd, A. K., and Raney, K. D. (2016) Yeast Helicase Pif1 Unwinds RNA:DNA Hybrids with Higher Processivity than DNA:DNA Duplexes. *Journal of Biological Chemistry* **291**, 5889-5901

216. Singh, S. P., Soranno, A., Sparks, M. A., and Galletto, R. (2019) Branched unwinding mechanism of the Pif1 family of DNA helicases. *Proceedings of the National Academy of Sciences* **116**, 24533

217. Zhou, R. B., Zhang, J. C., Bochman, M. L., Zakian, V. A., and Ha, T. (2014) Periodic DNA patrolling underlies diverse functions of Pif1 on R-loops and G-rich DNA. *Elife* **3**, 16

218. Ho, B., Baryshnikova, A., and Brown, G. W. (2018) Unification of Protein Abundance Datasets Yields a Quantitative Saccharomyces cerevisiae Proteome. *Cell Syst* **6**, 192-205.e193

219. Geronimo, C. L., and Zakian, V. A. (2016) Getting it done at the ends: Pif1 family DNA helicases and telomeres. *DNA Repair (Amst)* **44**, 151-158

220. Makovets, S., and Blackburn, E. H. (2009) DNA damage signalling prevents deleterious telomere addition at DNA breaks. *Nat. Cell Biol.* **11**, 1383-U1288

221. Barnes, C. E., English, D. M., and Cowley, S. M. (2019) Acetylation & Co: an expanding repertoire of histone acylations regulates chromatin and transcription. *Essays Biochem* **63**, 97-107

222. Aparicio, J. G., Viggiani, C. J., Gibson, D. G., and Aparicio, O. M. (2004) The Rpd3-Sin3 histone deacetylase regulates replication timing and enables intra-S origin control in Saccharomyces cerevisiae. *Mol Cell Biol* **24**, 4769-4780

223. Lin, Y. Y., Qi, Y., Lu, J. Y., Pan, X., Yuan, D. S., Zhao, Y., Bader, J. S., and Boeke, J. D. (2008) A comprehensive synthetic genetic interaction network governing yeast histone acetylation and deacetylation. *Genes Dev* **22**, 2062-2074

224. Billon, P., Li, J., Lambert, J. P., Chen, Y., Tremblay, V., Brunzelle, J. S., Gingras, A. C., Verreault, A., Sugiyama, T., Couture, J. F., and Cote, J. (2017) Acetylation of PCNA Sliding Surface by Eco1 Promotes Genome Stability through Homologous Recombination. *Mol Cell* **65**, 78-90

225. Robinson, P. J., An, W., Routh, A., Martino, F., Chapman, L., Roeder, R. G., and Rhodes, D. (2008) 30 nm chromatin fibre decompaction requires both H4-K16 acetylation and linker histone eviction. *J Mol Biol* **381**, 816-825

226. Saikrishnan, K., Powell, B., Cook, N. J., Webb, M. R., and Wigley, D. B. (2009) Mechanistic basis of 5'-3' translocation in SF1B helicases. *Cell* **137**, 849-859

227. Lohman, T. M., Tomko, E. J., and Wu, C. G. (2008) Non-hexameric DNA helicases and translocases: mechanisms and regulation. *Nat Rev Mol Cell Biol* **9**, 391-401

228. Bessler, J. B., Torres, J. Z., and Zakian, V. A. (2001) The Pif1p subfamily of helicases: region-specific DNA helicases? *Trends Cell Biol* **11**, 60-65

229. Lu, K. Y., Chen, W. F., Rety, S., Liu, N. N., Wu, W. Q., Dai, Y. X., Li, D., Ma, H. Y., Dou, S. X., and Xi, X. G. (2018) Insights into the structural and mechanistic basis of multifunctional S. cerevisiae Pif1p helicase. *Nucleic Acids Res* **46**, 1486-1500

230. Luo, J., Li, M., Tang, Y., Laszkowska, M., Roeder, R. G., and Gu, W. (2004) Acetylation of p53 augments its site-specific DNA binding both in vitro and in vivo. *Proc Natl Acad Sci U S A* **101**, 2259-2264

231. Boyes, J., Byfield, P., Nakatani, Y., and Ogryzko, V. (1998) Regulation of activity of the transcription factor GATA-1 by acetylation. *Nature* **396**, 594-598

232. Wang, R., Cherukuri, P., and Luo, J. (2005) Activation of Stat3 sequence-specific DNA binding and transcription by p300/CREB-binding protein-mediated acetylation. *J Biol Chem* **280**, 11528-11534

233. Cheng, X., Jobin-Robitaille, O., Billon, P., Buisson, R., Niu, H., Lacoste, N., Abshiru, N., Cote, V., Thibault, P., Kron, S. J., Sung, P., Brandl, C. J., Masson, J. Y., and Cote, J. (2018) Phospho-dependent recruitment of the yeast NuA4 acetyltransferase complex by MRX at DNA breaks regulates RPA dynamics during resection. *Proc Natl Acad Sci U S A* **115**, 10028-10033

234. Elfert, S., Weise, A., Bruser, K., Biniossek, M. L., Jägle, S., Senghaas, N., and Hecht, A. (2013) Acetylation of human TCF4 (TCF7L2) proteins attenuates inhibition by the HBP1 repressor and induces a conformational change in the TCF4::DNA complex. *PLoS One* **8**, e61867

235. Buchholz, I., Nestler, P., Köppen, S., and Delcea, M. (2018) Lysine residues control the conformational dynamics of beta 2-glycoprotein I. *Physical Chemistry Chemical Physics* **20**, 26819-26829

236. Buzovetsky, O., Kwon, Y., Pham, N. T., Kim, C., Ira, G., Sung, P., and Xiong, Y. (2017) Role of the Pif1-PCNA Complex in Pol delta-Dependent Strand Displacement DNA Synthesis and Break-Induced Replication. *Cell Rep* **21**, 1707-1714

237. Falquet, B., Olmezer, G., Enkner, F., Klein, D., Challa, K., Appanah, R., Gasser, S. M., and Rass, U. (2020) Disease-associated DNA2 nuclease-helicase protects cells from lethal chromosome under-replication. *Nucleic Acids Res*

238. Onwubiko, N. O., Borst, A., Diaz, S. A., Passkowski, K., Scheffel, F., Tessmer, I., and Nasheuer, H. P. (2020) SV40 T antigen interactions with ssDNA and replication protein A: a regulatory role of T antigen monomers in lagging strand DNA replication. *Nucleic Acids Research* **48**, 3657-3677

239. Bryant, E. E., Šunjevarić, I., Berchowitz, L., Rothstein, R., and Reid, R. J. D. (2019) Rad5 dysregulation drives hyperactive recombination at replication forks resulting in cisplatin sensitivity and genome instability. *Nucleic Acids Res* **47**, 9144-9159

240. Moruno-Manchon, J. F., Lejault, P., Wang, Y., McCauley, B., Honarpisheh, P., Morales Scheihing, D. A., Singh, S., Dang, W., Kim, N., Urayama, A., Zhu, L., Monchaud, D., McCullough, L. D., and Tsvetkov, A. S. (2020) Small-molecule G-quadruplex stabilizers reveal a novel pathway of autophagy regulation in neurons. *Elife* **9**

241. Gagou, M. E., Ganesh, A., Thompson, R., Phear, G., Sanders, C., and Meuth, M. (2011) Suppression of Apoptosis by PIF1 Helicase in Human Tumor Cells. *Cancer Research* **71**, 4998-5008

242. Gagou, M. E., Ganesh, A., Phear, G., Robinson, D., Petermann, E., Cox, A., and Meuth, M. (2014) Human PIF1 helicase supports DNA replication and cell growth under oncogenic-stress. *Oncotarget* **5**, 11381-11398

243. Chisholm, K. M., Aubert, S. D., Freese, K. P., Zakian, V. A., King, M. C., and Welcsh, P. L. (2012) A Genomewide Screen for Suppressors of Alu-Mediated Rearrangements Reveals a Role for PIF1. *Plos One* **7**, 10

244. Barrios, A., Selleck, W., Hnatkovich, B., Kramer, R., Sermwittayawong, D., and Tan, S. (2007) Expression and purification of recombinant yeast Ada2/Ada3/Gcn5 and Piccolo NuA4 histone acetyltransferase complexes. *Methods* **41**, 271-277

245. Langston, L. D., and O'Donnell, M. (2008) DNA polymerase delta is highly processive with proliferating cell nuclear antigen and undergoes collision release upon completing DNA. *J Biol Chem* **283**, 29522-29531

246. von der Haar, T. (2007) Optimized protein extraction for quantitative proteomics of yeasts. *PLoS One* **2**, e1078

247. Vester, K., Santos, K. F., Kuropka, B., Weise, C., and Wahl, M. C. (2019) The inactive C-terminal cassette of the dual-cassette RNA helicase BRR2 both stimulates and inhibits the activity of the N-terminal helicase unit. *J Biol Chem*

248. Rogers, C. M., Wang, J. C., Noguchi, H., Imasaki, T., Takagi, Y., and Bochman, M. L. (2017) Yeast Hrq1 shares structural and functional homology with the disease-linked human RecQ4 helicase. *Nucleic Acids Res* **45**, 5217-5230

249. Wold, M. S. (1997) Replication protein A: a heterotrimeric, single-stranded DNA-binding protein required for eukaryotic DNA metabolism. *Annu Rev Biochem* **66**, 61-92

250. Deng, S. K., Chen, H., and Symington, L. S. (2015) Replication protein A prevents promiscuous annealing between short sequence homologies: Implications for genome integrity. *Bioessays* **37**, 305-313

251. Binz, S. K., Sheehan, A. M., and Wold, M. S. (2004) Replication protein A phosphorylation and the cellular response to DNA damage. *DNA Repair (Amst)* **3**, 1015-1024

252. Fan, J., and Pavletich, N. P. (2012) Structure and conformational change of a replication protein A heterotrimer bound to ssDNA. *Genes Dev* **26**, 2337-2347

253. Iftode, C., Daniely, Y., and Borowiec, J. A. (1999) Replication protein A (RPA): the eukaryotic SSB. *Crit Rev Biochem Mol Biol* **34**, 141-180

254. Chen, R., and Wold, M. S. (2014) Replication protein A: single-stranded DNA's first responder: dynamic DNA-interactions allow replication protein A to direct single-strand DNA intermediates into different pathways for synthesis or repair. *Bioessays* **36**, 1156-1161

255. Bochkareva, E., Korolev, S., Lees-Miller, S. P., and Bochkarev, A. (2002) Structure of the RPA trimerization core and its role in the multistep DNA-binding mechanism of RPA. *EMBO J* **21**, 1855-1863

256. Wang, Q. M., Yang, Y. T., Wang, Y. R., Gao, B., Xi, X. G., and Hou, X. M. (2019) Human replication protein A induces dynamic changes in single-stranded DNA and RNA structures. *J Biol Chem* **294**, 13915-13927

257. Bartos, J. D., Willmott, L. J., Binz, S. K., Wold, M. S., and Bambara, R. A. (2008) Catalysis of strand annealing by replication protein A derives from its strand melting properties. *J Biol Chem* **283**, 21758-21768

258. Gibb, B., Ye, L. F., Gergoudis, S. C., Kwon, Y., Niu, H., Sung, P., and Greene, E. C. (2014) Concentration-dependent exchange of replication protein A on single-stranded DNA revealed by single-molecule imaging. *PLoS One* **9**, e87922

259. Ahmad, F., Patterson, A., Deveryshetty, J., Mattice, J., Pokhrel, N., Bothner, B., and Antony, E. (2020) Hydrogen-deuterium exchange reveals a dynamic DNA binding map of Replication Protein A. *bioRxiv*, 2020.2009.2004.283879

260. Gan, H., Yu, C., Devbhandari, S., Sharma, S., Han, J., Chabes, A., Remus, D., and Zhang, Z. (2017) Checkpoint Kinase Rad53 Couples Leading- and Lagging-Strand DNA Synthesis under Replication Stress. *Mol Cell* **68**, 446-455 e443

261. Guilliam, T. A., Jozwiakowski, S. K., Ehlinger, A., Barnes, R. P., Rudd, S. G., Bailey, L. J., Skehel, J. M., Eckert, K. A., Chazin, W. J., and Doherty, A. J. (2015) Human PrimPol is a highly error-prone polymerase regulated by single-stranded DNA binding proteins. *Nucleic Acids Res* **43**, 1056-1068

262. Martinez-Jimenez, M. I., Lahera, A., and Blanco, L. (2017) Human PrimPol activity is enhanced by RPA. *Sci Rep* **7**, 783

263. Koc, K. N., Stodola, J. L., Burgers, P. M., and Galletto, R. (2015) Regulation of yeast DNA polymerase delta-mediated strand displacement synthesis by 5'-flaps. *Nucleic Acids Res* **43**, 4179-4190

264. Zaher, M. S., Rashid, F., Song, B., Joudeh, L. I., Sobhy, M. A., Tehseen, M., Hingorani, M. M., and Hamdan, S. M. (2018) Missed cleavage opportunities by FEN1 lead to Okazaki fragment maturation via the long-flap pathway. *Nucleic Acids Res* **46**, 2956-2974

265. Gloor, J. W., Balakrishnan, L., Campbell, J. L., and Bambara, R. A. (2012) Biochemical analyses indicate that binding and cleavage specificities define the ordered processing of human Okazaki fragments by Dna2 and FEN1. *Nucleic Acids Res* **40**, 6774-6786

266. Brosh, R. M., Jr., Li, J. L., Kenny, M. K., Karow, J. K., Cooper, M. P., Kureekattil, R. P., Hickson, I. D., and Bohr, V. A. (2000) Replication protein A physically interacts with the Bloom's syndrome protein and stimulates its helicase activity. *J Biol Chem* **275**, 23500-23508

267. DeMott, M. S., Zigman, S., and Bambara, R. A. (1998) Replication protein A stimulates long patch DNA base excision repair. *J Biol Chem* **273**, 27492-27498

268. Nagelhus, T. A., Haug, T., Singh, K. K., Keshav, K. F., Skorpen, F., Otterlei, M., Bharati, S., Lindmo, T., Benichou, S., Benarous, R., and Krokan, H. E. (1997) A sequence in the N-terminal region of human uracil-DNA glycosylase with homology to XPA interacts with the C-terminal part of the 34-kDa subunit of replication protein A. *J Biol Chem* **272**, 6561-6566

269. Slupphaug, G., Mol, C. D., Kavli, B., Arvai, A. S., Krokan, H. E., and Tainer, J. A. (1996) A nucleotide-flipping mechanism from the structure of human uracil-DNA glycosylase bound to DNA. *Nature* **384**, 87-92

270. Jackson, S. P. (2002) Sensing and repairing DNA double-strand breaks. *Carcinogenesis* **23**, 687-696

271. McKinnon, P. J., and Caldecott, K. W. (2007) DNA strand break repair and human genetic disease. *Annu Rev Genomics Hum Genet* **8**, 37-55

272. Borgstahl, G. E., Brader, K., Mosel, A., Liu, S., Kremmer, E., Goettsch, K. A., Kolar, C., Nasheuer, H. P., and Oakley, G. G. (2014) Interplay of DNA damage and cell cycle signaling at the level of human replication protein A. *DNA Repair (Amst)* **21**, 12-23

273. Oakley, G. G., and Patrick, S. M. (2010) Replication protein A: directing traffic at the intersection of replication and repair. *Front Biosci (Landmark Ed)* **15**, 883-900

274. Anantha, R. W., Sokolova, E., and Borowiec, J. A. (2008) RPA phosphorylation facilitates mitotic exit in response to mitotic DNA damage. *Proc Natl Acad Sci U S A* **105**, 12903-12908

275. Dou, H., Huang, C., Singh, M., Carpenter, P. B., and Yeh, E. T. (2010) Regulation of DNA repair through deSUMOylation and SUMOylation of replication protein A complex. *Mol Cell* **39**, 333-345

276. Elia, A. E., Wang, D. C., Willis, N. A., Boardman, A. P., Hajdu, I., Adeyemi, R. O., Lowry, E., Gygi, S. P., Scully, R., and Elledge, S. J. (2015) RFWD3-Dependent Ubiquitination of RPA Regulates Repair at Stalled Replication Forks. *Mol Cell* **60**, 280-293

277. Marechal, A., Li, J. M., Ji, X. Y., Wu, C. S., Yazinski, S. A., Nguyen, H. D., Liu, S., Jimenez, A. E., Jin, J., and Zou, L. (2014) PRP19 transforms into a sensor of RPA-ssDNA after DNA damage and drives ATR activation via a ubiquitin-mediated circuitry. *Mol Cell* **53**, 235-246

278. Yu, H., Bu, C., Liu, Y., Gong, T., Liu, X., Liu, S., Peng, X., Zhang, W., Peng, Y., Yang, J., He, L., Zhang, Y., Yi, X., Yang, X., Sun, L., Shang, Y., Cheng, Z., and Liang, J. (2020) Global crotonylome reveals CDYL-regulated RPA1 crotonylation in homologous recombination-mediated DNA repair. *Sci Adv* **6**, eaay4697

279. Bedford, D. C., and Brindle, P. K. (2012) Is histone acetylation the most important physiological function for CBP and p300? *Aging (Albany NY)* **4**, 247-255

280. Wang, F., Marshall, C. B., and Ikura, M. (2013) Transcriptional/epigenetic regulator CBP/p300 in tumorigenesis: structural and functional versatility in target recognition. *Cell Mol Life Sci* **70**, 3989-4008

281. Bedford, D. C., Kasper, L. H., Fukuyama, T., and Brindle, P. K. (2010) Target gene context influences the transcriptional requirement for the KAT3 family of CBP and p300 histone acetyltransferases. *Epigenetics* **5**, 9-15

282. Hasan, S., El-Andaloussi, N., Hardeland, U., Hassa, P. O., Burki, C., Imhof, R., Schar, P., and Hottiger, M. O. (2002) Acetylation regulates the DNA end-trimming activity of DNA polymerase beta. *Mol Cell* **10**, 1213-1222

283. Mertins, P., Qiao, J. W., Patel, J., Udeshi, N. D., Clauser, K. R., Mani, D. R., Burgess, M. W., Gillette, M. A., Jaffe, J. D., and Carr, S. A. (2013) Integrated proteomic analysis of post-translational modifications by serial enrichment. *Nat Methods* **10**, 634-637

284. Gomes, X. V., Henricksen, L. A., and Wold, M. S. (1996) Proteolytic mapping of human replication protein A: evidence for multiple structural domains and a conformational change upon interaction with single-stranded DNA. *Biochemistry* **35**, 5586-5595

285. Lee, M. Y., Kim, M. A., Kim, H. J., Bae, Y. S., Park, J. I., Kwak, J. Y., Chung, J. H., and Yun, J. (2007) Alkylating agent methyl methanesulfonate (MMS) induces a wave of global protein hyperacetylation: implications in cancer cell death. *Biochem Biophys Res Commun* **360**, 483-489

286. Ramanathan, B., and Smerdon, M. J. (1986) Changes in nuclear protein acetylation in u.v.-damaged human cells. *Carcinogenesis* **7**, 1087-1094

287. Kim, C., Paulus, B. F., and Wold, M. S. (1994) Interactions of human replication protein A with oligonucleotides. *Biochemistry* **33**, 14197-14206

288. Brosey, C. A., Yan, C., Tsutakawa, S. E., Heller, W. T., Rambo, R. P., Tainer, J. A., Ivanov, I., and Chazin, W. J. (2013) A new structural framework for integrating replication protein A into DNA processing machinery. *Nucleic Acids Res* **41**, 2313-2327

289. Schubert, F., Zettl, H., Hafner, W., Krauss, G., and Krausch, G. (2003) Comparative thermodynamic analysis of DNA--protein interactions using surface plasmon resonance and fluorescence correlation spectroscopy. *Biochemistry* **42**, 10288-10294

290. Gibb, B., Silverstein, T. D., Finkelstein, I. J., and Greene, E. C. (2012) Single-stranded DNA curtains for real-time single-molecule visualization of protein-nucleic acid interactions. *Anal Chem* **84**, 7607-7612

291. Blackwell, L. J., and Borowiec, J. A. (1994) Human replication protein A binds single-stranded DNA in two distinct complexes. *Mol Cell Biol* **14**, 3993-4001

292. Glozak, M. A., Sengupta, N., Zhang, X., and Seto, E. (2005) Acetylation and deacetylation of non-histone proteins. *Gene* **363**, 15-23

293. Martinez-Balbas, M. A., Bauer, U. M., Nielsen, S. J., Brehm, A., and Kouzarides, T. (2000) Regulation of E2F1 activity by acetylation. *EMBO J* **19**, 662-671

294. Tell, G., Quadrifoglio, F., Tiribelli, C., and Kelley, M. R. (2009) The many functions of APE1/Ref-1: not only a DNA repair enzyme. *Antioxid Redox Signal* **11**, 601-620

295. Wan, F., and Lenardo, M. J. (2009) Specification of DNA binding activity of NF-kappaB proteins. *Cold Spring Harb Perspect Biol* **1**, a000067

296. Zhao, Y., Lu, S., Wu, L., Chai, G., Wang, H., Chen, Y., Sun, J., Yu, Y., Zhou, W., Zheng, Q., Wu, M., Otterson, G. A., and Zhu, W. G. (2006) Acetylation of p53 at lysine 373/382 by the histone deacetylase inhibitor depsipeptide induces expression of p21(Waf1/Cip1). *Mol Cell Biol* **26**, 2782-2790

297. Gronroos, E., Hellman, U., Heldin, C. H., and Ericsson, J. (2002) Control of Smad7 stability by competition between acetylation and ubiquitination. *Mol Cell* **10**, 483-493

298. Rausa, F. M., 3rd, Hughes, D. E., and Costa, R. H. (2004) Stability of the hepatocyte nuclear factor 6 transcription factor requires acetylation by the CREB-binding protein coactivator. *J Biol Chem* **279**, 43070-43076

299. Jeong, J. W., Bae, M. K., Ahn, M. Y., Kim, S. H., Sohn, T. K., Bae, M. H., Yoo, M. A., Song, E. J., Lee, K. J., and Kim, K. W. (2002) Regulation and destabilization of HIF-1alpha by ARD1-mediated acetylation. *Cell* **111**, 709-720

300. Shimazu, T., Komatsu, Y., Nakayama, K. I., Fukazawa, H., Horinouchi, S., and Yoshida, M. (2006) Regulation of SV40 large T-antigen stability by reversible acetylation. *Oncogene* **25**, 7391-7400

301. Grossman, S. R. (2001) p300/CBP/p53 interaction and regulation of the p53 response. *Eur J Biochem* **268**, 2773-2778

302. Cazzalini, O., Sommatis, S., Tillhon, M., Dutto, I., Bachi, A., Rapp, A., Nardo, T., Scovassi, A. I., Necchi, D., Cardoso, M. C., Stivala, L. A., and Prosperi, E. (2014) CBP and p300 acetylate PCNA to link its degradation with nucleotide excision repair synthesis. *Nucleic Acids Res* **42**, 8433-8448

303. Henricksen, L. A., Umbricht, C. B., and Wold, M. S. (1994) Recombinant replication protein A: expression, complex formation, and functional characterization. *J Biol Chem* **269**, 11121-11132

304. Wyka, I. M., Dhar, K., Binz, S. K., and Wold, M. S. (2003) Replication protein A interactions with DNA: differential binding of the core domains and analysis of the DNA interaction surface. *Biochemistry* **42**, 12909-12918

305. Stewart, J. A., Campbell, J. L., and Bambara, R. A. (2009) Significance of the dissociation of Dna2 by flap endonuclease 1 to Okazaki fragment processing in Saccharomyces cerevisiae. *J Biol Chem* **284**, 8283-8291

306. Sirbu, B. M., Couch, F. B., and Cortez, D. (2012) Monitoring the spatiotemporal dynamics of proteins at replication forks and in assembled chromatin using isolation of proteins on nascent DNA. *Nat Protoc* **7**, 594-605

307. Balakrishnan, L., Brandt, P. D., Lindsey-Boltz, L. A., Sancar, A., and Bambara, R. A. (2009) Long patch base excision repair proceeds via coordinated stimulation of the multienzyme DNA repair complex. *J Biol Chem* **284**, 15158-15172

308. Debrauwere, H., Loeillet, S., Lin, W., Lopes, J., and Nicolas, A. (2001) Links between replication and recombination in Saccharomyces cerevisiae: a hypersensitive requirement for homologous recombination in the absence of Rad27 activity. *Proc Natl Acad Sci U S A* **98**, 8263-8269

309. Murakami, Y., Eki, T., and Hurwitz, J. (1992) Studies on the initiation of simian virus 40 replication in vitro: RNA primer synthesis and its elongation. *Proc Natl Acad Sci U S A* **89**, 952-956

310. Garg, P., Stith, C. M., Sabouri, N., Johansson, E., and Burgers, P. M. (2004) Idling by DNA polymerase delta maintains a ligatable nick during lagging-strand DNA replication. *Genes Dev* **18**, 2764-2773

311. Turchi, J. J., Huang, L., Murante, R. S., Kim, Y., and Bambara, R. A. (1994) Enzymatic completion of mammalian lagging-strand DNA replication. *Proc Natl Acad Sci U S A* **91**, 9803-9807

312. Rossi, M. L., Purohit, V., Brandt, P. D., and Bambara, R. A. (2006) Lagging strand replication proteins in genome stability and DNA repair. *Chem Rev* **106**, 453-473

313. Kao, H. I., Campbell, J. L., and Bambara, R. A. (2004) Dna2p helicase/nuclease is a tracking protein, like FEN1, for flap cleavage during Okazaki fragment maturation. *J Biol Chem* **279**, 50840-50849

314. Stewart, J. A., Campbell, J. L., and Bambara, R. A. (2006) Flap endonuclease disengages Dna2 helicase/nuclease from Okazaki fragment flaps. *J Biol Chem* **281**, 38565-38572

315. Zheng, L., Jia, J., Finger, L. D., Guo, Z., Zer, C., and Shen, B. (2011) Functional regulation of FEN1 nuclease and its link to cancer. *Nucleic Acids Res* **39**, 781-794

316. Kao, H. I., Veeraraghavan, J., Polaczek, P., Campbell, J. L., and Bambara, R. A. (2004) On the roles of Saccharomyces cerevisiae Dna2p and Flap endonuclease 1 in Okazaki fragment processing. *J Biol Chem* **279**, 15014-15024

317. Masuda-Sasa, T., Imamura, O., and Campbell, J. L. (2006) Biochemical analysis of human Dna2. *Nucleic Acids Res* **34**, 1865-1875

318. Fortune, J. M., Stith, C. M., Kissling, G. E., Burgers, P. M., and Kunkel, T. A. (2006) RPA and PCNA suppress formation of large deletion errors by yeast DNA polymerase delta. *Nucleic Acids Res* **34**, 4335-4341

319. Stodola, J. L., and Burgers, P. M. (2016) Resolving individual steps of Okazaki-fragment maturation at a millisecond timescale. *Nat Struct Mol Biol* **23**, 402-408

320. Burgers, P. M. (2009) Polymerase dynamics at the eukaryotic DNA replication fork. *J Biol Chem* **284**, 4041-4045

321. Murante, R. S., Rust, L., and Bambara, R. A. (1995) Calf 5' to 3' exo/endonuclease must slide from a 5' end of the substrate to perform structure-specific cleavage. *J Biol Chem* **270**, 30377-30383

322. Henneke, G., Koundrioukoff, S., and Hubscher, U. (2003) Phosphorylation of human Fen1 by cyclin-dependent kinase modulates its role in replication fork regulation. *Oncogene* **22**, 4301-4313

323. Gloor, J. W., Balakrishnan, L., and Bambara, R. A. (2010) Flap endonuclease 1 mechanism analysis indicates flap base binding prior to threading. *J Biol Chem* **285**, 34922-34931

324. Hohl, M., Dunand-Sauthier, I., Staresincic, L., Jaquier-Gubler, P., Thorel, F., Modesti, M., Clarkson, S. G., and Scharer, O. D. (2007) Domain swapping between FEN-1 and XPG defines regions in XPG that mediate nucleotide excision repair activity and substrate specificity. *Nucleic Acids Res* **35**, 3053-3063

325. Huggins, C. F., Chafin, D. R., Aoyagi, S., Henricksen, L. A., Bambara, R. A., and Hayes, J. J. (2002) Flap endonuclease 1 efficiently cleaves base excision repair and DNA replication intermediates assembled into nucleosomes. *Mol Cell* **10**, 1201-1211

326. Stewart, J. A., Campbell, J. L., and Bambara, R. A. (2010) Dna2 is a structure-specific nuclease, with affinity for 5'-flap intermediates. *Nucleic Acids Res* **38**, 920-930

327. Zhou, C., Pourmal, S., and Pavletich, N. P. (2015) Dna2 nuclease-helicase structure, mechanism and regulation by Rpa. *Elife* **4**

328. Hübscher U, M. G., podust VN. (1996) In DNA Replication Accessory Proteins. Cold Spring Harbor NY. pp 525-543

329. Kuriyan, J., and O'Donnell, M. (1993) Sliding clamps of DNA polymerases. *J Mol Biol* **234**, 915-925

330. O'Donnell, M. E., Elias, P., Funnell, B. E., and Lehman, I. R. (1987) Interaction between the DNA polymerase and single-stranded DNA-binding protein (infected cell protein 8) of herpes simplex virus 1. *J Biol Chem* **262**, 4260-4266

331. Wu, Y., Rawtani, N., Thazhathveetil, A. K., Kenny, M. K., Seidman, M. M., and Brosh, R. M., Jr. (2008) Human replication protein A melts a DNA triple helix structure in a potent and specific manner. *Biochemistry* **47**, 5068-5077

332. Qureshi, M. H., Ray, S., Sewell, A. L., Basu, S., and Balci, H. (2012) Replication protein A unfolds G-quadruplex structures with varying degrees of efficiency. *J Phys Chem B* **116**, 5588-5594

333. Chen, R., Subramanyam, S., Elcock, A. H., Spies, M., and Wold, M. S. (2016) Dynamic binding of replication protein a is required for DNA repair. *Nucleic Acids Res* **44**, 5758-5772

334. Treuner, K., Ramsperger, U., and Knippers, R. (1996) Replication protein A induces the unwinding of long double-stranded DNA regions. *J Mol Biol* **259**, 104-112

335. Fortune, J. M., Pavlov, Y. I., Welch, C. M., Johansson, E., Burgers, P. M., and Kunkel, T. A. (2005) Saccharomyces cerevisiae DNA polymerase delta: high fidelity for base substitutions but lower fidelity for single- and multi-base deletions. *J Biol Chem* **280**, 29980-29987

336. Unk, I., Haracska, L., Gomes, X. V., Burgers, P. M., Prakash, L., and Prakash, S. (2002) Stimulation of 3'-->5' exonuclease and 3'-phosphodiesterase activities of yeast apn2 by proliferating cell nuclear antigen. *Mol Cell Biol* **22**, 6480-6486

337. Eckschlager, T., Plch, J., Stiborova, M., and Hrabeta, J. (2017) Histone Deacetylase Inhibitors as Anticancer Drugs. *Int J Mol Sci* **18**

338. Ononye, O. E., Sausen, C. W., Balakrishnan, L., and Bochman, M. L. (2020) Lysine Acetylation Regulates the Activity of Nuclear Pif1. *J Biol Chem*

339. Shi, W., Feng, Z., Zhang, J., Gonzalez-Suarez, I., Vanderwaal, R. P., Wu, X., Powell, S. N., Roti Roti, J. L., Gonzalo, S., and Zhang, J. (2010) The role of RPA2 phosphorylation in homologous recombination in response to replication arrest. *Carcinogenesis* **31**, 994-1002

340. Liu, L., Scolnick, D. M., Trievel, R. C., Zhang, H. B., Marmorstein, R., Halazonetis, T. D., and Berger, S. L. (1999) p53 sites acetylated in vitro by PCAF and p300 are acetylated in vivo in response to DNA damage. *Mol Cell Biol* **19**, 1202-1209

341. Ononye, O. E., Sausen, C. W., Bochman, M. L., and Balakrishnan, L. (2020) Dynamic regulation of Pif1 acetylation is crucial to the maintenance of genome stability. *Curr Genet*

342. Guo, Z., Zheng, L., Xu, H., Dai, H., Zhou, M., Pascua, M. R., Chen, Q. M., and Shen, B. (2010) Methylation of FEN1 suppresses nearby phosphorylation and facilitates PCNA binding. *Nat Chem Biol* **6**, 766-773

343. Abe, Y., Uehara, S., Okamura, K., Yajima, A., Saito, T., Yoshida, Y., Wagatsuma, S., and Mandai, M. (1993) [Possibility of vertical transmission of hepatitis C virus]. *Nihon Sanka Fujinka Gakkai Zasshi* **45**, 263-266

APPENDIX A. SUPPLEMENTARY FOR CHAPTER 2

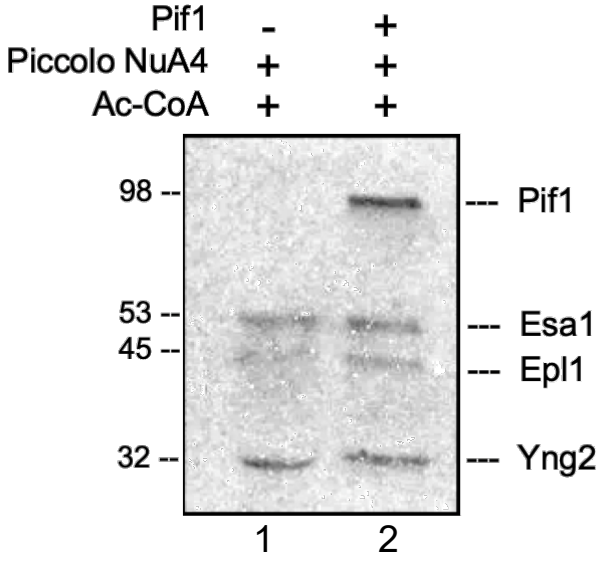

Figure A- 1. Piccolo NuA4 (Esa1) in vitro-acetylates Pif1

Recombinant NuA4 and full-length Pif1 were incubated along with 14C labelled-acetyl CoA as described in the Materials and Methods. The reaction products were separated on a 4-15% SDS-PAGE gel and subsequently subjected to autoradiography. Piccolo NuA4 (Esa1) was capable of robustly acetylating Pif1 in vitro (lane 2). The Esa1 subunit also underwent autoacetylation and acetylated the other subunits (Epl1 and Yng2) of the NuA4 complex (lanes 1 and 2).

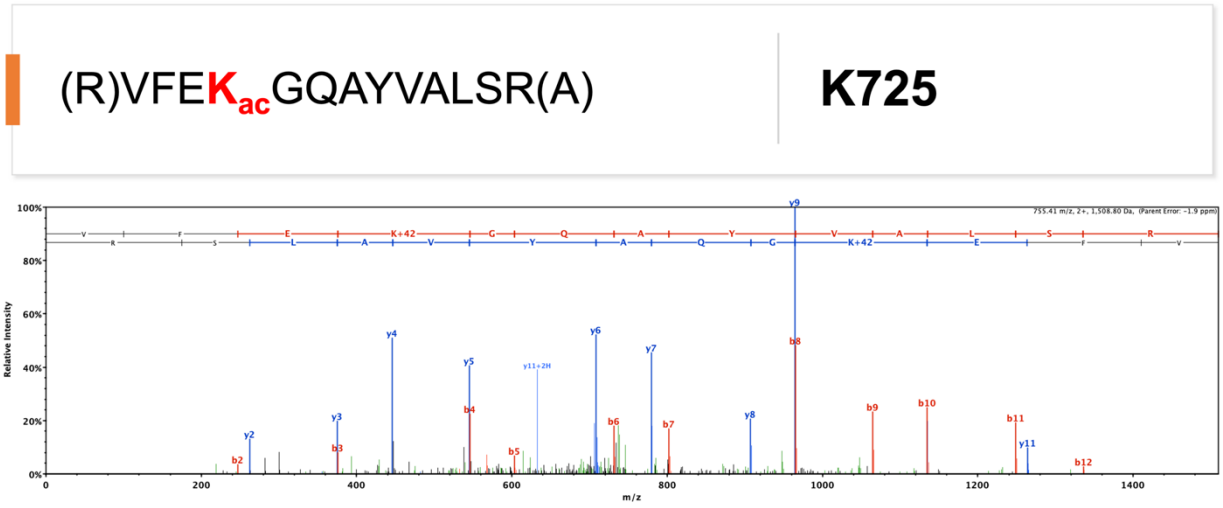

Figure A- 2. Spectra for Acetylated Pif1 Lysine 725

Representative spectra for lysine acetylation sites on Pif1 annotated on Scaffold (Proteome Software, Portland OR). The b-ions are labeled in red, and y-ions are labeled in blue. Neutral loss and other parent ion fragments are shown in green. The sequence of the acetylated peptide is denoted above the spectra with the acetylated lysine (K) highlighted in bold red font.

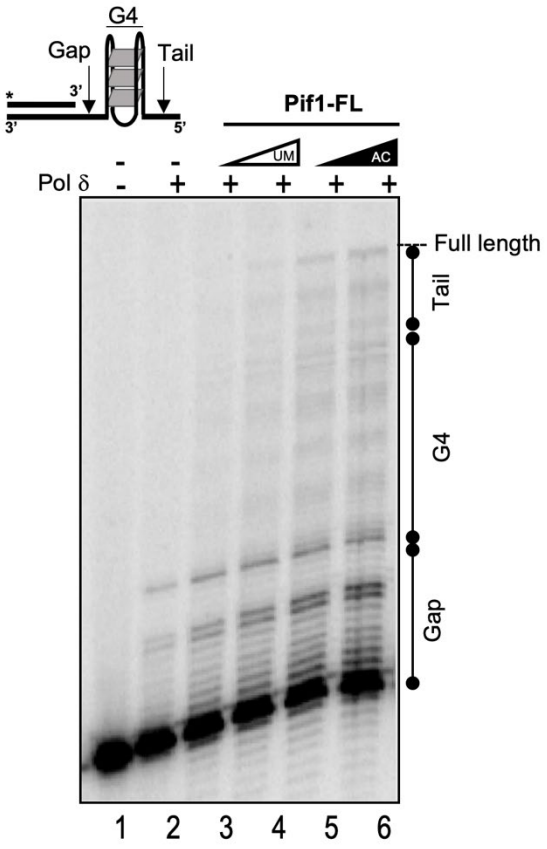

Figure A- 3. Pif1 resolves G4 structures to allow Pol δ synthesis.

The synthesis activity of 23 nM S. cerevisiae DNA polymerase delta (Pol δ) was assayed on 5 nM cMyc-G4 substrate in the absence (lane 1) and presence of increasing concentrations (5 and 10 nM) of UM-Pif1 (lanes 3, 4) and AC-Pif1 (lanes 5, 6). The reactions were performed in a reaction buffer containing 20 mM Tris HCl (pH 7.8), 8 mM $Mg(CH_3COO)_2$, 100 mM KCl, 1 mM DTT, 0.1 mg/mL BSA, 100 µM dNTPs, and 1 mM ATP for 10 min at 30ºC. Reactions were terminated using 2X termination dye and were immediately heated to 95°C and loaded onto a pre-warmed denaturing polyacrylamide gel (12% polyacrylamide, 7 M urea), and reaction products were separated by electrophoresis for 80 min at 80 W, subsequently dried, and analyzed.

Result: DNA pol δ alone was unable to synthesize on the G4 substrate past the gap region, indicating the presence of a stable G4 structure. However, in the presence of both UM-Pif1 and AC-Pif1, we observed synthesis past the gap and into the G4 region. The AC-Pif1 displayed the highest stimulation of Pol δ synthesis, including the formation of a full-length product, presumably because AC-Pif1 was more efficient at G4 structure resolution than UM-Pif1.

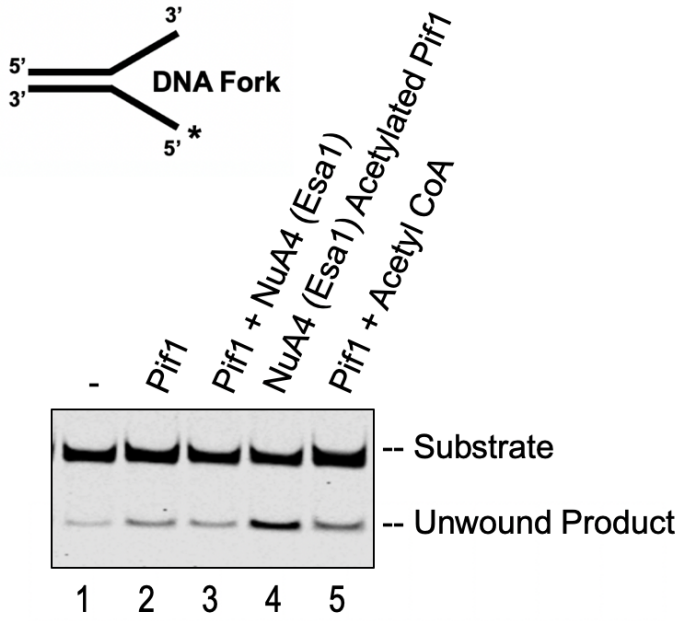

Figure A- 4. Stimulation of helicase activity is dependent on Pif1 acetylation alone.

Helicase assays was performed using an IR labeled DNA fork in the presence of one nanomolar of either UM-Pif1 (lane 2), Pif1 + Piccolo NuA4 (Esa1) (lane 3), AC-Pif1 (lane 4) or Pif1 + Acetyl CoA lithium salt as described in Materials and Methods.

Table A-1. Yeast genotypes used in this study.

Strain Number	**Genotype**
MBY623-638 and 662-669	*MATα can1Δ::STE2pr-Sp_his5 lyp1Δ his3Δ1 leu2Δ0 met15Δ0 ura3Δ0*
MBY703-706, 713-714, and 799	*MATα can1Δ::STE2pr-Sp_his5 lyp1Δ his3Δ1 leu2Δ0 ura3Δ0 met15Δ0*
MBY710, 711, and 715	*MATaa leu2-3,112 trp1-1 can1-100 ura3-1 ade2-1 his3-11,15*

Table A-2. List of yeast strains used in this study

Number	**Name**	**Description**
MBY623	*ura3::NatMX pESC-URA*	Empty vector control in a wild-type background
MBY624	*rpd3::NatMX pESC-URA*	Empty vector control in an *rpd3Δ* background
MBY625	*hda1::NatMX pESC-URA*	Empty vector control in an *hda1Δ* background
MBY626	*hda2::NatMX pESC-URA*	Empty vector control in an *hda2Δ* background
MBY627	*hda3::NatMX pESC-URA*	Empty vector control in an *hda3Δ* background
MBY628	*hos1::NatMX pESC-URA*	Empty vector control in a *hos1Δ* background
MBY629	*hos2::NatMX pESC-URA*	Empty vector control in a *hos2Δ* background
MBY630	*hos3::NatMX pESC-URA*	Empty vector control in a *hos3Δ* background
MBY631	*ura3::NatMX pESC-URA-PIF1*	Pif1 overexpression in a wild-type background
MBY632	*rpd3::NatMX pESC-URA-PIF1*	Pif1 overexpression in an *rpd3Δ* background
MBY633	*hda1::NatMX pESC-URA-PIF1*	Pif1 overexpression in an *hda1Δ* background
MBY634	*hda2::NatMX pESC-URA-PIF1*	Pif1 overexpression in an *hda2Δ* background
MBY635	*hda3::NatMX pESC-URA-PIF1*	Pif1 overexpression in an *hda3Δ* background
MBY636	*hos1::NatMX pESC-URA-PIF1*	Pif1 overexpression in a *hos1Δ* background

Table A-2 continued		
MBY637	*hos2::NatMX pESC-URA-PIF1*	Pif1 overexpression in a *hos2Δ* background
MBY638	*hos3::NatMX pESC-URA-PIF1*	Pif1 overexpression in a *hos3Δ* background
MBY662	*ura3::NatMX pESC-URA-PIF1ΔN*	Pif1ΔN overexpression in a *rpd3Δ* background
MBY663	*rpd3::NatMX pESC-URA-PIF1ΔN*	Pif1ΔN overexpression in an *hda1Δ* background
MBY664	*hda1::NatMX pESC-URA-PIF1ΔN*	Pif1ΔN overexpression in an *hda2Δ* background
MBY665	*hda2::NatMX pESC-URA-PIF1ΔN*	Pif1ΔN overexpression in an *hda3Δ* background
MBY666	*hda3::NatMX pESC-URA-PIF1ΔN*	Pif1ΔN overexpression in a *hos1Δ* background
MBY667	*hos1::NatMX pESC-URA-PIF1ΔN*	Pif1ΔN overexpression in a *hos2Δ* background
MBY668	*hos2::NatMX pESC-URA-PIF1ΔN*	Pif1ΔN overexpression in a *hos3Δ* background
MBY669	*hos3::NatMX pESC-URA-PIF1ΔN*	Pif1ΔN overexpression in a *rpd3Δ* background
MBY693	*esa1-414 pESC-URA*	Empty vector control in an *esa1-414* background
MBY694	*esa1-414 pESC-URA-PIF1*	Pif1 overexpression in an *esa1-414* background
MBY703	*gcn5Δ::KanMX pESC-URA empty vector*	Empty vector control in a *gcn5Δ* background
MBY704	*gcn5Δ::KanMX pESC-URA-PIF1*	Pif1 overexpression in a *gcn5Δ* background

Table A-2 continued		
MBY705	*rtt109Δ::KanMX pESC-URA empty vector*	Empty vector control in an *rtt109Δ* background
MBY706	*rtt109Δ::KanMX pESC-URA-PIF1*	Pif1 overexpression in an *rtt109Δ* background
MBY710	*WT MBY580 pESC-URA empty vector*	Empty vector control in a wild-type background
MBY711	*WT MBY580 pESC-URA-PIF1*	Pif1 overexpression in a wild-type background
MBY713	*gcn5Δ::KanMX pESC-URA-PIF1ΔN*	Pif1ΔN overexpression in a *gcn5Δ* background
MBY714	*rtt109Δ::KanMX pESC-URA-PIF1ΔN*	Pif1ΔN overexpression in an *rtt109Δ* background
MBY715	*WT MBY580 pESC-URA-PIF1ΔN*	Pif1ΔN overexpression in a wild-type background
MBY799	*esa1-414 pESC-URA-PIF1ΔN*	Pif1ΔN overexpression in an *esa1-414* background

Table A-3. Plasmids used in this study.

Number	Name	Description
pMB524	pESC-URA	Multi-copy vector enabling epitope tagging of genes cloned under the control of the bidirectional *GAL1,10* promoter
pMB526	pESC-URA-Pif1	Pif1 cloned into pESC-URA, enabling galactose induction and C-terminal FLAG tagging
pMB540	pESC-URA-Pif1ΔN	Pif1ΔN cloned into pESC-URA, enabling galactose induction and C-terminal FLAG tagging
pMB472	pSUMO-Pif1	Nuclear isoform of Pif1 cloned into the pSUMO vector for over-expression in *Escherichia coli*
pMB562	pSUMO-Pif1ΔN	Pif1ΔN cloned into the pSUMO vector for over-expression in *E. coli*
pST44	P6XHis-Epl1/Yng2/Esa1	Wild-type Esa1, Yng2 (2-18), and 6X His-Epl1 (51-380) cloned into the pST44 vector for over-expression in *E. coli*

Table A-4. Oligonucleotides used in this study. Capital letters = dNTP, small letters = NTP, and Bio - biotinylated.

Oligo name and length (nt)	Sequence (5' – 3')
T1 (45)	TTTTTTTTTTTTTTTTTTTTTTTTTGTGTCACTCACATAGCGTTC-Bio
D1 (45)	GAACGCTATGTGAGTGACACTTTTTTTTTTTTTTTTTTTTTTTTT
D2 (45)	gaacgcuaugugagugacacuuuuuuuuuuuuuuuuuuuuuuuu(O-methyl)u
D3 (20)	GAACGCTATGTGAGTGACAC
D4 (20)	GAACGCTATGugagugaca(O-methyl)c
D5 (65)	ACGTCATTGGTCTGGGGAGGGTGGGGAGGGTGGGGAAGGTTTTTCACTAATAAGTTCCGCGGCGG–Bio
T2 (21)	CCGCCGCGGAACTTATTAGTG
T50 (50)	TTTTTTTTTTTTTTTTTTTTTTTTTTTTTTTTTTTTTTTTTTTTTTTTTT

APPENDIX B. SUPPLEMENTARY FOR CHAPTER 3

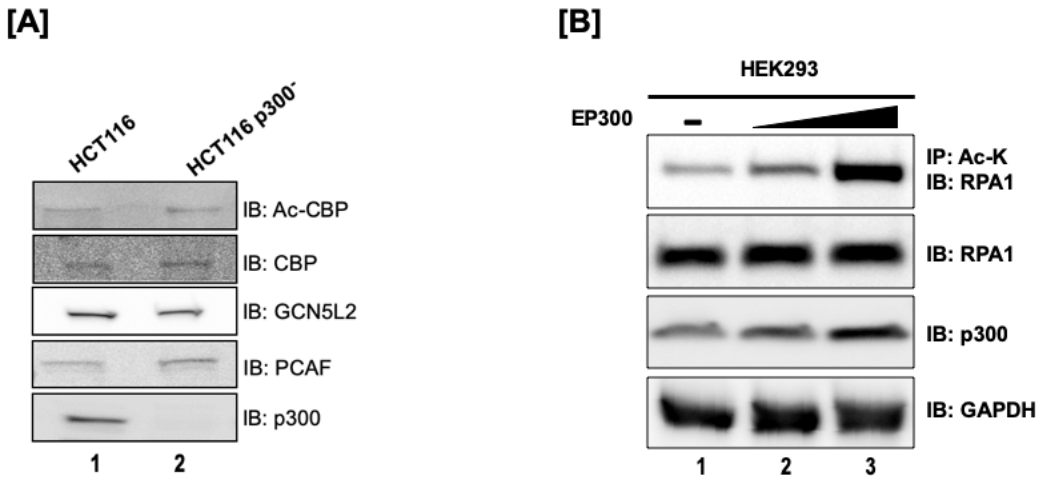

Figure B- 1. Probing for KATs in multiple lysates

(A) Immunoblot analysis of expression of specific KATs in wild-type HCT116 and HCT116p300- cell lysates (B) Acetylation of RPA1 Subunit. IP-western blot analysis of RPA1 acetylation in HEK293 cells transfected with EP300 overexpression construct.

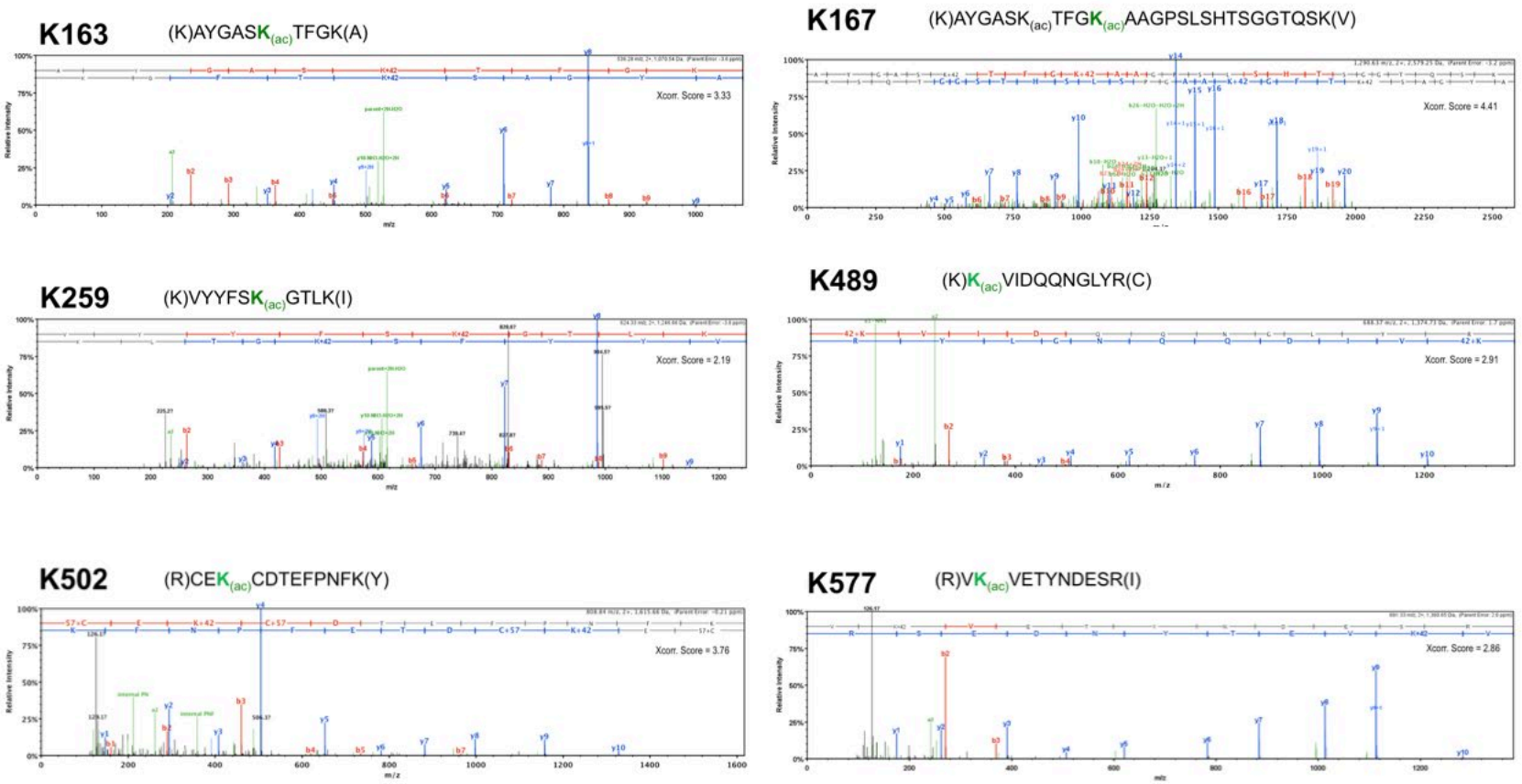

Figure B- 2. MS/MS spectra for *in vitro* acetylated RPA1.

Representative spectra for lysine acetylation sites on RPA1 annotated on Scaffold (Proteome Software, Portland OR). The b-ions are labeled in red and y-ions are labeled in blue. Neutral loss and other parent ion fragments are shown in green. Sequence of the acetylated peptide is denoted above the spectra with the acetylated lysine (K) highlighted in bold green font.

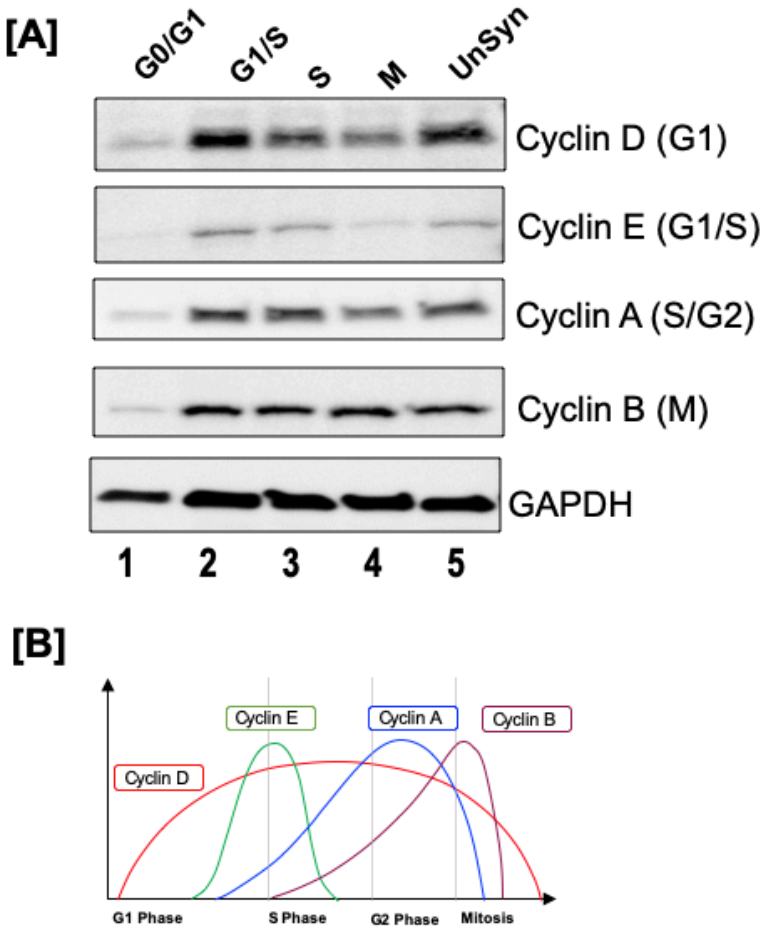

Figure B- 3. Probing for cyclins levels at various cell cycle phases

HEK293T Cells were synchronized during different phases using either serum starvation or specific chemicals as described in the Materials and Methods. (**A**) Synchronization in different cell phases were confirmed by probing for expression of specific cyclins in the different cell cycle phases; (**B**) Graphical representation of cyclins that have known expression patterns in different cell cycle phases.

	Neat Serum			Affinity Purity Fraction (Acetyl)		
		Plates coated with acetyl peptide	Plates coated with control peptide		Plates coated with acetyl peptide	Plates coated with control peptide
A	1:100	3.042***	3.050***	1:100	3.039***	0.212
B	1:1000	3.034***	3.048***	1:1000	3.039***	0.039
C	1:10,000	3.026***	2.827***	1:10,000	1.153	0.033
D	1:100,000	1.093	0.538	1:100,000	0.183	0.022

Figure B- 4. Testing the Specificity of RPAK163$_{ac}$ antibody

ELISA Analysis of Custom Affinity Pure Sera: Antigens (free peptides) were coated on ELISA strips at 10 µg/ml in coating buffer. The unbound antigen was washed and all remaining sites were blocked with buffer containing BSA. Anti-sera, including preimmune was diluted in 1:100, 1:1000, 1:10,000 and 1:100,000 and added in separate wells down the column. After 60 mins of antibody incubation, unbound antibodies were washed and the anti-rabbit IgG-HRP conjugate is added. The plates were washed again after 30 mins incubation. TMB substrate is then added and color developed for 15 mins. The reaction (blue color) is stopped by the addition of acid (turns blue to yellow).

The amount of yellow color (read at 450 nm with an ELIZA reader) is directly proportional to the amount of antibody. Color is read in Absorbance or OD (Optical density) units of 0.000-2.000. Reading above 2.000 were not considered to be linear, since it displayed too much yellow color. This is represented by *** indicating excess color. Upon further antibody dilution, the absorbance was readable (Abs. < 2.000). This is represented as A450 nm.

The ELISA assay showed that the antibodies were clearly detected in an antibody titre of 1:10,000 and 1:100,000 and blocking using the control peptide showed that the antibody was specific to the acetylated peptide.

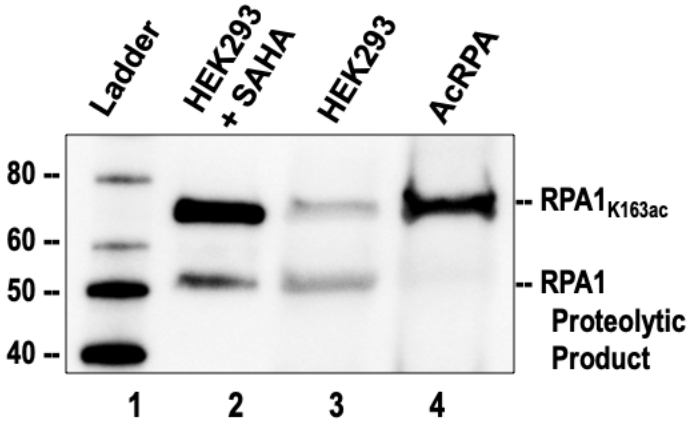

Figure B- 5. Testing the Specificity of RPAK163$_{ac}$ antibody

HEK293T cell lysates (from either untreated or treated for 24 hours with 10mM suberoylanilide hydroxamic acid (SAHA) to induce cellular hyperacetylation) were separated on a 4-20% gradient gel and subject to immunoblotting using the RPA1K$_{163ac}$ antibody (1:10,000 dilution). In vitro acetylated RPA (AcRPA) served as a positive control.

The RPA1K163ac antibody recognized two products in the cell lysate, the 70 kDa RPA1 and the 55 kDa RPA1 proteolytic product.

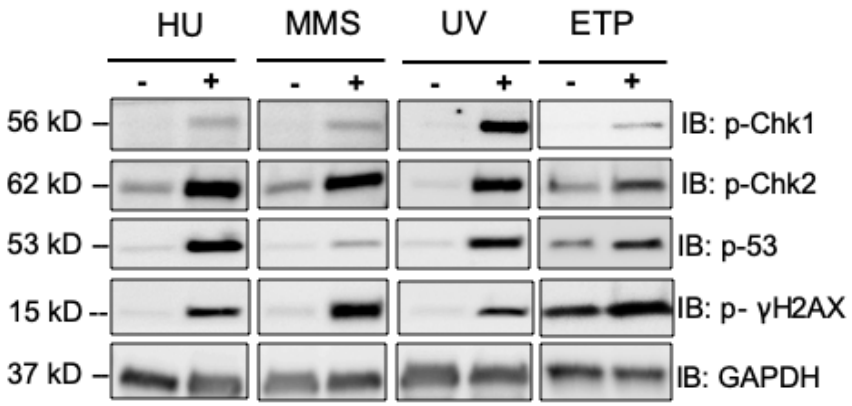

Figure B- 6. Markers of DNA Damage

HEK293T cell lysates treated with different DNA damaging agents (as described in Materials and Methods) were immunoblotted with antibodies against different DNA damage markers to confirm induction of DNA damage in our experiments. Cell lysates for HU and ETP were harvested 6 hours post-treatment and MMS and UV were harvested 12 hours post-treatment.

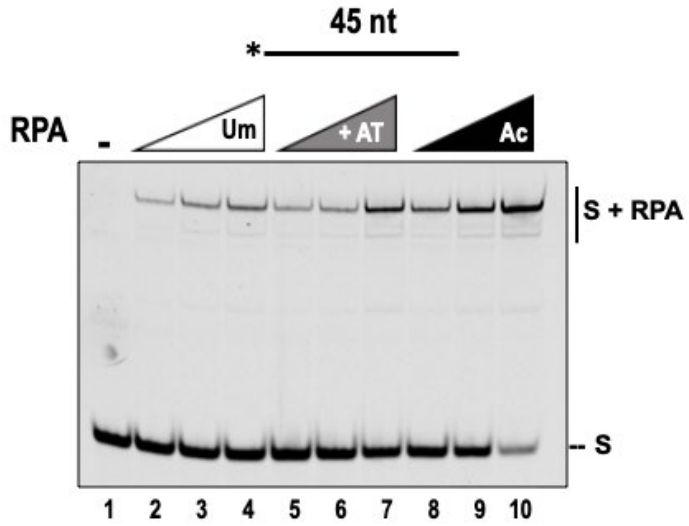

Figure B- 7. RPA acetylation and not the presence of p300 improves ssDNA binding affinity.

Five nanomolar of IR labeled 45 nt ssDNA substrate was incubated with increasing concentrations (5, 10, 25 nM) of Um-RPA, RPA + p300 (in the absence of acetyl CoA) or Ac-RPA, and the reactions were incubated for 10 min at 37°C and reactions were subsequently separated on a 6% polyacrylamide gel. The labeled substrate is depicted above the gel with the asterisk indicating 5' of the IR-700 label. The substrate alone and the complexes containing RPA-bound substrate are indicated beside the gel at the right

Table B-1. Oligonucleotides used in this study

All sequences are written in the 5' – 3' direction

Oligonucleotide	**Sequence**
20	TTC ACG CCT GTT AGT TAA TT
24	TTC ACG CCT GTT AGT TAA TTC ACT
29	TTC ACG CCT GTT AGT TAA TTC ACT GGC CG
30	TTC ACG AGA TTT ACT TAT TTC ACT GGC CGT
32	TTC ACG CCT GTT AGT TAA TTC ACT GGC CGT AC
45	TTC ACT ATA ACT ACC TAA TCT TCT GGC CGT ACT GAA CTA CTG ACA

Oligonucleotides containing TAMRA were labelled on the 5' end while those containing biotin were labelled on the 3' end.